

1994

# The Structural Basis for Kinetic and Allosteric Differences Between Two Bacterial Phosphofructokinases.

Walton Malcolm Byrnes

*Louisiana State University and Agricultural & Mechanical College*

Follow this and additional works at: [https://digitalcommons.lsu.edu/gradschool\\_disstheses](https://digitalcommons.lsu.edu/gradschool_disstheses)

---

## Recommended Citation

Byrnes, Walton Malcolm, "The Structural Basis for Kinetic and Allosteric Differences Between Two Bacterial Phosphofructokinases." (1994). *LSU Historical Dissertations and Theses*. 5859.

[https://digitalcommons.lsu.edu/gradschool\\_disstheses/5859](https://digitalcommons.lsu.edu/gradschool_disstheses/5859)

This Dissertation is brought to you for free and open access by the Graduate School at LSU Digital Commons. It has been accepted for inclusion in LSU Historical Dissertations and Theses by an authorized administrator of LSU Digital Commons. For more information, please contact [gradetd@lsu.edu](mailto:gradetd@lsu.edu).

## **INFORMATION TO USERS**

This manuscript has been reproduced from the microfilm master. UMI films the text directly from the original or copy submitted. Thus, some thesis and dissertation copies are in typewriter face, while others may be from any type of computer printer.

**The quality of this reproduction is dependent upon the quality of the copy submitted.** Broken or indistinct print, colored or poor quality illustrations and photographs, print bleedthrough, substandard margins, and improper alignment can adversely affect reproduction.

In the unlikely event that the author did not send UMI a complete manuscript and there are missing pages, these will be noted. Also, if unauthorized copyright material had to be removed, a note will indicate the deletion.

Oversize materials (e.g., maps, drawings, charts) are reproduced by sectioning the original, beginning at the upper left-hand corner and continuing from left to right in equal sections with small overlaps. Each original is also photographed in one exposure and is included in reduced form at the back of the book.

Photographs included in the original manuscript have been reproduced xerographically in this copy. Higher quality 6" x 9" black and white photographic prints are available for any photographs or illustrations appearing in this copy for an additional charge. Contact UMI directly to order.

# **UMI**

A Bell & Howell Information Company  
300 North Zeeb Road, Ann Arbor, MI 48106-1346 USA  
313/761-4700 800/521-0600



THE STRUCTURAL BASIS FOR KINETIC AND ALLOSTERIC DIFFERENCES  
BETWEEN TWO BACTERIAL PHOSPHOFRUCTOKINASES

A Dissertation  
Submitted to the Graduate Faculty of the  
Louisiana State University and  
Agricultural and Mechanical College  
in partial fulfillment of the  
requirements for the degree of  
Doctor of Philosophy

in

The Department of Biochemistry

by  
Walton Malcolm Byrnes  
B. S., Xavier University of Louisiana, 1981  
December 1994

**UMI Number: 9524438**

---

**UMI Microform Edition 9524438**  
**Copyright 1995, by UMI Company. All rights reserved.**

**This microform edition is protected against unauthorized  
copying under Title 17, United States Code.**

---

**UMI**  
**300 North Zeeb Road**  
**Ann Arbor, MI 48103**

## **Acknowledgments**

There are many people without whom this dissertation would not have come to pass. To these people I owe a debt of sincere gratitude. I thank Dr. Simon H. Chang, my advisor, for his professional and financial support. I thank also the members of my advisory committee, Dr. Eric Achberger, Dr. Sue Bartlett, Dr. Ding Shih, and Dr. Ezzat Younathan, for their guidance and advice. Two people deserve special thanks: Sr. Mary Carl Malmstrom, S.B.S., my friend and mentor at Xavier who never spoke a discouraging word despite my wanderings since graduating from Xavier in 1981, and my Uncle Alva B. O'Brien, whose encouragement and kind help led to my returning to graduate school. I am also grateful to my parents, V. Malcolm and Christine F. Byrnes, and my family, who have supported and encouraged me during the last six years. Finally, my deepest gratitude and appreciation are saved for my wife, Noni, whose patience, love, understanding and sacrifice (also money) have carried me through these last few months of preparation.

## Preface

This dissertation is divided into three major parts: a general introduction or literature review (chapter 1), a presentation of the results and a discussion of the results (chapters 2, 3, and 4), and some concluding statements and suggestions for future studies (chapter 5). Chapters 2, 3, and 4 form the core of the dissertation. Each of these three chapters is presented in the form of a manuscript consisting of Introduction, Materials and Methods, Results, and Discussion sections. Chapter 2 has been published (Byrnes, M., Zhu, X., Younathan, E. S., & Chang, S. H. (1994) *Biochemistry* 33, 3424-3431), chapter 3 has been accepted for publication in the *Journal of Biological Chemistry*, and chapter 4 is currently being submitted to *Biochemistry*. Some of the kinetic results presented in Tables 4.2, 4.3, and 4.4—those for the *E. coli* PFK mutants—were obtained by Dr. Isabelle Auzat, who came from the Laboratoire d'Enzymologie-CNRS in France to visit the Chang laboratory in March, 1994. There may be some overlap in the introductory sections of the three core chapters. Chapter 1 is designed to be an "umbrella" introduction that will hopefully provide a comprehensive review of the bacterial PFK literature, including information not included in the core chapter introductions. Finally, chapter 5 sums up the whole body of work and proposes some specific future experiments. Hopefully, one or more of the suggested future experiments in chapter 5 will ignite someone's interest in pursuing further studies of bacterial PFK.

## Table of Contents

ACKNOWLEDGEMENTS .....	ii
PREFACE .....	iii
LIST OF TABLES .....	v
LIST OF FIGURES .....	vi
LIST OF ABBREVIATIONS AND SYMBOLS.....	viii
ABSTRACT .....	x
CHAPTER ONE: .....	1
General Introduction	
CHAPTER TWO: .....	39
Kinetic Characteristics of Phosphofructokinase from <i>Bacillus stearothermophilus</i> : MgATP Non-allosterically Inhibits the Enzyme	
CHAPTER THREE: .....	71
A Chimeric Bacterial Phosphofructokinase Exhibits Cooperativity in the Absence of Heterotropic Regulation	
CHAPTER FOUR: .....	107
The Role of Residue 161 in the Allosteric Transitions of Two Bacterial Phosphofructokinases	
CHAPTER FIVE: .....	133
Conclusions and Future Studies	
LITERATURE CITED .....	140
APPENDIX: Permission Letter .....	145
VITA .....	148



## List of Tables

1.1	Active Site Residues. . . . .	6
1.2	Effector Site Residues. . . . .	7
1.3	Residues Important for Catalysis . . . . .	15
1.4	Kinetic and Allosteric Parameters for <i>E. coli</i> PFK . . . . .	27
1.5	Residues Important for Homotropic Cooperativity of <i>E. coli</i> PFK . . . . .	34
2.1	Product Inhibition Patterns for the Reverse Reaction . . . . .	49
2.2	Alternative Nucleoside Triphosphate (NTP) Substrates . . . . .	59
2.3	Product and Dead-end Inhibition Patterns for the Forward Reaction . . . . .	61
3.1	Kinetic Parameters for ChiPFK and the Native Enzymes . . . . .	85
3.2	Dissociation Constants and Maximum Fluorescence Changes for Fru-6P and AMPPNP Binding to <i>E. coli</i> PFK . . . . .	98
3.3	Changes in Intrinsic Fluorescence Induced by Ligand Binding to <i>E. coli</i> PFK and the Chimeric PFK . . . . .	99
4.1	Mutagenic Oligonucleotides . . . . .	114
4.2	Steady-state Kinetic Parameters for Wild-type and Mutant PFKs . . . . .	119
4.3	PEP Inhibition of Wild-type and Mutant PFKs . . . . .	121
4.4	Activation of EcPFK and Its Mutants by GDP . . . . .	124
4.5	Activation of BsPFK and Its Mutants by GDP and Fru-6P . . . . .	128

## List of Figures

1.1	The Glycolytic Pathway . . . . .	3
1.2	Sequences of the PFKs from <i>E. coli</i> and <i>B. stearothermophilus</i> . . . . .	5
1.3	The Bacterial PFK Tetramer . . . . .	9
1.4	The Proposed Transition State of <i>E. coli</i> PFK . . . . .	13
1.5	The Open-to-Closed Conformational Change . . . . .	18
1.6	The Proposed Reaction Cycle of <i>E. coli</i> PFK . . . . .	19
1.7	The Effector Site of <i>E. coli</i> PFK . . . . .	22
1.8	Co-ordinated Movement of the 8H and 6F Loops . . . . .	32
1.9	Reorganization of the 6F Loop . . . . .	33
2.1	Initial Velocity Patterns for the Reverse Reaction . . . . .	47
2.2	Saturation Curves and Initial Velocity Plots with Respect to Fru-6P . . . . .	51
2.3	Dependence of the BsPFK-catalyzed Reaction Rate on MgATP Concentration . . . . .	56
2.4	MgATP Inhibition of the Mutant GV212 Enzyme . . . . .	58
2.5	AMPPNP Inhibition Patterns . . . . .	63
3.1	Molecular Graphics Image of the Chimeric Subunit . . . . .	80
3.2	Structural Properties of the Chimeric PFK . . . . .	82
3.3	Dependence of PFK Activity on Fru-6P Concentration . . . . .	86
3.4	Dependence of PFK Activity on MgATP Concentration when Fru-6P Concentration is Low (50 $\mu$ M) . . . . .	88
3.5	Effect of PEP and GDP on PFK Activity . . . . .	91
3.6	Protection of (A) Native <i>E. coli</i> PFK and (B) Chimeric PFK Against Thermal Inactivation . . . . .	93
3.7	Effect of AMPPNP on the Fru-6P-Dependent Cooperative Behavior of Chimeric PFK . . . . .	96
3.8	Combined Effects of Fru-6P and AMPPNP on Intrinsic Fluorescence of the Chimeric PFK . . . . .	100

4.1	Reorganization of the 6F Loop (156-162) of <i>B. stearrowthermophilus</i> PFK . . . .	110
4.2	The Amino Acid Sequences of the 6F Loops of <i>B. stearrowthermophilus</i> PFK, <i>E. coli</i> PFK, and the Five Mutant Enzymes . . . .	111
4.3	Fructose 6-phosphate Saturation Curves for <i>B. stearrowthermophilus</i> PFK (○) and <i>E. coli</i> PFK (●) . . . . .	117
4.4	PEP Inhibition of <i>B. stearrowthermophilus</i> PFK (○) and <i>E. coli</i> PFK (●) . . . . .	120
4.5	GDP Activation of <i>E. coli</i> PFK . . . . .	123
4.6	Activation of PEP-Inhibited <i>B. stearrowthermophilus</i> PFK . . . . .	126

## List of Abbreviations and Symbols

- PFK = phosphofructokinase (ATP:  $\beta$ ,D-fructose 6-phosphate 1-phosphotransferase)
- BsPFK = phosphofructokinase from *Bacillus stearothermophilus*
- EcPFK = phosphofructokinase from *Escherichia coli*
- ChiPFK = the chimeric phosphofructokinase
- Bs EQ161 = mutant *B. stearothermophilus* PFK having a glutamine at position 161
- Bs EA161 = mutant *B. stearothermophilus* PFK having an alanine at position 161
- Ec QE161 = mutant *E. coli* PFK having a glutamate at position 161
- Ec QA161 = mutant *E. coli* PFK having an alanine at position 161
- Ec QR161 = mutant *E. coli* PFK having an arginine at position 161
- Fru-6P = fructose 6-phosphate
- PEP = phosphoenolpyruvate
- GDP = guanosine 5'-diphosphate
- Fru-1,6BP = fructose 1,6-bisphosphate
- Ara-5P = Arabinose 5-phosphate
- AMPPCP =  $\beta$ , $\gamma$ -methyleneadenosine 5'-triphosphate
- AMPPNP = adenylymidodiphosphate
- $K_{is}$  and  $K_{ii}$  = equilibrium constants for dissociation of an inhibitor from its inhibitory complex with the enzyme, as determined from slope and intercept replots, respectively
- $K_{act}^{GDP}$  = the equilibrium constant for dissociation of GDP from the effector site, as determined from the GDP activation profile
- $I_{1/2}$  = the half-saturation concentration for an inhibitor
- DTT = dithiothreitol
- SDS-PAGE = sodium dodecylsulfate polyacrylamide gel electrophoresis

X-gal = 5-bromo-4-chloro-3-indoyl- $\beta$ ,D-galactoside

IPTG = isopropyl- $\beta$ ,D-thiogalactoside

MWC = model of allosteric behavior proposed by Monod, Wyman, and Changeux

## Abstract

The fructose 6-phosphate (Fru-6P) saturation curve for phosphofructokinase (PFK) from *E. coli* is sigmoidal in the presence of saturating MgATP levels, while the corresponding curve for *B. stearothermophilus* PFK is essentially hyperbolic. Sigmoidality can be due to apparent cooperativity arising from the kinetic mechanism of an enzyme. We have determined the kinetic mechanism of *B. stearothermophilus* PFK (BsPFK). BsPFK was found to obey a non rapid-equilibrium random mechanism similar to the one *E. coli* PFK (EcPFK) follows. Substrate inhibition by MgATP was observed. We propose that substrates bind to BsPFK through two alternative pathways, one of which is slower. The substrate inhibition arises in part from reaction flux through the slower pathway.

Although EcPFK and BsPFK obey similar kinetic mechanisms, they are inhibited differently by MgATP: EcPFK is profoundly inhibited, BsPFK only weakly. The structural basis for this difference could be closure of the active site *via* a conformational transition that occurs in EcPFK, but not BsPFK. To investigate the importance of this transition for MgATP inhibition of EcPFK, we have constructed a chimeric enzyme (ChiPFK) that contains the "rigid" ATP-binding domain of BsPFK grafted onto the remainder of the EcPFK subunit. Our results indicate that ChiPFK is locked in an "open" structure resembling the activated form of EcPFK. It is insensitive to heterotropic regulation. Nevertheless, ChiPFK exhibits residual cooperativity. Possible explanations for the cooperativity are discussed.

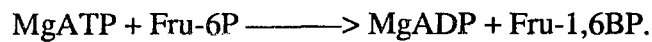
The 6F loop is proposed to be important in PFK allosteric behavior. Residues along the loop are largely conserved between BsPFK and EcPFK, except for 161, which is a glutamate in BsPFK, and a glutamine in EcPFK. Using site-directed mutagenesis, Glu 161 of BsPFK has been changed to glutamine and alanine. Similarly, Gln 161 of

EcPFK has been changed to glutamate, arginine and alanine. Of the five mutants, one, QA161, was particularly interesting. Though activated normally by GDP, it was completely insensitive to PEP inhibition. This indicates that the hydrogen-bonding ability of residue 161 is critical for PEP inhibition of EcPFK, and that GDP activation and PEP inhibition follow different structural pathways.

**Chapter 1**  
**General Introduction**



Phosphofructokinase (PFK, ATP:  $\beta$ -D-fructose 6-phosphate 1-phosphotransferase, EC 2.7.1.11) is a key regulatory enzyme of glycolysis. Positioned near the top of the glycolytic pathway (Fig. 1.1), PFK catalyzes the first committed step of the pathway, the MgATP-dependent phosphorylation of fructose 6-phosphate (Fru-6P) to produce MgADP and fructose 1,6-bisphosphate (Fru-1,6BP):



A divalent  $\text{Mg}^{++}$  ion, as well as a monovalent  $\text{NH}_4^+$  or  $\text{K}^+$  ion, is required for the catalysis. The enzymatic activity of PFK, hence flux through the glycolytic pathway, is regulated by a number of metabolites. In mammalian cells, the regulation is complex, with ATP and citrate serving as inhibitors of the enzyme, and Fru-6P, ADP, AMP and  $\text{P}_i$  as well as fructose 2,6-bisphosphate, serving as activators (see Uyeda, 1979 for a review). In bacteria, however, regulation of PFK is simpler, involving the activator ADP (or GDP) and the inhibitor phosphoenolpyruvate (PEP). Exceptions to this are the PFKs from the bacteria *Lactococcus bulgaricus* and *Spiroplasma citri*, which are regulated by PEP but not ADP (Auzat *et al.*, 1994). ATP also inhibits bacterial PFK, but the potency of the inhibition varies from one bacterial species to another. For example, ATP inhibits *Escherichia coli* PFK strongly at low Fru-6P concentration, but *Bacillus stearothermophilus* PFK only weakly.

The genes for both *E. coli* PFK and *B. stearothermophilus* PFK have been cloned (Hellinga & Evans, 1985; French & Chang, 1987), and the three-dimensional structures of the two enzymes have been determined from X-ray diffraction studies (Shirakihara & Evans, 1988; Evans *et al.*, 1981). The cloning of the genes has made possible not only a deduction of the primary structures (amino acid sequences) of the enzymes, but also high-level expression of the enzymes in PFK-deficient *E. coli* cells (Hellinga & Evans, 1985; French *et al.*, 1987), and site-directed mutagenesis for the

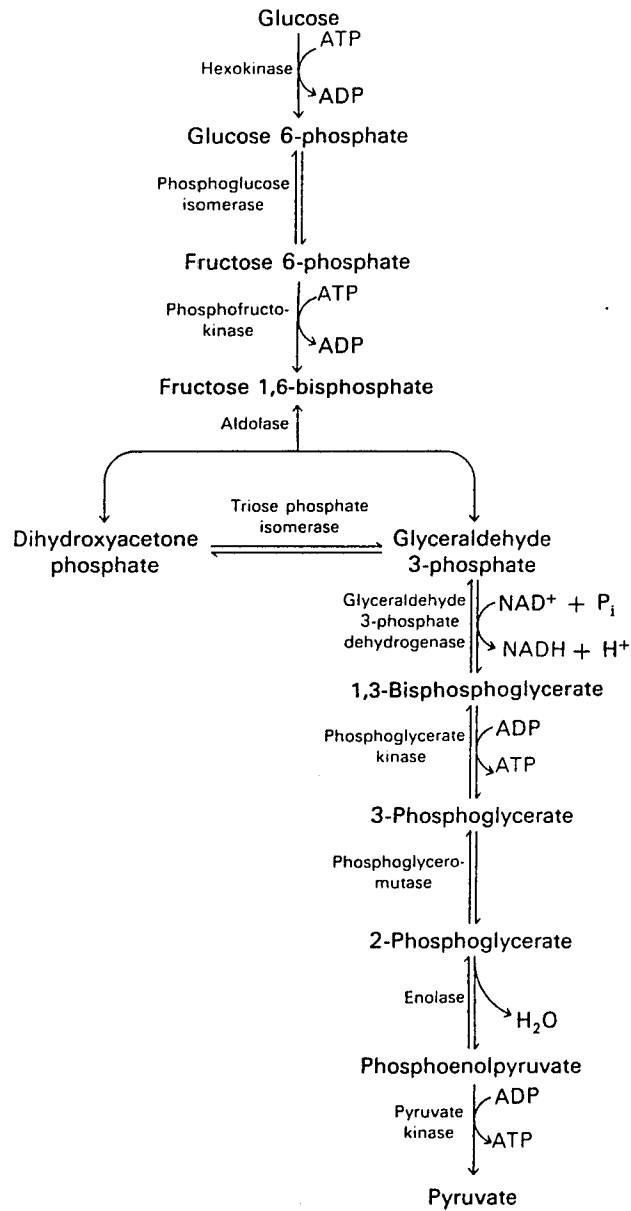


**FIGURE 1.1. The Glycolytic Pathway.** (Taken with permission from Stryer (1988) *Biochemistry*, 3rd. ed., W. H. Freeman and Co., New York. Copyright 1988 W. H. Freeman and Co.).

purpose of structure-function studies. High-level expression has resulted in purer, more homogeneous crystals of *B. stearrowthermophilus* PFK, which has in turn allowed a higher-resolution X-ray structure (Schirmer & Evans, 1990). The availability of high-resolution structures of the proteins has in turn spawned structure-function studies using site-directed mutagenesis and recombinant DNA, which confirm or deny predictions made from the crystal structures. Thus, recombinant DNA technology and site-directed mutagenesis on one hand, and X-ray crystallography on the other, have been used together to unravel the intricacies of PFK catalysis and regulation. Furthermore, the combination of site-directed mutagenesis, recombinant DNA methods, and X-ray crystallography with classical enzymology and ligand binding studies allows one to undertake a very comprehensive study of the structure and function of PFK, and indeed any regulatory enzyme.

### **Bacterial PFK Structure**

The primary structures of *E. coli* PFK (EcPFK) and *B. stearrowthermophilus* PFK (BsPFK) are shown in Fig. 1.2. These structures were deduced from the nucleotide sequences of their genes (Hellings & Evans, 1985; French & Chang, 1987), but a partial amino acid sequence of BsPFK had been determined some time earlier (Kolb *et al.*, 1980) from an analysis of cyanogen bromide and other peptic fragments. Examination of the two sequences in Fig. 1.2 reveals that EcPFK and BsPFK share 55% amino acid identity. Moreover, a comparison among the amino acids that bind substrates in the active site (Table 1.1) and effectors in the regulatory site (Table 1.2) of the two enzymes shows that most of the residues are either identical or conserved between the two. This close homology between EcPFK and BsPFK is in contrast to the complete lack of homology observed between EcPFK and the non-allosteric PFK from *E. coli* (the two are designated PFK 1 and PFK 2, respectively), whose gene has also been cloned and sequenced (Daldal, 1984). (PFK 2 accounts for about 10% of the total PFK activity in wild-type *E. coli* cells). The PFK 2 enzyme has been purified and studied in terms of

1	10	20	30	40
<i>E. coli</i>	MIKKIGVLTSGGDAPGMNAAIRGVVRSALTEGLEVMGIYDGYLGLYED RM			
<i>B. st</i>	<u>MKRIGVLTSGGDS</u> <u>PGMNAAIRSVVRKAIYHG</u> <u>VEVYGVYHGYAGLIAG NI</u>			
	$\beta$ -A	$\alpha$ -1	$\beta$ -B	$\alpha$ -2
50	60	70	80	90
	VQLDRYSVSDMINRGGTFLGSRPFPEFRD ENIRAVAIENLKKRGIDALVV			
	<u>KKLEVGDVGDIIHRGGTILYTARCP</u> <u>EFKT</u> <u>EEGOKKGI</u> <u>EGLK</u> <u>KHGIEGLVV</u>			
	$\beta$ -C	$3_{10}$ -4A	$\alpha$ -4	$\beta$ -D
100	110	120	130	140
	IGGDGSYMGAMRLTEMGFPCIGLPGTIDNDIKGTDYTIGFF TALSTVVEA			
	<u>IGGDGSYOGAKK</u> <u>LTEHGF</u> <u>CPVGP</u> <u>TIDNDIP</u> <u>GTDF</u> <u>TIGF</u> <u>D TALNTVIDA</u>			
	$\alpha$ -5	$\beta$ -E		$\alpha$ -6
150	160	170	180	190
	IDRLRDTSSSHQORISVVEVMGRYCGDLTLAAAIAGGCEFVVVPEVEFSRE			
	<u>IDKIRD</u> <u>TATSHERTYVIEVMGRHAGDIAL</u> <u>WSGLAGGAETIL</u> <u>IPEADYDMN</u>			
	$\beta$ -F	$\alpha$ -7	$\beta$ -G	
200	210	220	230	240
	DLVNEIKAGIAKGGKHAIVAITEHMCVDDELAHFIEKETGRETRATVL GH			
	<u>DVIARL</u> <u>KRGHERG</u> <u>KKHSII</u> <u>IIVAE</u> <u>GVG</u> <u>SGVDF</u> <u>GR</u> <u>IOEAT</u> <u>GF</u> <u>ETRV</u> <u>TVL GH</u>			
	$\alpha$ -8	$\beta$ -H	$\alpha$ -9	$\beta$ -I
250	260	270	280	290
	IQRGGSPVPYDRILASRMGAYAIIDLLAGYGGRCVGIQNEQLVHHD IIDA			
	<u>VORGGSP</u> <u>TAFDRV</u> <u>LASRLGAR</u> <u>AVELL</u> <u>LEGK</u> <u>GGRCV</u> <u>GIQNN</u> <u>QLVD</u> <u>HD</u> <u>IAEA</u>			
$3_{10}$ -10	$\alpha$ -11	$\beta$ -J	$\beta$ -K	$\alpha$ -12
300	310	320		
	IENMKRPFKGDWLDCAKKLY			
	<u>LA-NKHT</u> <u>IDORMYAL</u> <u>SKELSI</u>			
	$\alpha$ -13			

**FIGURE 1.2.** Sequences of the PFKs from *E. coli* and *B. stearothermophilus*. The residues of EcPFK are numbered from 0 to 319, while those of BsPFK are from 1 to 320. Residues identical between the two are *bolded*. A gap at position 302 of BsPFK allows alignment of the C-termini. Positions  $\alpha$ -helices and  $\beta$ -strands are indicated by *horizontal lines*. Corrections of the BsPFK sequence due to French & Chang (1987) are in *italics*.

**TABLE 1.1**  
*Active Site Residues*

A. Fru-1,6BP Binding.

Residue No.	Ec	Bs	Interactions
125	Thr	Thr	H bond to 1-phosphate
127	Asp	Asp	Catalytic residue, H bond to O(3)
129	Asp	Asp	Binds water attached to Mg <sup>++</sup>
162*	Arg	Arg	Binds 6-phosphate
169	Met	Met	Hydrophobic contact to O(2), O(3)
170	Gly	Gly	Main-chain H bond to O(3)
171	Arg	Arg	Near 1-phosphate
222	Glu	Glu	H bond to O(4)
243*	Arg	Arg	Binds 6-phosphate
249	His	His	Binds 6-phosphate
252	Arg	Arg	H bond to 6-phosphate and O(2)

B. ADP Binding.

Residue No.	Ec	Bs	Interactions
11	Gly	Gly	Main-chain amide H bond to $\beta$ -P
41	Tyr	Tyr	Contact with ribose
72	Arg	Arg	Bridges ADP $\alpha$ P and Fru-1,6BP P's
73	Phe	<u>Cys</u>	Main-chain bonds to ribose OH
77	Arg	<u>Lys</u>	Hydrophobic contact with adenine
103	Asp	Asp	Binds to Mg <sup>++</sup>
104	Gly	Gly	Main-chain amide bond to $\beta$ -P
105	Ser	Ser	H bonds to $\beta$ -P from OH and NH
107	Met	<u>Gln</u>	Hydrophobic contact with adenine
108	Gly	Gly	Contacts adenine

Ec, *E. coli* PFK; Bs, *B. stearothermophilus* PFK. Residues indicated are those that interact with products because the crystal structure was determined with products in the active site. \*, from another subunit. *Underlined* residues are different between Ec and Bs. (From Shirakihara, Y., & Evans, P. R. (1988) *J. Mol. Biol.* 204, 973-994).

**TABLE 1.2**  
*Effector Site Residues*

ADP Binding.

Residue No.	Ec	Bs	Interactions
21*	Arg	Arg	H bond to $\beta$ -P and $Mg^{++}$ via water
25*	Arg	Arg	H bond to $\beta$ -phosphate
54*	Arg	<u>Val</u>	H bond to $\alpha$ -P and C terminus
55*	Tyr	<u>Gly</u>	Stacks against adenine ring
58*	Ser	<u>Gly</u>	H bond to 1-P and Arg 25
59*	Asp	Asp	Main chain to $\beta$ -P, bond to $O_{(3)}$
154	Arg	Arg	Two H bonds to $\beta$ -P
185	Gly	Gly	Main chain carbonyl bond to $Mg^{++}$
187	Glu	Glu	Carboxyl binds to $Mg^{++}$
211	Lys	Arg	Alternative to Arg 54
213	Lys	Lys	H bond to C-terminus and Glu 187
214	Lys	Lys	Main chain amide H bond to $O_{(4)}$
215	His	His	Bond to $Mg^{++}$ via water
C terminus	Tyr	<u>Ile</u>	H bond to Arg 54 in <i>E. coli</i>

Ec, *E. coli*; Bs, *B. stearothermophilus*. The effector site is formed between the two subunits of the rigid PFK dimer. The *asterisks* indicate residues from one of the two subunits. Note that Arg 54 of *E. coli* PFK is replaced by Arg 211 in *B. stearothermophilus* PFK. (From Shirakihara, Y., & Evans, P. R. (1988) *J. Mol. Biol.* 204, 973-994).

its enzymology (Babul, 1978), its regulation by ATP (Kotlarz & Buc, 1981; Guixe & Buc, 1985), its dimer-tetramer equilibrium (Kotlarz & Buc, 1989), its kinetic mechanism (Campos *et al*, 1984), and its possible physiological function (Daldal *et al.*, 1982; Daldal & Fraenkel, 1983; Torres & Babul, 1991). Because of its apparent unrelatedness to EcPFK and BsPFK, however, PFK 2 will not be discussed further.

Both BsPFK and EcPFK are tetramers of four identical subunits, each composed of 319 amino acids (320 for BsPFK). The subunit molecular mass is  $35,000 \pm 1,000$  daltons. The subunit structures of the two enzymes are remarkably similar: they share the same secondary structural elements, and their  $\alpha$ -carbon traces are nearly superimposable. Fig. 1.3 is a schematic representation of the bacterial PFK tetramer. Each subunit has two domains, a large one and a small one. The catalytic site is located within the cleft formed between the two domains: it binds the substrates Fru-6P and ATP, as well as the essential  $Mg^{++}$  ion. (The binding site of the  $NH_4^+$  ion has not been located yet). Movement of the two domains relative to each other in EcPFK allows the active site to open and close, a process that is important for catalysis (Evans, 1992) and may be important for allosteric regulation as well. Three of the residues important for catalysis (see Table 1.1) lie on a polypeptide loop (residues 125 to 129) connecting the two domains. All of the residues that bind ATP are from the large domain, while those that bind Fru-6P are from the small domain, but include two residues, Arg 162 and Arg 243, from across the dimer-dimer interface. As will be shown below, Arg 162 is directly involved in the allosteric transition.

The bacterial PFK tetramer can be thought of as a dimer of rigid dimers A:B and C:D (Fig. 1.3). The A-B and C-D interfaces (there are two in the tetramer) are called regulatory interfaces because they form the four effector sites. The A:B-C:D dimer-dimer interface is called the active interface because it forms part of the four Fru-6P sites. The regulatory interface has more contact area than the active interface (about twice as much), so it is considerably more stable. Subunit A has no contact with subunit

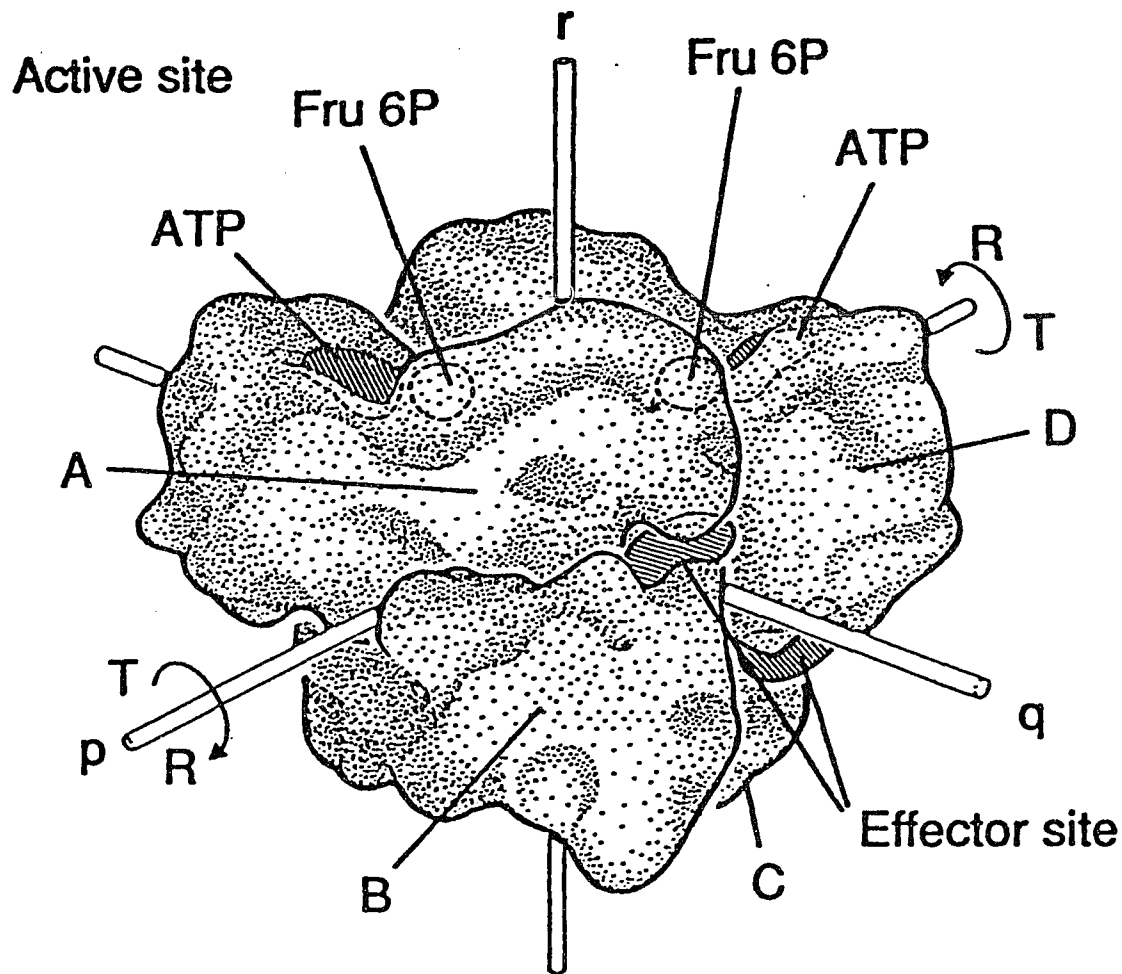
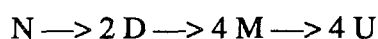


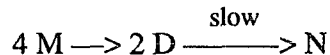
**FIGURE 1.3. The Bacterial PFK Tetramer.** The A, B, C, and D subunits are indicated, as are the locations of the ATP and Fru-6P sites, and the effector sites. r, p, and q are the axes of symmetry. The directions of rotation in the T → R and R → T transitions are indicated. (Taken with permission from Evans, P. R. (1992) *Proc. Robert A. Welch Found. Conf. on Chem. Res. XXXVI. Regulation of Proteins by Ligands*, pp. 39-54).



C; likewise B has no contact with D. J.-R. Garel and co-workers have studied the dissociation (Le Bras *et al.*, 1989; Deville-Bonne *et al.*, 1989) and re-association (Martel & Garel, 1984; Teschner & Garel, 1989) of EcPFK in the chaotropic agents potassium thiocyanate, guanidinium hydrochloride, and urea. The protein is found to dissociate in an ordered, stepwise, and reversible manner according to the following scheme



where N represents native EcPFK, D a dimeric species, M a monomeric species, and U the unfolded monomer. Reassociation proceeds by the reverse scheme



involving two bimolecular events, the second of which is the slower, rate-limiting step. The species "D" was shown to be the regulatory dimer (A:B or C:D above) since its disappearance or appearance was correlated with the enhancement or quenching, respectively, of the intrinsic fluorescence of a unique tryptophan (Trp 311) that is situated along the regulatory interface. Saturating levels of Fru-6P were found to retard dissociation of the native tetramer into dimers, presumably because interactions of Fru-6P with Arg 162 and Arg 243 across the active interface serve to "cross-link" the dimers together. The strength of the interaction is so strong, in fact, that the pathway of urea-induced dissociation is modified, causing the regulatory interface to become distorted first. The weakened tetramer then falls apart into monomers in an all-or-none process (Teschner *et al.*, 1990). Fru-6P also prevents inactivation and dissociation of a proteolyzed EcPFK tetramer which is not stable in its absence (Le Bras & Garel, 1985). It is interesting that several features of bacterial PFK geometry, i.e., that the tetramer is a dimer of dimers having two kinds of interfaces (regulatory and active) and that Fru-6P interacts with residues across the active interface, have been predicted by these dissociation/reassociation studies independent of other structural data.

The tetramer of the PFK from rabbit muscle is about twice the size of the bacterial one (subunit molecular masses are 82,000 *versus* 35,000 daltons), and its N- and C-halves show clear homology to BsPFK and to each other (Poorman *et al.*, 1984; Lee *et al.*, 1987). Because of this, Poorman *et al.* (1984) have proposed that eucaryotic PFK arose from a procaryotic progenitor by series gene duplication and divergence. Furthermore, because the N-half of rabbit muscle PFK has a higher homology to BsPFK than does the C-half, and because it has key catalytic residues that the C-half does not have, Poorman *et al.* (1984) have suggested that the N-half contains the catalytic site, while the C-half contains the regulatory site(s). Alignment of amino acid sequences based on the Poorman model has been used as a guide for site-directed mutagenesis of rabbit muscle PFK cDNA (Li *et al.*, 1993), which has been cloned and sequenced (Li *et al.*, 1990).

### **The Active Site and Catalysis**

X-ray diffraction studies have identified the amino acid residues that bind ATP and Fru-6P in the active sites of EcPFK and BsPFK (Evans *et al.*, 1981; Shirakihara & Evans, 1988). These are listed in Table 1.1. As can be seen from the table, all of the residues that bind Fru-6P are the same between EcPFK and BsPFK, while those that bind ATP are almost all the same. Those that are different are Phe 73 (Cys in BsPFK), Arg 77 (Lys), and Met 107 (Gln). These differences are probably not significant since residue 73 interacts with the ribose hydroxyl group *via* its main chain amide and carbonyl groups, Lys is similar to Arg, and residue 107 interacts with the adenine ring of ATP by hydrophobic contact. The strict conservation of active site residues between EcPFK and BsPFK is surprising given their very different responses to Fru-6P when the MgATP level is high: sigmoidal for EcPFK *versus* hyperbolic for BsPFK.

Two different kinds of studies have been done to determine the reaction mechanism of PFK, i.e., the manner in which the phosphoryl group is transferred from ATP to Fru-6P in the PFK-catalyzed reaction. First, <sup>31</sup>P-NMR has been used to

determine the stereochemical course of phosphoryl transfer in both the BsPFK- and rabbit muscle PFK-catalyzed reactions. It was found that the transfer involves an inversion of configuration at the phosphorous atom of the transferred phosphoryl group, which is indicative of an in-line nucleophilic attack of the 1-hydroxyl group of Fru-6P on the  $\gamma$ -phosphate of ATP (Jarvest *et al.*, 1981). Second, site-directed mutagenesis has identified Asp 127, which is conserved among all known PFKs, as the key catalytic residue (Hellinga & Evans, 1987). When Asp 127 was mutated to Ser in EcPFK, the catalytic rate constant  $k_{cat}$  dropped 18,000-fold for the forward reaction, and 3,100-fold for the reverse reaction, indicating that Asp 127 is critical for catalysis. From these results, and from the proximity of Asp 127 to the attacking 1-hydroxyl of Fru-6P, Hellinga & Evans (1987) have proposed that it acts as the general base to increase the nucleophilicity of the Fru-6P 1-hydroxyl group. Studies of the pH-dependence of EcPFK activity have confirmed the important role of Asp 127 in catalysis, and have suggested a secondary role for Asp 129 (Auzat & Garel, 1992; Laine *et al.*, 1992).

Site-directed mutagenesis in conjunction with X-ray crystallography has identified the residues important for stabilizing the EcPFK transition state and coordinating the  $Mg^{++}$  ion in the active site. Fig. 1.4 depicts the pentacoordinate transition state complex proposed by Berger & Evans (1992). Residues important for stabilizing the transition state include Arg 72, Thr 125, and possibly Gly 11. Arg 72 is proposed to help neutralize the negative charge of the transferring phosphate. Mutation of Arg 72 to His changes the pH-dependence of enzyme activity (Zheng & Kemp, 1994) and lowers the  $k_{cat}$  100-fold. This result indicates that Arg 72 plays a role in catalysis; it also suggests that phosphoryl transfer is associative rather than dissociative since an associative mechanism would be helped by a positive charge in the vicinity, while a dissociative mechanism would be hindered. An interaction with Thr 125 is also proposed to help stabilize the transition state since mutation of Thr 125 to Ala decreases  $k_{cat}$  900-fold in the forward reaction, and 3,200-fold in the reverse reaction (Berger &

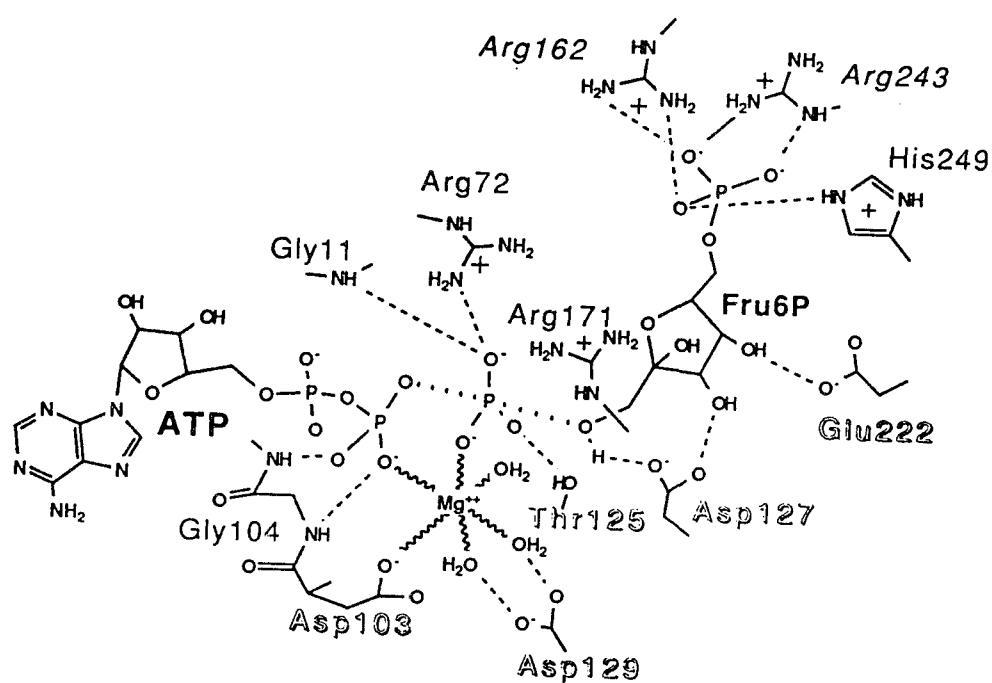


**FIGURE 1.4. The Proposed Transition State of *E. coli* PFK.** Residues Arg 162 and Arg 243 are from an adjacent subunit. (Taken with permission from Berger, S. A., and Evans, P. R. (1992) *Biochemistry* 31, 9237-9242. Copyright 1992 American Chemical Society).

Evans, 1992). Thr 125 also interacts with the neutral oxygen of the  $\gamma$ -phosphate of ATP before transfer (Auzat *et al.*, 1994a). Gly 11, which is proposed to hydrogen-bond to an oxygen of the transferred phosphoryl group *via* its main chain amide group (Fig. 1.4), has not yet been mutated and studied. Finally, site-directed mutagenesis has identified residues Asp 103 and Asp 129 as important for catalysis; they are involved in coordination of the essential  $Mg^{++}$  ion (Berger & Evans, 1992). A list of the residues involved in catalysis and their roles is presented in Table 1.3.

### **The Kinetic Mechanism**

The kinetic mechanism of an enzyme is a description of the way that substrates bind to and products are released from the active site before and after catalysis. The kinetic mechanism of several PFKs including rabbit muscle PFK (Bar-Tana & Cleland, 1974a,b), *Ascaris suum* PFK (Rao *et al.*, 1987), *E. coli* PFK (Deville-Bonne *et al.*, 1991b), and a non-allosteric PFK from *Lactobacillus plantarum* (Simon & Hofer, 1978) as well as others, *e.g.*, PFKs from heart and liver, the PFK from *Dictyostelium discoideum*, and *E. coli* PFK 2, have been determined. Generally, the methodology used to determine the kinetic mechanism of an enzyme is the one formulated by W. W. Cleland (1963, 1979). The method involves constructing double-reciprocal plots for initial velocity studies, as well as product and dead-end (non-reactive substrate analog) inhibition studies. The patterns of lines obtained identify the kinetic mechanism, and fitting the data to the appropriate initial velocity equations generates a set of parameters that quantitatively describe the kinetic mechanism.

Initial velocity plots are double-reciprocal plots of data obtained by varying the concentration of one substrate while keeping the concentration of the other constant at different fixed levels near the  $K_m$  value. Two families of double-reciprocal lines are obtained for a bi-substrate reaction: one family for each substrate. Convergence of both families of lines indicates that the kinetic mechanism is sequential, meaning that both substrates must bind to the enzyme before catalysis can occur. If one family of lines

**TABLE 1.3**  
*Residues Important for Catalysis*

<b>Residue</b>	<b>Mutation</b>	<b>Fold Drop in <math>k_{cat}</math></b>	<b>Function</b>
Asp 127	—>Ser	18,000	general base
Asp 129	—>Ser	960	binds $Mg^{++}$
Thr 125	—>Ala	890	binds $\gamma$ -phosphate
Arg 72	—>His	100	binds $\gamma$ -phosphate
Asp 103	—>Ala	28	binds $Mg^{++}$
Arg 171	—>Ser	3	binds Fru-1,6BP 1-P

does not converge, but the lines are parallel, then the mechanism is ping-pong, meaning that one substrate binds and is released before the second binds. Actually, PFK must necessarily follow a sequential rather than a ping-pong kinetic mechanism because the reaction mechanism of PFK involves in-line nucleophilic attack, not a phosphoenzyme intermediate that would be formed if a ping-pong mechanism were involved. It comes as no surprise, then, that the kinetic mechanisms of all the PFKs mentioned above are proposed to be sequential.

However, differences are present among the PFKs listed above in terms of whether the kinetic mechanism is ordered or random, whether rapid-equilibrium or steady-state. The patterns of lines obtained from product and dead-end inhibition plots generally establish whether the mechanism is random or ordered: if random, the plots will converge; if ordered, one of the inhibition plots with respect to the substrate that binds first will contain parallel lines. If the substrates do not bind in rapid-equilibrium, *i.e.*, if their binding and/or release is slow relative to catalysis, then initial velocity and inhibition plots will have curved lines. However, the degree of curvature may be small; under these conditions, the curvature may not be evident and lines that would normally converge may appear to be parallel. This was the case for rabbit muscle PFK (Bar-Tana & Cleland, 1974a,b).

By application of the methodology outlined above, Bar-Tana & Cleland (1974a,b) established that the kinetic mechanism of rabbit muscle PFK involves sequential, random, non-rapid equilibrium binding of substrates Fru-6P and ATP. Rao *et al.* (1987) found that the mechanism of *A. suum* PFK is predominantly steady-state ordered with MgATP binding first to the enzyme, but there exists some degree of randomness, *i.e.*, Fru-6P can bind first to a small extent. The kinetic mechanism of *E. coli* PFK, like that of rabbit muscle PFK, is steady-state random (Deville-Bonne *et al.*, 1991b; Johnson & Reinhart, 1992; Zheng & Kemp, 1992), while the kinetic mechanism of the PFK from *L. plantarum* is proposed to be ordered with Fru-6P binding first, but a

random mechanism is not ruled out (Simon & Hofer, 1978). All but the last of these four PFKs are allosteric. Therefore, determination of their kinetic mechanisms is complicated by their cooperative behavior. It is of interest to unequivocally determine the kinetic mechanism of PFK. As stated by Uyeda (1978): "The final determination of the [kinetic] mechanism may come from the use of non-allosteric PFK." *B.*

*Stearothermophilus* PFK is non-allosteric in the absence of inhibitor PEP. Thus, it is a good candidate for finally laying to rest the kinetic mechanism of PFK.

### **The Open-to-Closed Conformational Change of *E. coli* PFK**

The crystal structure of the EcPFK tetramer complexed with its reaction products MgADP and Fru-1,6BP (Shirakihara & Evans, 1988) was found to contain an asymmetrical unit composed of two subunits: one "open", the other "closed." Superimposition of the  $\alpha$ -carbon traces of the open and closed subunits reveals that they have substantially different conformations in the outer helical layer of their large domains, around the ATP-binding site (Fig. 1.5). The regions that are different include residues 41 to 49 (helix 2), 71 to 95 (helices 4a and 4), and 101 to 118 (helix 5) of the large domain. In addition, residues 303 to 309 near the C-terminal end appear to be in different positions in the open *versus* closed subunit structures. Presumably, an open-to-closed conformational change can occur within the EcPFK subunit. One effect of the conformational change is closure of the active site, which brings the two substrates Fru-6P and MgATP, which are too far apart in the open structure, closer together so that reaction can occur (Evans, 1992). The closing and opening of the active site is postulated to be an integral part of the catalytic cycle, as shown in Fig. 1.6. Substrates bind to the open subunit, it closes, phosphoryl transfer takes place, products are formed, the subunit opens, and products are released.

Evans (1992) does not attribute any allosteric significance to the open-to-closed conformational change. Nevertheless, it may be important for the mechanism by which ATP "allosterically" inhibits EcPFK, and Fru-6P overcomes that inhibition (discussed in





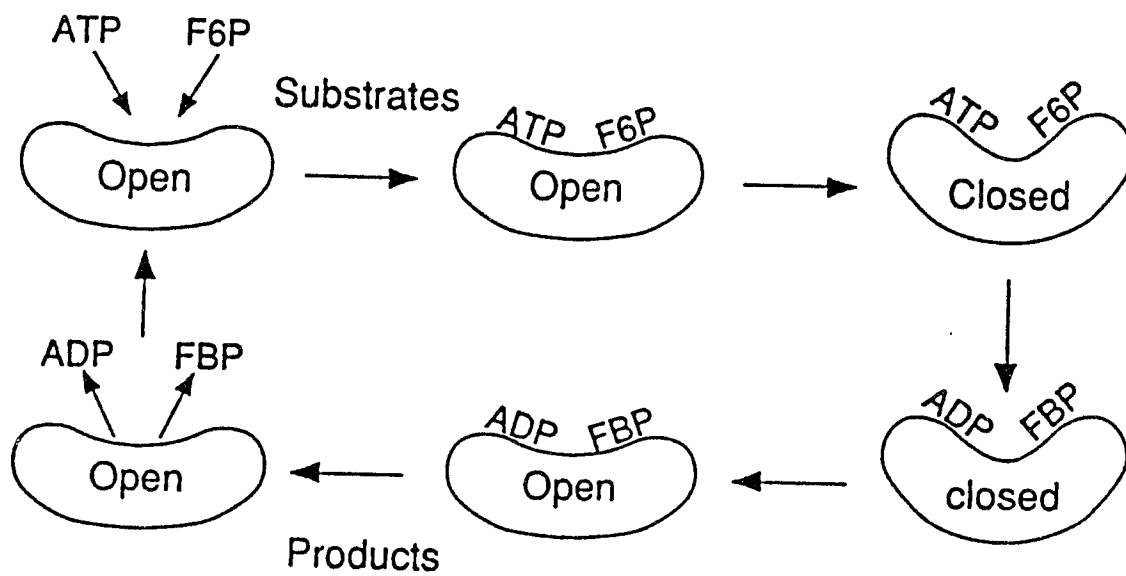


**FIGURE 1.6. The Proposed Reaction Cycle of *E. coli* PFK.** (Taken with permission from Evans, P. R. (1992) *Proc. Robert A. Welch Found. Conf. on Chem. Res.* XXXVI. *Regulation of Proteins by Ligands*, pp. 39-54).

more detail below). It may also be involved in GDP activation of the ATP-inhibited enzyme. Garel and co-workers have identified a region near the C-terminus of EcPFK that acts as a "built-in" effector; its removal by proteolysis makes the enzyme dependent upon Fru-6P for stability, and destroys the sensitivity of the enzyme to allosteric effectors PEP and GDP (Le Bras & Garel, 1982; Le Bras & Garel, 1986). Removal of this C-terminal region also causes the cooperativity of the enzyme with respect to Fru-6P to drop two-fold (the Hill number falls from 4.0 to 2.0). The position of the proposed built-in effector has been localized to a stretch of 30 amino acid residues (between 280 and 310) near the C-terminal end (Serre & Garel, 1990). An examination of Fig. 1.5 shows that the residues at the C-terminus that move during the open-to-closed transition are squarely within this 30-amino acid region. Furthermore, the loop between  $\beta$ -strands J and K (the J-K loop) which is found to move between the unliganded (Rypniewski & Evans, 1989) and open liganded (Shirakihara & Evans, 1988) forms of the EcPFK subunit, is also within the region identified by Serre & Garel (1990). Rypniewski & Evans (1989) have shown that the J-K loop of EcPFK moves toward the catalytic loop composed of residues 125 to 138 as the subunits go from unliganded to substrate-liganded structures. Specific hydrogen bonds are formed between residues in the J-K loop and those in the catalytic loop, and others hydrogen bonds are broken, during this process. The importance of the C-terminal "effector" region (residues 280 to 310) for EcPFK allosteric behavior can be explored using site-directed mutagenesis, and also by constructing chimeric Bs/Ec PFKs (see chapter five).

X-ray crystallography shows that, unlike EcPFK, the large (ATP-binding) domain of BsPFK remains rigid during the allosteric transition of the enzyme (Schirmer & Evans, 1990). There is no evidence that the BsPFK subunit undergoes an open-to-closed conformational change. The lack of this conformational change in BsPFK, along with the corresponding lack of allosteric inhibition of BsPFK by MgATP suggests that

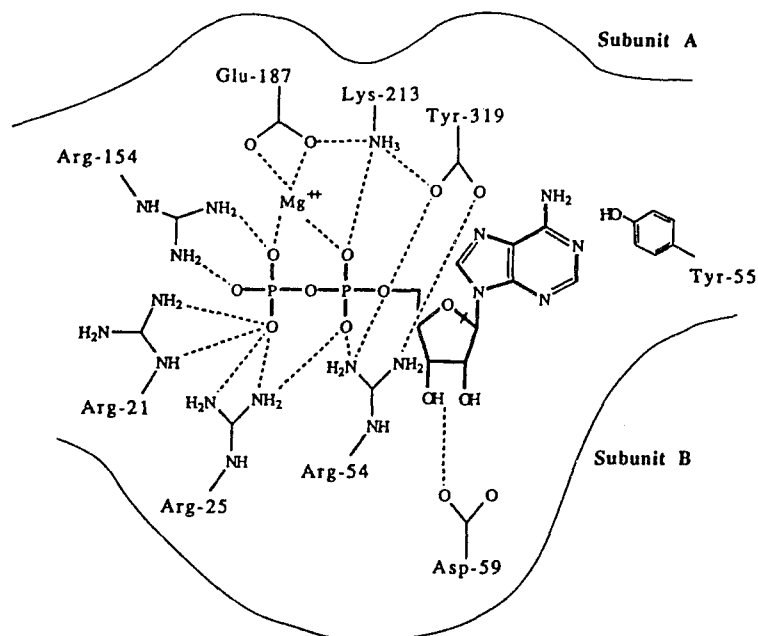
the two phenomena—the conformational change and inhibition—may be associated in EcPFK.

### The Effector Site

The effector sites of EcPFK and BsPFK lie in deep clefts between subunits related by the molecular p axis, *i.e.*, between subunits of the rigid dimer (Fig. 1.3). The effector site residues that bind the activator MgADP and the inhibitor PEP have been identified by X-ray crystallography (Evans *et al.*, 1981; Shirakihara & Evans, 1988). As can be seen from Table 1.2, half of the residues in the site are contributed by one subunit of the rigid dimer; the other half by the other subunit. Schematic diagrams of the effector site of EcPFK with MgADP bound, as well as with PEP bound, are shown in Figs. 1.7A and 1.7B, respectively. Using site-directed mutagenesis, several effector site mutants have been created, and analyzed for their ability to bind GDP and PEP. Truncation of each of the positively-charged residues Arg 21, Arg 25, Arg 54, Arg 154, and Lys 213 to Ala in EcPFK weakens the binding of both MgGDP and PEP by 2 to 3 kcal/mole, a result consistent with the disruption of charged hydrogen bonds important for effector binding (Lau & Fersht, 1989). Mutation of Tyr 55 to Gly has no effect on the  $K_T(\text{PEP})$  and only a small effect on  $K_R(\text{GDP})$ , indicating that the proposed hydrophobic interaction between residue 55 and the purine ring of ADP or GDP is not critical (Lau *et al.*, 1987). Thus, the key interactions for effector binding appear to be with the phosphates of GDP (or ADP), or the phosphate and carbonyl of PEP, as indicated in Fig 1.7.

In BsPFK, Arg 211 replaces Arg 54, and residue 54 is a valine in BsPFK (Table 1.2). Valdez *et al.* (1988) have mutated Arg 25, Asp 59 and Arg 211 in BsPFK. As expected, both arginine residues were found to be important for effector binding. Asp 59, on the other hand, was found not to be essential, probably because its interaction with effector is *via* its main-chain amide and carbonyl groups. Interestingly, the Arg 25

A



B

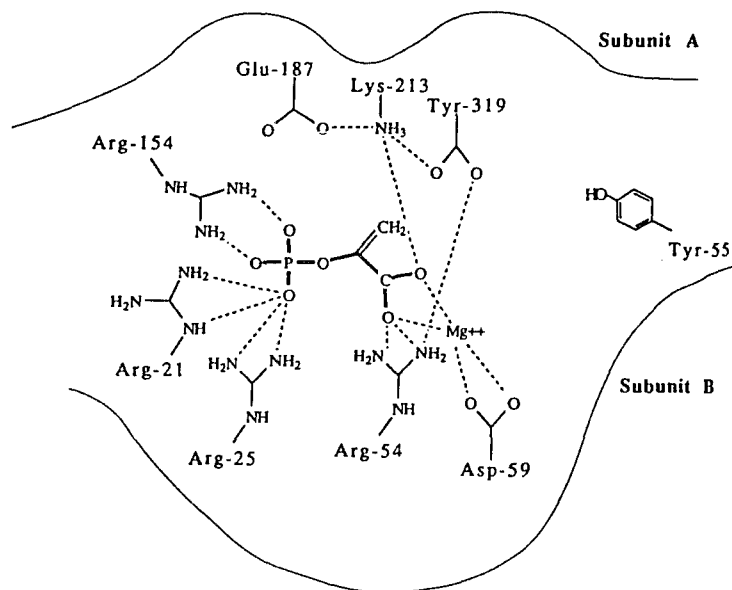


**FIGURE 1.7. The Effector Site of *E. coli* PFK.** Proposed structure of the effector site with (A) ADP, and (B) PEP bound. Subunits A and B are the subunits of the rigid dimer. (Taken with permission from Lau, F. T., & Fersht, A. R. (1989) *Biochemistry* 28, 6841-6847. Copyright 1989 American Chemical Society).

—> Ala mutant had a two-fold higher  $S_{1/2}^{\text{Fru-6P}}$  value, and exhibited sigmoidality ( $n=2.0$ ). Thus, a mutation at the effector site can affect the active site.

Glu 187 in another residue at the effector site whose mutation affects the active site. Glu 187 is proposed to help coordinate the  $\text{Mg}^{++}$  ion essential for GDP (or ADP) binding. Its mutation to Ala causes PEP to activate the enzyme rather than inhibit it (Lau & Fersht, 1987). The mutation also affects the homotropic interactions of Fru-6P binding. At low Fru-6P concentration, the mutant enzyme is more than 100-fold more active than wild-type in the presence of 10 mM PEP, and the cooperativity with respect to Fru-6P drops from 3.7 to 1.1. Auzat *et al.* (1994b) have found that the mutation Glu 187 —> Asp destroys PEP inhibition, but not GDP activation, at pH 8.2. However, mutation of Glu 187 to Leu destroys both inhibition and activation. Thus, the function of Glu 187 is to discriminate between PEP and GDP binding in the effector site.

#### **PFK and the Allosteric Model of Monod, Wyman and Changeux**

Bacterial PFK is allosterically inhibited by PEP and activated by ADP (or GDP). In addition, the substrate MgATP apparently "allosterically" inhibits *E. coli* PFK when Fru-6P concentrations are low, causing the Fru-6P saturation curve to be highly sigmoidal in the presence of a saturating concentration of MgATP. (MgATP does not inhibit *B. stearothermophilus* PFK by the same mechanism. The Fru-6P saturation kinetics of BsPFK are essentially hyperbolic). The word "allosteric" refers to an effect on the binding of a ligand that results from the binding of the same or another ligand at a distinct, specific site (Monod *et al.*, 1965). An allosteric interaction can be either homotropic or heterotropic. It is homotropic when between identical ligands, heterotropic when between different ligands. According to these definitions, the positive cooperativity observed in the Fru-6P saturation curve of EcPFK would be the result of homotropic allosteric interactions between Fru-6P molecules binding to distinct sites on the protein. On the other hand, the effects of PEP and GDP in decreasing and

increasing, respectively, the cooperativity of Fru-6P binding would be due to heterotropic allosteric interactions between the effectors and Fru-6P.

*E. coli* PFK was one of the first enzymes shown to obey the concerted model of Monod, Wyman, and Changeux (the MWC model; 1965). Many of the regulatory and structural properties of the enzyme have since been interpreted in terms of the model. Therefore, it is useful to present its basic tenets and show how it has been applied to EcPFK (Blangy *et al.*, 1968). The MWC model is simple and elegant; it assumes that a symmetry of allosteric effects due to ligand binding is correlated to protein molecular symmetry. A number of regulatory enzymes besides PFK, including *E. coli* aspartate transcarbamylase (Kantrowitz & Lipscomb, 1988) and rabbit muscle glycogen phosphorylase (Barford & Johnson, 1989), obey the MWC model.

Paraphrasing Monod *et al.*(1965), the MWC model makes the following statements: (1) the protomers (subunits) of oligomeric allosteric proteins are symmetrically arranged relative to an axis of symmetry, (2) the distinct ligand binding sites (one per protomer) are also symmetrically arranged, (3) the conformation of one protomer is constrained by its association with the others, *i.e.*, protomers are allosterically-linked, (4) the allosteric oligomer can reversibly exist in two (at least) conformational states, (5) because of this, the affinity of the binding site for its ligand is altered when a transition occurs from one state to the other, and (6) molecular symmetry is conserved in the allosteric transition.

Suppose F is a ligand with differential affinity toward two states of the oligomer. In the absence of F, the oligomer is in equilibrium between the two states  $R_0$  and  $T_0$ ; the equilibrium constant for the  $R_0 \longleftrightarrow T_0$  transition is L, the "allosteric constant" ( $L = T_0/R_0$ ). We define  $K_R$  and  $K_T$  as the microscopic dissociation constants for ligand F from a specific binding site in the R and T states, respectively. After writing equilibrium equations for the binding of F to the R and T states, the following

expression, which describes the fraction of sites on the oligomer actually occupied by ligand F, *i.e.*, the "saturation function"  $Y_F$ , can be written:

$$Y_F = \frac{Lc\alpha(1+c\alpha)^{n-1} + \alpha(1+\alpha)^{n-1}}{L(1+c\alpha)^n + (1+\alpha)^n} \quad (\text{eqn. 1})$$

where  $L = T_O/R_O$  is the allosteric constant;  $c = K_R/K_T$  is the non-exclusive binding constant, a measure of the affinity of ligand F for the R state *versus* the T state;  $\alpha = F/K_R$  is the normalized concentration of ligand F; and  $n$  is the number of homologous binding sites on the protein for F. Equation 1 describes homotropic interactions among ligands F. The cooperativity of the response of the oligomer to F depends on the values of  $L$  and  $c$ . Cooperativity is pronounced when  $L$  is large, *i.e.*, when  $T_O$  is strongly favored in the  $R_O \rightleftharpoons T_O$  equilibrium, and when  $c$  is small. When  $c$  is very small, as is proposed to be the case for EcPFK (Blangy *et al.*, 1968), the saturation function reduces to

$$Y_F = \frac{\alpha(1+\alpha)^{n-1}}{L + (1+\alpha)^n} \quad (\text{eqn. 2})$$

When the ligand F has no preference for either the T or the R state, *i.e.*, when  $c = 1$ , and  $L$  is small, the equation reduces to  $Y_F = F/(K_R + F)$ , which is the Michaelis-Menten equation.

The MWC model also describes heterotropic interactions between different ligands. Assume that a substrate S has significant affinity for its binding site in only one state, *e.g.*, R, and that of two other allosteric ligands I and A, I has affinity only for the T-state while A has affinity only for the R-state. The effects of ligands I and A will be to displace the equilibrium between R and T states, so that  $L$  becomes  $L'$ , a new apparent allosteric constant.  $L' = L[(1 + \beta)^n / (1 + \gamma)^n]$ , where  $\beta = I/K_I$ , and  $\gamma = A/K_A \cdot K_I$



and  $K_A$  are the microscopic dissociation constants for I and A from the T and R states, respectively. Finally, the saturation function for S,  $Y_S$ , is given by:

$$Y_S = \frac{\alpha(1 + \alpha)^{n-1}}{L \frac{(1 + \beta)^n}{(1 + \gamma)^n} + (1 + \alpha)^n} \quad (\text{eqn. 3})$$

Using the MWC model, we can distinguish two kinds of allosteric systems involving a substrate S and an effector F: (1) a **K system**. Both F and S have differential affinities toward the T and R states, *i.e.*, both are allosteric, and (2) a **V system**. S has the same affinity for both states. In this case, F does not affect binding of S, and *vice-versa*. But, F can affect the catalytic rate, either as an activator (positive V system) or as an inhibitor (negative V system).

Blangy, Buc and Monod (1968) have shown that *E. coli* PFK obeys the MWC model, at least in the presence of an ATP concentration close to its  $K_m$ . From a thorough analysis of steady-state kinetic data in terms of the model, the kinetic and allosteric parameters in Table 1.4 were obtained. Based on these parameters, one can conclude that (i) unliganded EcPFK exists overwhelmingly in the T state (only one molecule in 4 million will be in the R state since  $L = 4 \times 10^6$ ), (ii) the oligomer contains 4 protomers, (iii) ATP has no preference for either T or R and thus is not an allosteric ligand ( $K_R = K_T$ ), (iv) Fru-6P prefers the R state by a ratio of 2,000 to 1 ( $c = 5 \times 10^{-4}$ ), (v) GDP binds almost exclusively to the R-state, and (vi) PEP binds almost exclusively to the T-state.

Several of the afore-mentioned predictions about EcPFK based on the MWC model have been shown to be untrue over the course of time. First, X-ray diffraction studies of unliganded EcPFK (Rypniewski & Evans, 1989) have shown that the unliganded enzyme resembles the form that has a high affinity for Fru-6P, *i.e.*, the

**TABLE 1.4**  
*Kinetic and Allosteric Parameters for E. coli PFK*

Ligand	$K_R$ (mM)	$K_T$ (mM)
ATP	0.06	0.06
Fru-6P	0.0125	25
ADP	0.025	1.3
GDP	0.04	>40
PEP	>750	0.75
$n = 4$	$L = 4 \times 10^6$	$c = 5 \times 10^{-4}$

R-state form. Using equilibrium dialysis, Deville-Bonne *et al.* (1992) have shown that  $L=2$ . Second, ATP is now known to be involved in the allosteric response of EcPFK. It profoundly inhibits the enzyme when Fru-6P concentration is low (Kundrot & Evans, 1991). Fluorescence studies show that the ATP analog AMPPCP causes the Fru-6P binding profile to become sigmoidal (Deville-Bonne *et al.*, 1992). This result suggests that antagonistic interactions between MgATP and Fru-6P are involved in EcPFK homotropic cooperativity. ATP has been termed an "allosteric" inhibitor of EcPFK (Evans, 1992). Third, GDP can super-activate EcPFK that is already saturated by Fru-6P, increasing  $k_{cat}$  10 to 20% (Deville-Bonne *et al.*, 1991a). Thus, GDP affects not only the binding of Fru-6P, but also the catalytic rate, and indicates (at least) that EcPFK is not a perfect K-system enzyme. Finally, the observations that (i) both  $k_{cat}$  and the Hill number for Fru-6P saturation are pH-dependent and (ii) Hill numbers can be as high as 6.0, suggests that the cooperativity of EcPFK has a kinetic origin. Hill numbers higher than the number of binding sites (4 for Fru-6P binding to EcPFK) are not predicted by the MWC model; they arise when the enzyme does not operate at equilibrium. Such non-equilibrium conditions, which can result in kinetic cooperativity, are present when catalysis is fast relative to either substrate binding and/or release, or an essential structural transition. The resulting kinetic cooperativity can then add to the binding cooperativity, causing the Hill number to increase to values beyond the number of binding sites.

Blangy *et al.* (1968) were not the first to investigate the regulation of *E. coli* PFK. Atkinson & Walton (1965) studied the mutual effects of Fru-6P, ATP, AMP, and  $Mg^{++}$  on the rate of the EcPFK-catalyzed reaction. Their results show clearly that ATP negatively regulates the enzyme when its concentration is saturating (above 1.0 mM). The complex patterns of curved lines that Atkinson and Walton obtained stand in stark contrast to the graceful patterns obtained by Blangy *et al.* (1968), which fit the MWC

model so perfectly, albeit under a very limited set of experimental conditions (0.1 mM ATP). One must wonder if Blangy *et al.* (1968) read the 1965 paper, which states:

"... the whole kinetic picture [for PFK] depends on the initial assay conditions. Thus, if a relatively high concentration of ATP were used in determining rate as a function of Fru-6P and Mg<sup>++</sup> concentrations, and if just saturating levels of Fru-6P and Mg<sup>++</sup> were used in turn to study the rate *versus* ATP concentration ... a self-consistent set of [kinetic parameters] would be obtained. If, however, the same procedure were repeated with a lower initial concentration of ATP, a completely different but equally self-consistent set of values would result. More intensive kinetic analysis of either set of results could obviously not yield generally applicable parameters."

In conclusion to this section, the MWC model does partially describe the regulation of EcPFK (and BsPFK). However, it is inadequate and too simple to account completely for PFK cooperative behavior. Other models, such as those involving kinetic cooperativity arising from a slow transition (Frieden, 1970; Ainslie *et al.*, 1972) or from the kinetic mechanism (Ferdinand, 1966; Sweeny & Fisher, 1968) may prove to be important.

### The Hill Equation

Because the concerted model is not valid for PFK under many conditions, its equation (equation 2) was not used to fit the sigmoidal substrate saturation data obtained for EcPFK or BsPFK. Rather, the Hill equation (Hill, 1910), which assumes no particular model and is more empirical, was used. The general form of the Hill equation that is used to describe saturation of a protein by a ligand is:

$$\log \frac{Y}{1-Y} = h \log [A] - \log K \quad (\text{eqn. 4})$$

where Y is the degree of saturation of the protein by ligand, [A] is the concentration of free ligand, and K is a constant. A plot of  $\log (Y/(1-Y))$  *versus*  $\log [A]$  gives a straight line, the slope of which is the Hill number h (or n<sub>H</sub>). The Hill number describes the cooperativity of the response of the protein to ligand. The ligand concentration at

half-saturation,  $[A]_{1/2}$ , is equal to  $K^{1/n}$ . The form of the Hill equation generally used in studying the sigmoidality of saturation curves obtained from kinetic data is:

$$v = \frac{V_{\max} [A]^h}{[A]^h + A_{1/2}^h} \quad (\text{eqn. 5})$$

In this form, the binding term  $Y/(1-Y)$  has been replaced by the kinetic term  $v/(V_{\max}-v)$ .

### **A Structural Model for the PFK Allosteric Transition**

Although the MWC model is now known to be too simple to explain the regulation of bacterial PFK, it has been used extensively to make sense of differences in protein conformation found to exist in X-ray structures obtained under different conditions (Evans & Hudson, 1979; Evans *et al.*, 1981; Evans *et al.*, 1986; Shirakihara & Evans, 1988; Schirmer & Evans, 1990). Schirmer & Evans (1990) have proposed a structural model for the allosteric transition of *B. stearotherophilus* PFK based on X-ray diffraction data obtained from crystals under two different conditions: (a) in the presence of the inhibitor 2-phosphoglycolate (an analog of PEP), when the enzyme is presumably in its T-state, and (b) in the presence of the substrate Fru-6P and activator MgADP, when BsPFK is in the R-state. A comparison of the T- and R-state structures of the tetramer reveals that the structural changes accompanying an ostensible T-to-R transition can be described as three separate events that occur simultaneously: (1) rotation of the two rigid dimers A:B and C:D by  $7^\circ$  relative to each other, (2) a passive change along the "active" dimer-dimer interface that allows an ordered layer of water molecules to come in between the two dimers, and (3) the coordinated back-and-forth movement of a pair of loops, the 8H and 6F loops, that are situated between the effector and active sites. This last change involves the switching of two residues, Glu 161 and Arg 162, into and out of the active site. It is described in more detail below.

The 8H loop (residues 211 to 216) lines one edge of the effector cleft (Fig. 1.8). In the absence of effector, the cleft is open. Binding of inhibitor PEP pulls the 8H loop inward, closing the cleft and placing the enzyme in the T-state. Binding of ADP (or GDP), on the other hand, pushes the 8H loop away from the effector site and places BPFK in the R-state. Movement of the 8H loop is coordinated with a reorganization of the 6F loop (residues Thr 156 to Arg 162) along the dimer-dimer interface. In the T-to-R transition, Glu 161, which points into the active site across the dimer-dimer interface in the T-state, rotates away. At the same time, Arg 162 swings around into the active site, occupying the position formerly occupied by Glu 161 (Fig. 1.9). The positively-charged guanidinium groups of Arg 162 and Arg 243 favorably interact with the negative charges of the phosphate of the incoming Fru-6P, thereby increasing its binding affinity. The R-to-T transition involves the reverse sequence of events, with Glu 161 swinging back into the active site and Arg 162 rotating away. In this way, the binding of GDP and PEP at the effector site trigger the heterotropic allosteric transition and alter the affinity of the active site for Fru-6P.

An interaction important for stabilizing the T-state structure of BsPfk is the salt bridge between Arg 72 and Glu 241. This salt bridge is absent in the R-state but present in the T-state (Fig. 1.9). Thus, Arg 72, which is critical for catalysis, is sequestered away by Glu 241 when the enzyme undergoes the R-to-T transition.

#### **The Active Site, Cooperativity, and the Role of ATP**

Site-directed mutagenesis has identified a number of residues in the active site of EcPfk (and one in BsPfk) important for the enzyme's cooperative response to Fru-6P. These residues are listed in Table 1.5. As mentioned above, Arg 162 and Arg 243 bind the phosphate group of Fru-6P from across the dimer-dimer interface (Shirakihara & Evans, 1988). When these two residues are changed to Ser, the cooperativity drops significantly (Berger & Evans, 1990). The same happens when Arg 72 is changed to a

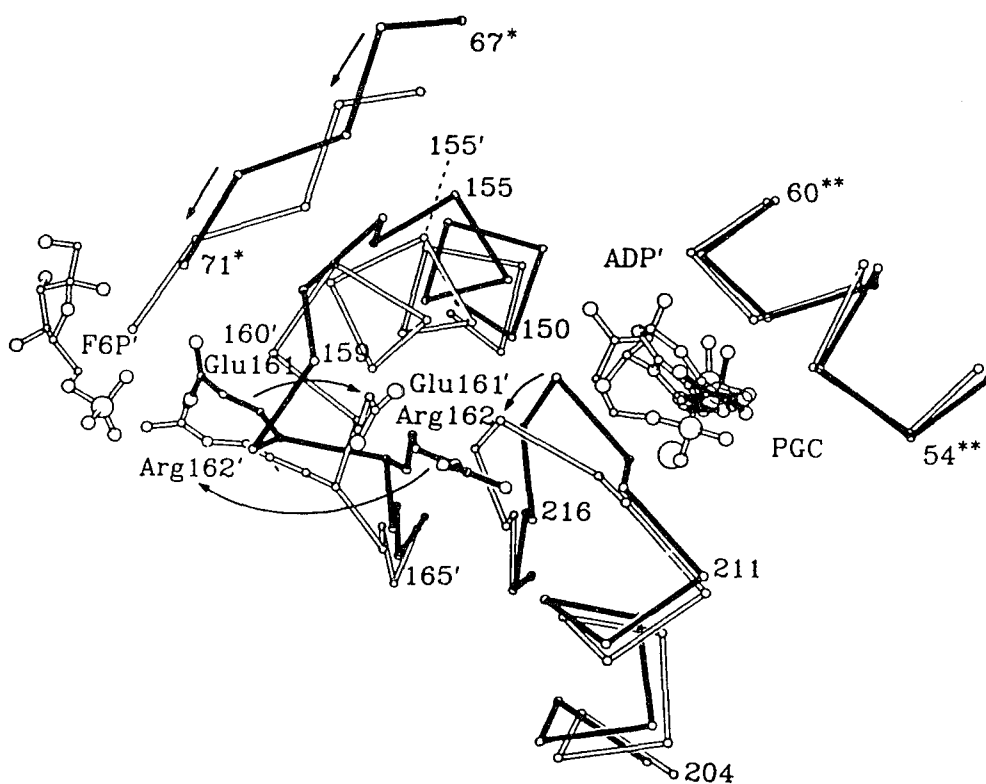


**FIGURE 1.8. Co-ordinated Movement of the 8H and 6F Loops.** The region between the effector site and active site that undergoes large structural change between the T-state (solid lines) and R-state (open lines). 8H loop: residues 211-216; 6F loop: residues 156-162. \*\*, residues from the same dimer. \*, residues from the other dimer. PGC, the inhibitor 2-phosphoglycolate, which binds to the T-state. ADP and Fru-6P bind to the R-state. R-state residues are *primed*. (Taken with permission from Schirmer, T., & Evans, P. R. (1990) *Nature* 343, 140-145. Copyright 1990 Macmillan Magazines, Limited).

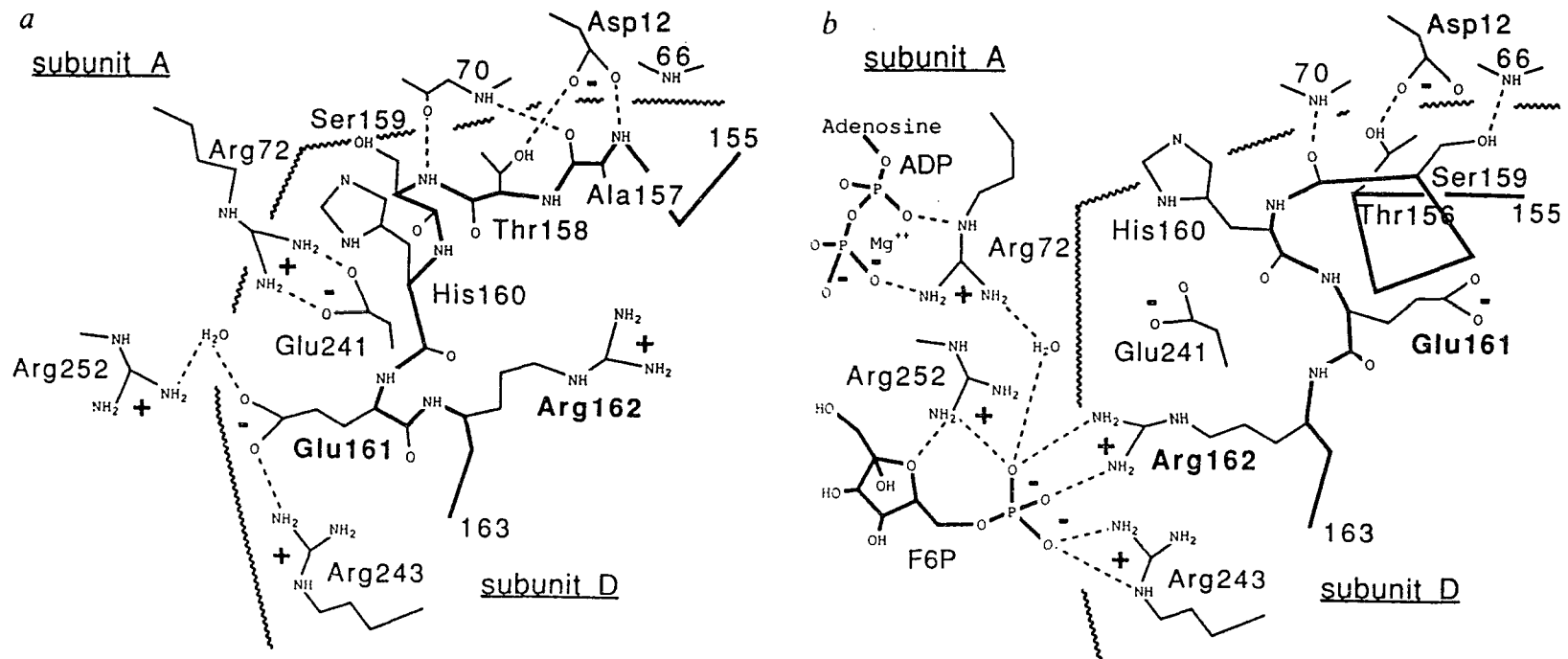


**FIGURE 1.9. Reorganization of the 6F Loop.** a, the T-state structure, showing Glu 161 at the active site. b, the R-state structure, showing Arg 162 and Arg 243 interacting with the phosphate group of Fru-6P. The wavy line represents the interface between dimers. (Taken with permission from Schirmer, T., & Evans, P. R. (1990) *Nature* 343, 141-145. Copyright 1990 Macmillan Magazines, Limited).



**TABLE 1.5**  
*Residues Important for Homotropic Cooperativity of E. coli PFK*

Mutation	Fold Increase in $S_{1/2}^{\text{Fru-6P}}$	Hill Number*
R 162—>S	7	2.1
R 243—>S	30	2.7
R 72—>S	1	2.2
S 159—>N	>1000	(1)
T 156—>(GS)	>100	(1)
D 129—>S	4	2.7
T 125—>A	1.6	1
D 127—>Y	1.5	1
R 252—>A**	1500	N. A.

\*, the Hill numbers in parentheses are only estimates since saturation with respect to Fru-6P was not achieved. \*\*, from *B. stearothermophilus* PFK. N. A., not applicable.

Ser (Table 1.5). Threonine 156 and Ser 159 are within the 6F loop of EcPFK (as is Arg 162), which becomes reorganized during the allosteric T-to-R transition. Mutation of either of these residues severely affects Fru-6P binding, and the mutant enzymes appear to be locked in the T-state since their catalytic rate constants are very low (about 100-fold lower than wild-type) and their Fru-6P saturation profiles are hyperbolic (Kundrot & Evans, 1991). Arg 252 is proposed to bind to the ribose hydroxyl of Fru-6P.

Mutation of Arg 252 to Ala in BsPFK severely lowers the affinity of the enzyme for Fru-6P and also lowers the cooperativity of its response to Fru-6P when inhibited by PEP (Valdez *et al.*, 1989). Finally, Thr 125 binds the  $\gamma$ -phosphate of ATP and helps stabilize the transition state, while Asp 129 helps coordinate the  $Mg^{++}$  ion. Mutation of Thr 125 and Asp 129 to Ala and Ser, respectively, both cause a 100-fold drop in  $k_{cat}$  and a moderate increase in  $S_{1/2}^{Fru-6P}$ , but have somewhat different effects on cooperativity. The mutation Thr 125 $\rightarrow$ Ala completely abolishes cooperativity (Hill number is 1.0), while the Asp 129 $\rightarrow$ Ser mutation reduces it ( $n_H$  drops from 4 to 2.7). Thus, Thr 125 appears to be critical for cooperativity, but Asp 129 is less important. Auzat *et al.* (1994a) have further shown that an interaction between Thr 125 and the  $\gamma$ -phosphate of ATP is involved not only in the cooperative response of EcPFK to Fru-6P, but also in its response to PEP. The observation that mutation of a residue that interacts directly with the  $\gamma$ -phosphate of ATP, *e.g.*, Thr 125, abolishes cooperativity, while mutation of other active site residues, *e.g.*, Asp 129, simply lowers cooperativity, suggests that the  $\gamma$ -phosphate itself is essential for the cooperative response.

A growing body of experimental evidence indicates that antagonistic interactions between ATP and Fru-6P in the active site of EcPFK trigger the conformational change associated with the homotropic allosteric transition. Deville-Bonne *et al.* (1991b) have found that MgATP antagonizes the binding of Fru-6P in the active site of EcPFK, and *vice-versa*. Fluorescence studies support this finding. Whereas titration of the intrinsic fluorescence of EcPFK with Fru-6P gives a hyperbolic

binding curve, titration with Fru-6P in the presence of AMPPCP (Deville-Bonne *et al.*, 1992) gives a sigmoidal curve ( $n_H$  is above 2). A Lys 213—> Ala mutant EcPFK enzyme that is insensitive to heterotropic regulation but retains homotropic cooperativity has also been used to study the effect of ATP on Fru-6P binding (Berger & Evans, 1991). As with the wild-type enzyme, ATP induces positive cooperativity in the Fru-6P binding curve of the mutant. Thus, ATP (or AMPPCP) can induce positive cooperativity in the Fru-6P binding curve of EcPFK. Interestingly, the converse is also true: Fru-6P induces positive cooperativity ( $n_H$  is 2.0) in the AMPPCP binding curve (Deville-Bonne *et al.*, 1992). Zheng & Kemp (1992) propose that antagonistic interactions between ATP (*via* its  $\gamma$ -phosphate group) and Fru-6P are important for "allosteric" ATP inhibition and cooperativity, but suggest a purely kinetic origin for the cooperativity. In contrast, Johnson & Reinhart (1992) maintain that an inter-active site interaction mediated through protein conformational change is partly responsible for the antagonism between Fru-6P and MgATP. Interestingly, Johnson & Reinhart (1994) found that MgADP in the effector site requires the presence of MgATP in the active site to activate the enzyme; in its absence, MgADP actually inhibits Fru-6P binding. Thus, whatever the mechanism of ATP inhibition, it appears that Fru-6P cannot act as a cooperative substrate by itself, but requires the presence of MgATP beside it in the active site in order to fulfill its role as a "cooperative" ligand.

The mechanism by which MgATP inhibits EcPFK has been investigated (Zheng & Kemp, 1992) but has not been conclusively determined. An intriguing possibility for the mechanism is that ATP inhibition is mediated by closure of the active site. If subsequent Fru-6P binding, i.e., Fru-6P binding after MgATP, causes re-opening of the active site *via* a transition that is slow relative to catalysis, the result could be sigmoidality in the Fru-6P saturation curve.

### **Mutation of Leucine 178 to Tryptophan**

Leu 178 is close to neither the active site nor the effector site, yet it appears to be involved in the heterotropic allosteric response of *E. coli* PFK. Its mutation to Trp causes specific suppression of heterotropic cooperativity but allows retention of homotropic cooperativity. In other words, the mutant enzyme cannot be inhibited by PEP or activated by GDP, but its Fru-6P saturation curve is highly sigmoidal (Serre *et al.*, 1990). This result is important because it shows that heterotropic and homotropic effects can be uncoupled; thus, they probably involve different conformational changes. Such a result is not predicted by the MWC model, which assumes a common conformational change for both homotropic and heterotropic allosteric responses. Presumably, Leu 178 lies along the structural pathway for transmission of heterotropic, but not homotropic, signals.

### **Fluorescence Studies**

Both BsPFK and EcPFK have a unique tryptophan residue. It is at position 179 in BsPFK and position 311 in EcPFK. The intrinsic fluorescence of Trp 179 of BsPFK is largely insensitive to the binding of substrates or allosteric effectors (Kim *et al.*, 1993). Thus, it is not possible to use intrinsic fluorescence to probe conformational changes associated with allostery in BsPFK. It may be possible, however, to use site-directed mutagenesis to strategically place a tryptophan residue in the right place in BsPFK, allowing the fluorescence to be sensitive to conformational changes without disrupting protein structure. This would open up a whole new set of binding studies for BsPFK (discussed in chapter five).

Unlike Trp 179 of BsPFK, Trp 311 of EcPFK is responsive to conformational changes induced in the enzyme by the binding of substrates and effectors. Saturation of the enzyme with Fru-6P causes a 20% decrease in intrinsic fluorescence. ADP causes a similar 20% decrease, but ATP (or AMPPCP) causes a 10% increase and PEP binding results in a 5 to 10% increase (Berger & Evans, 1991; Deville-Bonne *et al.*, 1992).

Thus, Fru-6P and ADP appear to place the enzyme in a low-fluorescence state, while ATP (or AMPPCP) and PEP place the enzyme in a high-fluorescence state. A number of fluorescence studies have been performed on wild-type and mutant EcPFK enzymes (Berger & Evans, 1991; Deville-Bonne *et al.*, 1992; Johnson & Reinhart, 1992; Johnson & Reinhart, 1994; Auzat *et al.*, 1994a). These studies have contributed significantly to our knowledge of the regulation of EcPFK, especially in regard to the role that ATP plays (see discussion above).

### **Objectives of Dissertation Research**

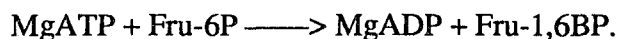
The objectives are threefold: (1) to determine the kinetic mechanism of *B. stearothermophilus* PFK using initial velocity and inhibition studies, (2) to investigate the role of the open-to-closed conformational transition in allosteric regulation of *E. coli* PFK by constructing a chimeric PFK that contains the "rigid" large (ATP-binding) domain of *B. stearothermophilus* PFK grafted onto the remainder of the *E. coli* PFK subunit, and (3) to uncover the importance of residue 161 in the allosteric transitions of both *B. stearothermophilus* PFK and *E. coli* PFK using site-directed mutagenesis.

## Chapter 2

### **Kinetic Characteristics of Phosphofructokinase from *Bacillus stearothermophilus*: MgATP Non-allosterically Inhibits the Enzyme**

(Reprinted with permission from Byrnes, M., Zhu, X., Younathan, E. S., and Chang, S. H. (1994) *Biochemistry* 33, 3424-3431. Copyright 1994 American Chemical Society.)

Phosphofructokinase (PFK, EC 2.7.1.11) catalyzes the first committed step of glycolysis, the transfer of a terminal phosphate from ATP to  $\beta$ ,D-fructose 6-phosphate (Fru-6P) to form ADP and  $\beta$ -fructose 1,6-bisphosphate (Fru-1,6BP):



The allosteric PFK from the thermophilic bacterium *B. stearothermophilus*, like its counterpart from *E. coli*, is a tetramer of identical subunits, each composed of 319 amino acids (320 for *E. coli* PFK). Fifty-five percent of the amino acids are identical between the two bacterial enzymes (French and Chang, 1987). Both *B. stearothermophilus* PFK (BsPFK) and *E. coli* PFK (EcPFK) are allosterically inhibited by phospho(enol)pyruvate (PEP). This inhibition is reversed by the activators adenosine diphosphate (ADP) and guanosine diphosphate (GDP) (Valdez *et al.*, 1989; Blangy *et al.*, 1968).

A comparison between the crystal structures of BsPFK and EcPFK (Evans *et al.*, 1981; Shirakihara and Evans, 1988) reveals striking structural similarity. The two enzymes have all the same secondary structural elements, and their subunit  $\alpha$ -carbon traces are nearly superimposable. In both enzymes, the subunit is divided into a large and a small domain, with the active site located within the subunit in a cleft between the two domains. The active site residues that bind substrates are either the same or similar between the two enzymes.

Despite the high degree of structural similarity between BsPFK and EcPFK, there is a significant kinetic difference between them. Steady-state initial velocity studies reveal that whereas saturation of EcPFK by Fru-6P is highly cooperative in the presence of saturating MgATP (Blangy *et al.*, 1968), saturation of BsPFK by Fru-6P shows little or no cooperativity under the same conditions (Valdez *et al.*, 1989). Fructose 6-phosphate saturation of BsPFK is cooperative, however, in the presence of

PEP (Valdez *et al.*, 1989). Thus, BsPFK resembles the PFK from the extreme thermophilic bacterium *Flavobacterium thermophilum* (Yoshida, 1972), which likewise displays a hyperbolic Fru-6P saturation profile that becomes sigmoidal in the presence of PEP. Schirmer and Evans (1990) have proposed a structural model for the allosteric transition of BsPFK based on X-ray diffraction data.

Although the structure of BsPFK has been extensively investigated, its kinetic characteristics have remained largely unstudied. For example, although the amino acid residues involved in binding the substrates MgATP and Fru-6P have been known for some time (Evans *et al.*, 1981), the kinetic mechanism has not been studied. Several observations suggest that there are differences between the active site regions of BsPFK and EcPFK: (i) the active site structure of BsPFK is more open than that of EcPFK (Shirakihara and Evans, 1988), (ii) significant binding of GDP occurs in the active site of BsPFK (Valdez *et al.*, 1989), but not in the active site of EcPFK (Blangy *et al.*, 1968), and (iii) the large (ATP-binding) domain of EcPFK moves as the enzyme changes conformation from a "closed" to an "open" subunit structure (Shirakihara and Evans, 1988), whereas the large domain of BsPFK remains essentially rigid during the allosteric transition of the enzyme (Schirmer and Evans, 1990).

These observations have stimulated our interest in studying the kinetic characteristics of the BsPFK-catalyzed reaction in both the forward and reverse directions. Initial velocity, product inhibition, and mixed alternate substrate studies of the reverse reaction indicate that the kinetic mechanism is sequential random. Product and dead-end inhibition studies of the forward reaction corroborate this result. However, initial velocity studies of the forward reaction indicate that MgATP is a non-allosteric substrate inhibitor, and the binding of MgATP is a non rapid-equilibrium process. Based on these results, it is proposed that substrate binding proceeds *via* two alternative steady-state pathways, with one pathway kinetically favored over the other.



Substrate inhibition by MgATP is proposed to result from both abortive binding of MgATP in the Fru-6P site and reaction flux through the disfavored pathway.

### Materials and Methods

*Enzymes and Chemicals*—NADH, NADP<sup>+</sup>, Fru-6P, ATP, Fru-1,6BP, ADP, PEP, Ara-5P, AMPPCP, and the auxiliary enzymes for the coupled PFK activity assays were all obtained from Sigma Chemical Co. (St. Louis, MO). The Cibacron Blue 3GA-agarose (type 3000-CL-L) resin was also obtained from Sigma. Restriction endonucleases used for cloning were obtained from either New England Biolabs (Beverly, MA) or United States Biochemical (Cleveland, OH).

*Expression and Purification of PFK*—BsPFK was expressed in PFK-deficient *E. coli* cells (DF1020 cells) from a recombinant plasmid constructed by cloning the *bspfk* gene (French and Chang, 1987) into the EcoRI/HindIII sites of pUC18. The enzyme was subsequently purified by a three-step procedure (Valdez *et al.*, 1989) involving (1) sonication, (2) heat-treatment at 70°C, and (3) chromatography on a Cibacron blue 3GA affinity column. The purified enzyme preparation had a specific activity of 160 units/mg. Its purity was demonstrated by the presence of a single band on an SDS-polyacrylamide gel stained with Coomassie Brilliant Blue dye. The purified enzyme solution was dialyzed at 4°C in 100 mM Tris-Cl, pH 7.4, containing 1 mM dithiothreitol and 50% glycerol, and stored at -20°C. Protein concentration was determined using the Bio-Rad (Richmond, CA) protein assay.

### *Site-directed Mutagenesis, and Expression and Purification of Mutant BsPFK*

The site-directed mutagenesis procedure to mutate the *bspfk* gene, as well as the procedures for expression and purification of the mutant enzyme, are to be described separately (Zhu *et al.*, manuscript in preparation).

*Kinetic Assays*—The initial velocity of the PFK-catalyzed reaction in the forward direction was measured at 30°C in 100 mM Tris-Cl, pH 8.2, containing 10 mM MgCl<sub>2</sub> and 5 mM NH<sub>4</sub>Cl by coupling the production of either Fru-1,6BP or ADP to the

oxidation of NADH (0.20 mM.) (The saturation curves with respect to substrates Fru-6P and MgATP obtained at 30°C were similar to those obtained at 60°C, except that the  $k_{cat}$  was lower at 30°C. Fru-6P saturation was non-cooperative at both temperatures, and substrate inhibition was apparent with high MgATP at both temperatures). The Fru-1,6BP-coupled assay utilized the auxiliary enzymes aldolase (20  $\mu\text{g/ml}$ ), triosephosphate isomerase (10  $\mu\text{g/ml}$ ) and  $\alpha$ -glycerophosphate dehydrogenase (10  $\mu\text{g/ml}$ ), while the ADP-coupled assay utilized pyruvate kinase (10  $\mu\text{g/ml}$ ), phospho(enol)pyruvate (PEP, 200  $\mu\text{M}$ ) and lactate dehydrogenase (10  $\mu\text{g/ml}$ .) The ADP-coupled assay system could not be used for Fru-6P saturation studies since PEP is an allosteric inhibitor with respect to Fru-6P; however, PEP at this concentration (200  $\mu\text{M}$ ) does not alter MgATP saturation behavior. The ATP-regenerating system that utilizes creatine kinase and creatine phosphate, which is required for the EcPFK activity assay, was found to be unnecessary since ADP has little or no activating effect on BsPFK (in the absence of PEP). In all forward reaction assays, the free  $\text{Mg}^{++}$  concentration was kept 5 to 10 mM in excess of the ATP concentration to avoid inhibition by free ATP. Typically, assays were initiated by the addition of 0.10  $\mu\text{g}$  of PFK. Since the BsPFK assay generally involved an initial nonlinear phase, a 1- or 2-minute lag period was allowed prior to recording the  $\text{Abs}_{340}$  change over time, which was done for at least one minute. A thermostatted Hitachi UV-2000 spectrophotometer was used for these measurements. Duplicate assays were run for each data point. Initial velocities are expressed in units of  $\mu\text{mole}$  of product formed per minute.

Initial velocity measurements in the reverse direction were similar to those in the forward direction, except that the production of either Fru-6P or ATP was coupled to the reduction of  $\text{NADP}^+$  (0.20 mM). Assays were run at pH 8.2, and  $\text{Mg}^{++}$  concentration was kept 9 to 10 mM in excess of the ADP concentration. For the Fru-6P-coupled assay, the auxiliary enzymes phosphoglucoisomerase (10  $\mu\text{g/ml}$ ) and glucose 6-phosphate dehydrogenase (10  $\mu\text{g/ml}$ ) were used, whereas for the ATP-coupled assay,

hexokinase (20  $\mu\text{g/ml}$ ), glucose (3 mM) and glucose 6-phosphate dehydrogenase (10  $\mu\text{g/ml}$ ) were used. Typically, assays were initiated with the addition of 2.0  $\mu\text{g}$  of PFK.

*Treatment of Kinetic Data*—Initial velocity data for the forward reaction were fit to either the Michaelis-Menten equation (eqn. 6), the Hill equation (eqn. 7), the initial velocity equation for a rapid-equilibrium sequential mechanism (eqn. 8; Cleland, 1963), or the initial velocity equation for a sequential random mechanism assuming steady-state (non rapid-equilibrium) conditions (eqn. 9; Ferdinand, 1966). In equations 6-12 below, [A] and [B] represent the concentrations of substrates A and B, and  $V_{\text{max}}$  is the maximum velocity. In equation (6),  $K_m$  is the Michaelis constant, whereas in eqn. (7),  $[A]_{1/2}$  is the concentration of substrate at half-saturation and  $n$  is the Hill coefficient. In equation (8),  $K_{ia}$  is the equilibrium constant for dissociation of substrate A from the binary complex EA (E represents enzyme). There is an analogous constant,  $K_{ib}$ , for dissociation of B from EB.  $K_a$  and  $K_b$  are equilibrium constants for dissociation of A and B, respectively, from the ternary complex EAB. In equation (9), the terms  $i$ ,  $j$ ,  $k$ ,  $l$ , and  $m$  are complex functions of [B] and the rate constants for the various steps in Scheme I (see Discussion section). As such,  $i$ - $m$  have no physical significance.

$$v = \frac{V_{\text{max}} [A]}{[A] + K_m} \quad (\text{eqn. 6})$$

$$v = \frac{V_{\text{max}} [A]^n}{[A]_{1/2} + [A]^n} \quad (\text{eqn. 7})$$

$$v = \frac{V_{\text{max}} [A] [B]}{K_{ia} K_b + K_b [A] + K_a [B] + [A] [B]} \quad (\text{eqn. 8})$$

$$v = \frac{i [A]^2 + j [A]}{k + l [A]^2 + m [A]} \quad (\text{eqn. 9})$$

Initial velocity data for product inhibition, dead-end inhibition and alternate substrate studies were first plotted graphically as double-reciprocal plots. On the basis of these primary plots, the inhibition patterns were identified, and each data set was fit to the equation for either linear competitive (eqn. 10), linear non-competitive (eqn. 11), or linear uncompetitive (eqn. 12) inhibition (Cleland, 1979). In equations 10-12, the constant  $K$  is the equilibrium constant for dissociation of varied substrate  $A$  from the ternary complex  $EAB$ , whereas  $K_{is}$  and  $K_{ii}$  are equilibrium constants for dissociation of inhibitor  $I$  from its inhibitory complex, as determined from slope and intercept replots, respectively.

$$v = \frac{V_{\max} [A]}{K (1 + [I]/K_{is}) + [A]} \quad (\text{eqn. 10})$$

$$v = \frac{V_{\max} [A]}{K (1 + [I]/K_{is}) + [A] (1 + [I]/K_{ii})} \quad (\text{eqn. 11})$$

$$v = \frac{V_{\max} [A]}{K + [A] (1 + [I]/K_{ii})} \quad (\text{eqn. 12})$$

All curve-fitting to equations 6-12 was performed by non-linear regression analysis using the program INPLOT (GraphPad, Inc., San Diego, CA).

## Results

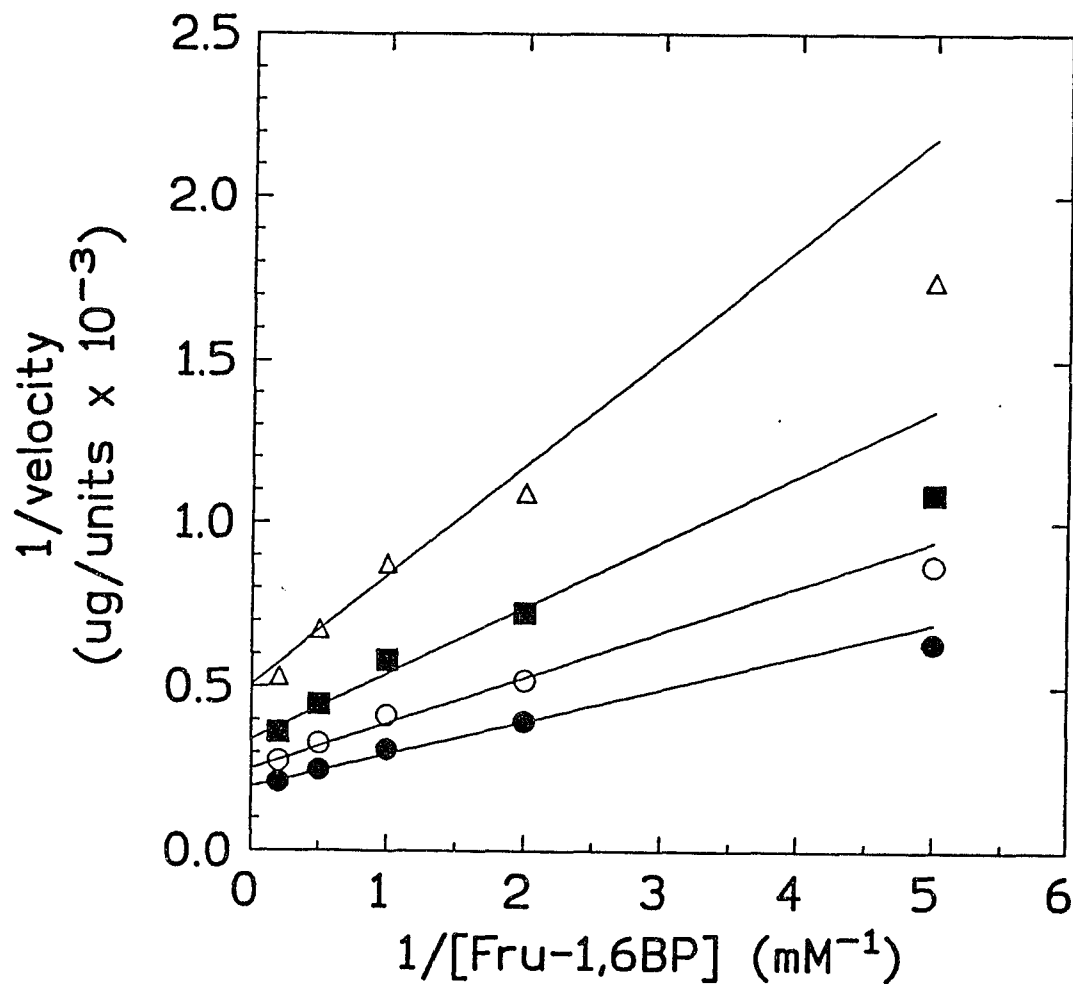
*The Reverse Reaction: Initial Velocity, Product Inhibition and Mixed Alternate Substrate Studies*—Because the kinetic behavior of BsPFK in the forward direction is more complex than in the reverse direction, studies on the latter are presented first. The turnover number  $k_{\text{cat}}$  of the reverse reaction ( $3.2 \text{ s}^{-1}$ ) was about 35-fold lower than that of the forward reaction ( $112 \text{ s}^{-1}$ ). This compares well to the 40-fold lower value for the reverse reaction of EcPFK relative to its forward reaction (Hellinga and Evans, 1987).

Initial velocity studies were performed on the reverse reaction by varying Fru-1,6BP concentration while keeping MgADP concentration constant at different fixed levels, and *vice-versa*. Double-reciprocal plots were constructed for both sets of data. The families of lines obtained for both (Figs. 2.1A & 2.1B) intersect to the left of the ordinate, a result which denotes a sequential kinetic mechanism. The initial velocity data were fit to the equation for a rapid-equilibrium random or ordered bireactant mechanism (eqn. 8), assuming that A is MgADP and B is Fru-1,6BP. The following parameters were obtained by performing nonlinear regression analysis of the initial velocity data (Cleland, 1979) using eqn. (8):  $k_{cat} = 3.2 \pm 0.2 \text{ s}^{-1}$ ,  $K_a = 0.11 \pm 0.01 \text{ mM}$ ,  $K_b = 0.44 \pm 0.05 \text{ mM}$ ,  $K_{ia} = 0.33 \pm 0.04 \text{ mM}$ , and  $K_{ib} = 0.19 \pm 0.08 \text{ mM}$ .

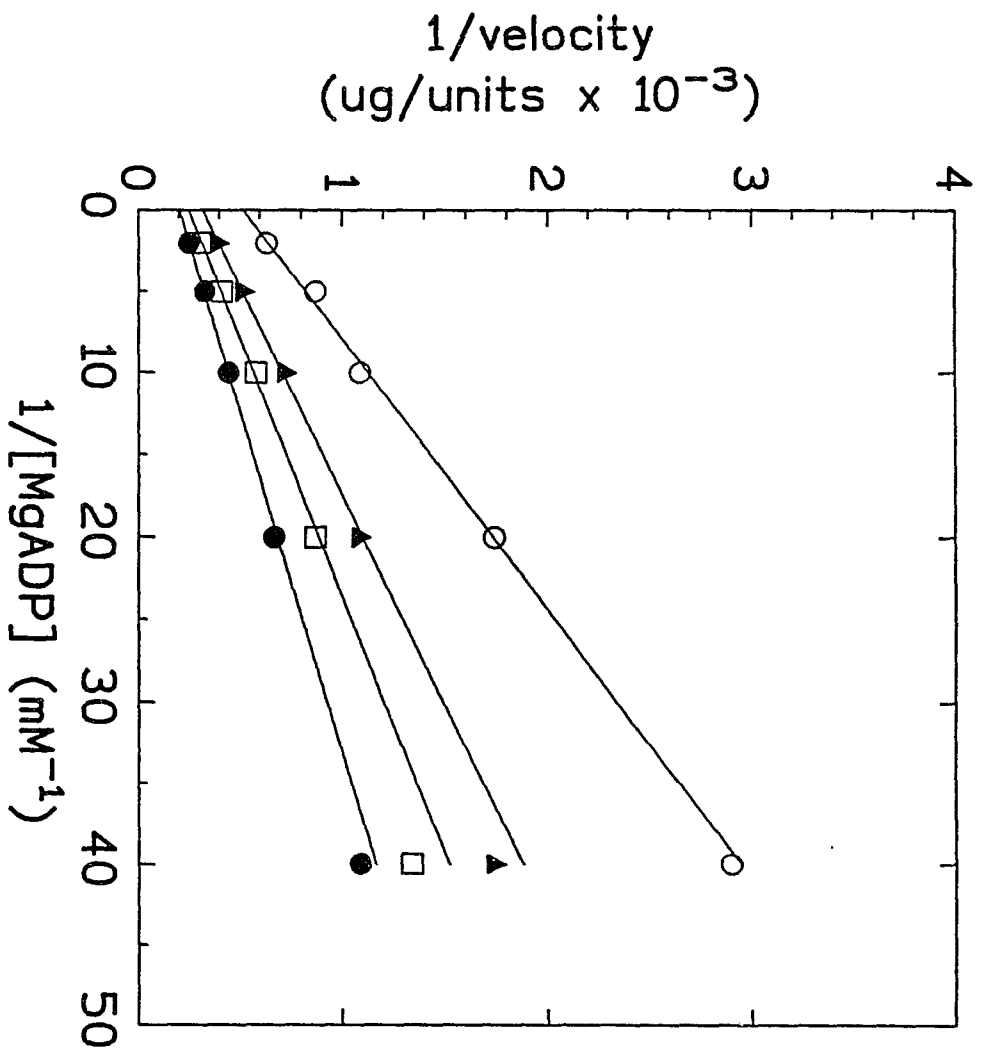
Product inhibition studies were also performed on the reverse reaction to further distinguish whether its mechanism is random or ordered. For these studies, the concentration of one substrate (Fru-1,6BP or MgADP) was varied while the other was kept constant at a fixed level in the absence or presence of different amounts of one of the two products (Fru-6P or MgATP). Four sets of product inhibition data were obtained. The data from each inhibition study were fit to the equation for either linear competitive (eqn. 10), linear noncompetitive (eqn. 11), or linear uncompetitive (eqn. 12) inhibition. Table 2.1 lists the pertinent kinetic parameters obtained, and the patterns of lines observed in double-reciprocal plots. The results are consistent with a rapid-equilibrium random mechanism in the reverse direction. The noncompetitive product inhibition by Fru-6P with respect to MgADP indicates the formation of a dead-end E-MgADP-Fru-6P complex. However, the equations for both competitive and noncompetitive inhibition fit equally well to the data for inhibition by MgATP with respect to Fru-1,6BP, a result which indicates that the dead-end E-MgATP-Fru-1,6BP complex probably does not form readily, if it forms at all.

Additional evidence that the mechanism in the reverse direction is random was obtained from studies using GDP, which can function as an alternate substrate for the

A



**FIGURE 2.1. Initial Velocity Patterns for the Reverse Reaction.** (A) Plot of the reciprocal of initial velocity *versus* the reciprocal of Fru-1,6BP concentration at different fixed levels of MgADP: ( $\Delta$ ) 0.05 mM, ( $\blacksquare$ ) 0.10 mM, ( $\circ$ ) 0.20 mM, and ( $\bullet$ ) 0.5 mM MgADP. (B) Plot of the reciprocal of initial velocity *versus* the reciprocal of MgADP concentration at different fixed levels of Fru-1,6BP: ( $\circ$ ) 0.20 mM, ( $\blacktriangle$ ) 0.50 mM, ( $\square$ ) 1.0 mM, and ( $\bullet$ ) 2.0 mM. The lines were drawn using linear equations containing parameters generated from direct curve-fitting to equation (8). Initial velocities (units/ug) were measured using the Fru-6P-coupled assay.

**B**

**TABLE 2.1**  
*Product Inhibition Patterns for the Reverse Reaction*

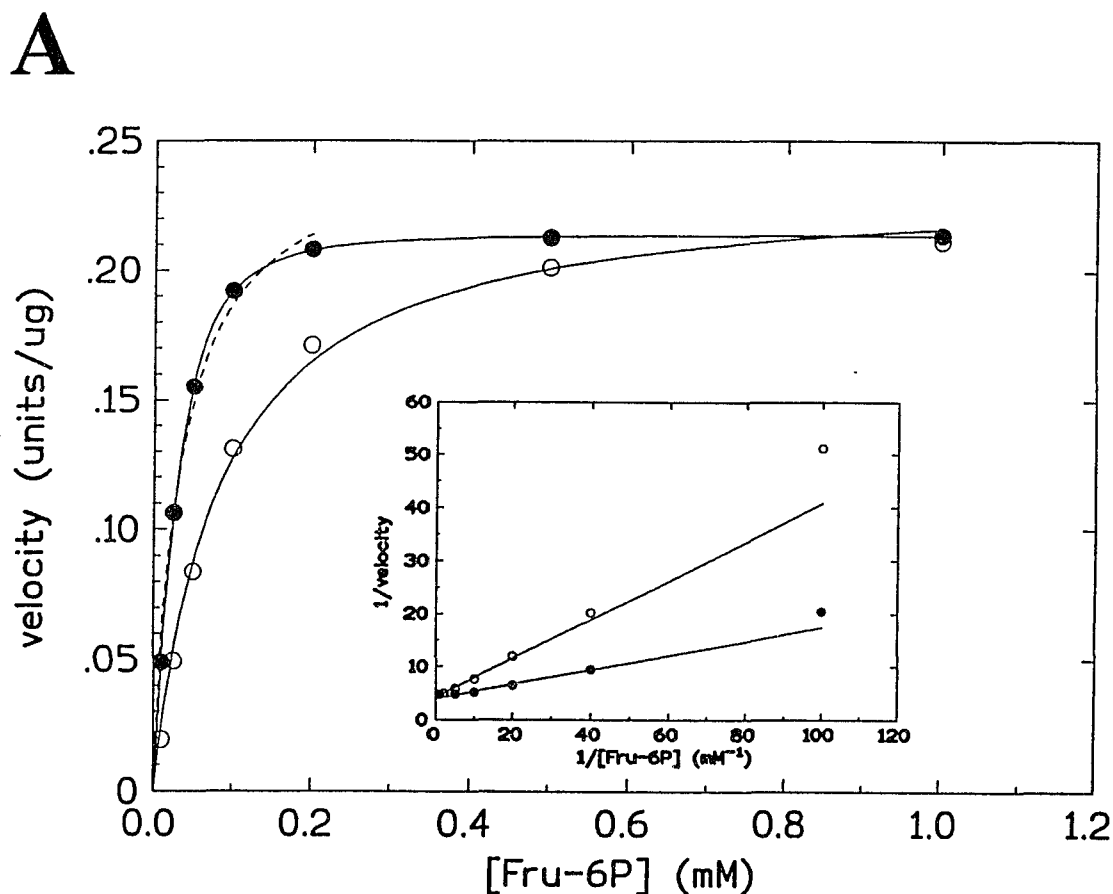
[Fru-1,6BP] (mM)	[MgADP] (mM)	inhibitor	pattern <sup>a</sup>	K <sub>iS</sub> ( $\mu$ M)	K <sub>iI</sub> ( $\mu$ M)
varied	0.91	MgATP <sup>b</sup>	NC (or C)	52 $\pm$ 4	676 $\pm$ 47
0.50	varied	MgATP	C	14 $\pm$ 1	N.A.
0.50	varied	Fru-6P <sup>c</sup>	NC	7 $\pm$ 2	55 $\pm$ 11
varied	0.91	Fru-6P	C	6 $\pm$ 0.5	N.A.

<sup>a</sup>NC= noncompetitive; C=competitive inhibition. <sup>b</sup>When MgATP was the product inhibitor, the Fru-6P-coupled assay was used. <sup>c</sup>When Fru-6P was the product inhibitor, the ATP-coupled assay was used. N.A., not applicable.

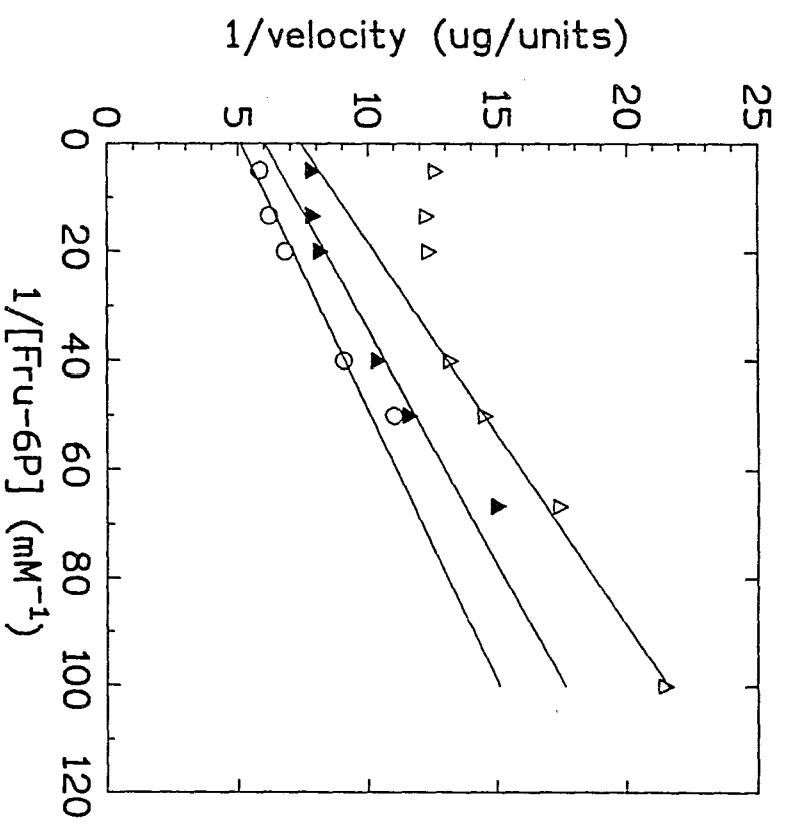


reverse reaction. When GDP is added to a PFK assay in which  $\text{NADP}^+$  reduction is coupled to ATP *via* hexokinase (see Methods section), which will not accept GTP as a substrate, the GTP produced in the reverse PFK reaction is not detected and “inhibition” results. The curvature or linearity of double-reciprocal plots for initial velocity studies in the presence of GDP can provide evidence as to whether the mechanism is ordered with ADP (GDP) binding first (curved plots), or random (linear plots). As expected, the plots obtained showed that GDP is a competitive “inhibitor” with respect to MgADP and a noncompetitive “inhibitor” with respect to Fru-1,6BP, indicating that ADP (or GDP) can bind first to the enzyme in either an ordered or a random mechanism. More significantly, the plots were linear. This result is consistent with a random mechanism, since nonlinear inhibition would have been observed had the mechanism been ordered. A similar result has been reported for rabbit muscle PFK (Hanson *et al.*, 1973). Altogether, the results of both the product inhibition and the mixed alternate substrate studies in the reverse direction are consistent with a rapid-equilibrium random mechanism that includes the formation of an abortive E-MgADP-Fru-6P complex.

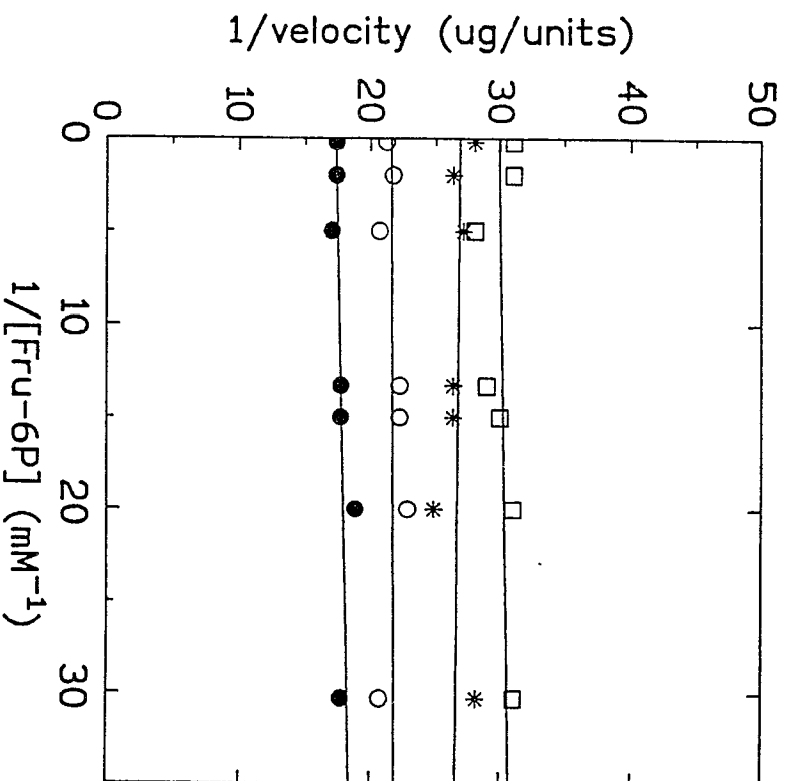
*The Forward Reaction: Fructose 6-phosphate Saturation of BsPFK*—Valdez and coworkers (1989) showed that Fru-6P saturation of BsPFK is hyperbolic. Our findings confirm this result, and further indicate that simple Michaelis-Menten kinetics cannot fully explain the saturation behavior of BsPFK. As shown in Fig. 2.2A (*dashed curve*), in the presence of varied Fru-6P concentrations that are less than about one-third the fixed MgATP concentration, the Fru-6P saturation data fit the Michaelis-Menten equation well ( $R^2=0.994$ ). A  $K_m(\text{Fru-6P})$  of 0.03 mM is obtained under these conditions. However, when the  $[\text{Fru-6P}]/[\text{MgATP}]$  ratio is greater than about one-third (Fig. 2.2A, *upper curve*), a flattening is observed. Thus, when analyzed over the entire 0.01 to 1.0 mM range, the saturation data fit the Michaelis-Menten equation less well ( $R^2=0.988$ ).



**FIGURE 2.2. Saturation Curves and Initial Velocity Plots with Respect to Fru-6P.** (A) Fru-6P Saturation Curves. Dependence of the velocity of the BsPFK-catalyzed reaction on Fru-6P concentration in the presence of (●) 0.5 mM or (○) 10.0 mM MgATP. The upper curve was generated by fitting the data to eqn. (9), whereas the lower curve was generated by curve-fitting to eqn. (6). The dashed line was generated by fitting the data between 0.01 and 0.2 mM Fru-6P in the upper curve to eqn. (6). (inset) Double-reciprocal plots of the same data. The lines were drawn using linear equations containing parameters generated from fitting the data between 0.01 and 0.2 mM Fru-6P to eqn (6). Initial velocities (units/ug) were measured using the Fru-1,6BP-coupled assay. (B) Initial velocity plot. Reciprocal of initial velocity *versus* reciprocal of Fru-6P concentration between 0.01 and 0.20 mM Fru-6P in the presence of (Δ) 0.05, (▲) 0.10, and (○) 0.20 mM MgATP. The lines were drawn using linear equations containing parameters generated by direct fitting of a selected range of data points to eqn. (8). (C) Initial velocity plot. Reciprocal of initial velocity *versus* reciprocal of Fru-6P concentration between 0.033 and 5.0 mM Fru-6P in the presence of different fixed low levels of MgATP: (□) 0.04, (\*), 0.05, (○) 0.067, and (●) 0.10 mM. Lines were generated by linear regression analysis.

**B**

C



In the presence of high levels of MgATP (greater than  $30 \times K_M$ ) Fru-6P saturation curves do not flatten within the normal 0.01 to 1.0 mM Fru-6P concentration range. Rather, saturation follows Michaelis-Menten kinetics (Fig. 2.2A, *lower curve*) throughout the entire range. Inhibition by MgATP is apparent, and this inhibition appears competitive with respect to Fru-6P (Fig. 2.2A, *inset*). Indeed, when Fru-6P saturation data collected in the presence of fixed levels of MgATP equal to 0.5 mM, 5.0 mM and 10.0 mM are analyzed according to the method of Cleland (1979), the data fit the equation for linear competitive inhibition (eqn. 10) well, yielding a linear slope replot and a  $K_{is}$  of  $5.2 \pm 0.5$  mM. A Hill coefficient of  $1.05 \pm 0.05$  is obtained for each of the three saturation curves. Thus, MgATP inhibition is not associated with cooperative Fru-6P binding as it is for EcPFK, where Hill coefficients increase from 1.4 to 3.6 in the presence of fixed MgATP concentrations ranging from very low levels to above-saturating levels (Johnson and Reinhart, 1992).

The flattening effect observed in the Fru-6P saturation curve when the  $[\text{Fru-6P}]/[\text{MgATP}]$  ratio is greater than about one-third is seen in double-reciprocal plots as a leveling-off of the slope near the  $1/v$  axis. This leveling-off effect is evident in Fig. 2.2B, which shows initial velocity plots with respect to variable Fru-6P concentration at different fixed levels of MgATP near its  $K_M$  value. These results indicate that MgATP concentration is rate-limiting when the  $[\text{MgATP}]/[\text{Fru-6P}]$  ratio is less than two or three. The effect is more apparent in Fig. 2.2C, which shows that the reaction rate remains steady and independent of Fru-6P concentration between 0.033 and 5.0 mM in the presence of fixed MgATP concentrations at or below its  $K_M$  value (0.1 mM). Overall, these studies suggest that MgATP binds to BsPFK under non rapid-equilibrium conditions, and that the rate of catalysis is faster than the rate of MgATP binding. [The deviation from linearity at low Fru-6P concentration in the presence of 0.1 and 0.2 mM MgATP in Fig. 2.2B is most likely the result of substrate binding via a kinetically-disfavored pathway (see Discussion section)].

The linear regions of the plots in Fig. 2.2B can be fit to the initial velocity equation for a sequential bireactant mechanism in rapid-equilibrium (eqn. 8), assuming A is MgATP and B is Fru-6P. When this is done, the following kinetic parameters are obtained:  $k_{cat} = 112 \pm 7 \text{ s}^{-1}$ ,  $K_a = 40 \pm 27 \text{ }\mu\text{M}$ ,  $K_b = 2 \pm 18 \text{ }\mu\text{M}$ , and  $K_{ib} = 68 \pm 43 \text{ }\mu\text{M}$ . The double-reciprocal lines generated from curve-fitting to eqn. (8) intersect to the left of the ordinate and on the abscissa, a result consistent with a sequential mechanism in the forward direction.

*MgATP Saturation and Substrate Inhibition*—The Michaelis-Menten equation fits the MgATP saturation data well ( $R^2 = 0.996$ ) in the presence of saturating Fru-6P as long as the varied MgATP concentration is below ten-fold the fixed Fru-6P concentration (Fig. 2.3, *thick dashed line*). A  $K_m(\text{MgATP})$  of 0.1 mM is obtained under these conditions. However, inhibition becomes apparent at high MgATP concentrations (Fig. 2.3), and this inhibition is more pronounced at the lower Fru-6P concentration (*lower curve*). Furthermore, as the fixed level of Fru-6P is decreased, the inhibition becomes apparent at a lower MgATP concentration. The saturation curves tend to rise to a maximum, then decrease to a plateau.

The inhibition by high levels of MgATP results in non-linear double-reciprocal plots with respect to variable MgATP concentration. As shown in Figure 2.3 (*inset*), the double-reciprocal plots pass through a minimum, then bend upward as they approach the  $1/v$  axis. This initial velocity pattern is indicative of substrate inhibition (Segel, 1975a) by high levels of MgATP. Because of their upward curvature, the lines do not intersect to the left of the ordinate. Thus, the initial velocity data with respect to MgATP do not fit the equation for a sequential bireactant mechanism in rapid equilibrium (eqn. 8).

*MgATP Saturation of the GV212 BsPFK Mutant*—It is conceivable that the inhibition exhibited by MgATP results from the binding of MgATP in a site other than the active site, e.g., the effector site. In order to address this possibility, the ability of

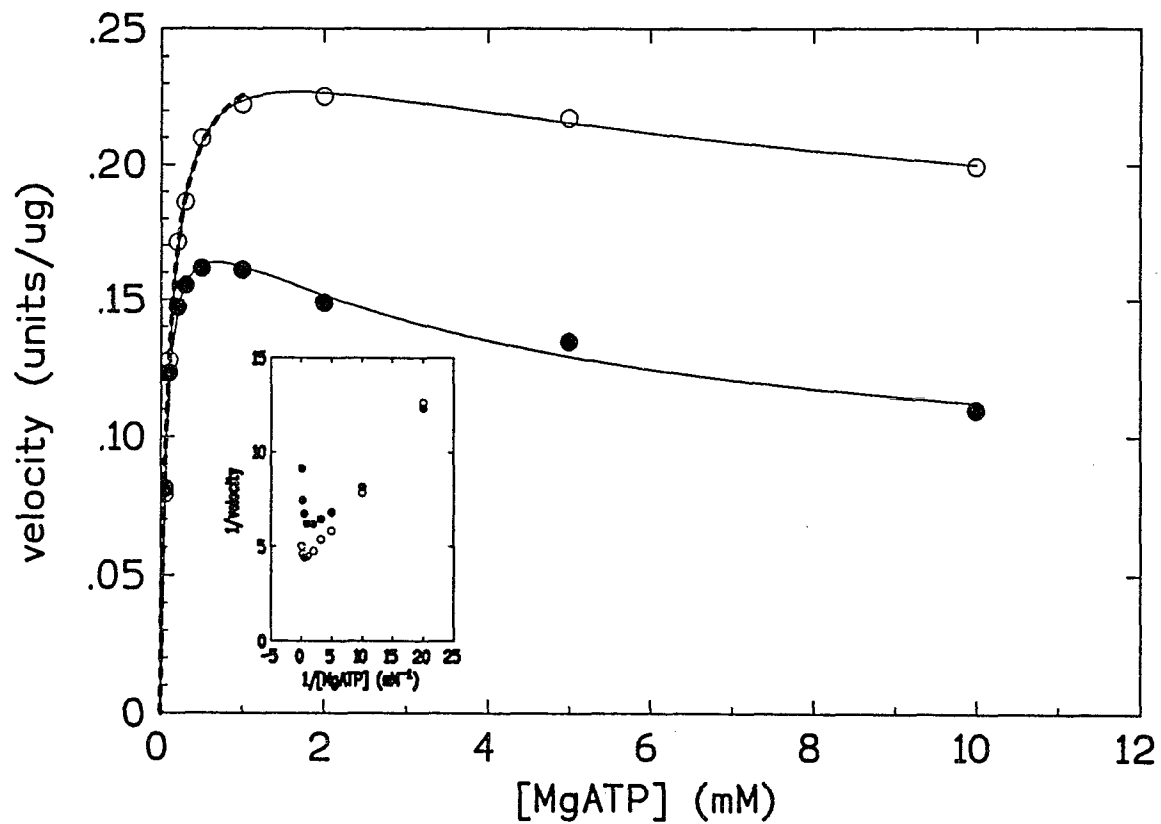


**FIGURE 2.3.** Dependence of the BsPFK-catalyzed Reaction Rate on MgATP concentration. Fru-6P concentration was kept fixed at (●) 0.05 mM or (○) 0.2 mM. Both curves were generated by fitting the data to eqn. (9). The thick dashed line was generated by fitting the data between 0.05 and 1.0 mM in the upper curve to eqn. (6). (*inset*) Double-reciprocal plots of the same data.

MgATP to inhibit a mutant BsPFK enzyme that has the glycine at position 212 replaced with a valine (GV212) was investigated. Glycine 212 is located at the hinge of the 8H loop, which has been proposed to be important in the BsPFK allosteric transition (Schirmer and Evans, 1990). Residue 212 is situated along the border of the effector binding cleft near the site where the purine ring of a bound ADP or GDP molecule would be located.

We have found that PEP inhibition of the GV212 mutant cannot be reversed by GDP or ADP, and that neither ADP nor GDP bind well to the effector site (Zhu *et al.*, manuscript in preparation). Presumably, binding of MgATP in the effector site would likewise be disrupted. Figure 2.4 shows that the ability of MgATP to inhibit the enzyme is unaffected by the mutation (the curves appear nearly identical). This observation suggests that the inhibition is not due to the binding of MgATP in the effector site.

*Alternative Nucleoside Triphosphate (NTP) Substrates*—In addition to ATP, the nucleoside triphosphates GTP, UTP and CTP can all serve as phosphoryl donors in the BsPFK-catalyzed reaction. All four NTPs display saturation profiles similar to those in Fig. 2.3, which tend to rise to a maximum, then drop to a plateau at high MgNTP concentrations. Surprisingly, although the four NTPs have different Michaelis constants (Table 2.2), they all give the same relative velocity ( $v/V_{\max}$ ) at a concentration of 10 mM (not shown). Thus, they inhibit BsPFK to essentially the same extent when present at high (10 mM) concentration.

*Product and Dead-end Inhibition Studies of the Forward Reaction*—Product inhibition studies as well as dead-end inhibition studies using the non-reactive ATP analogs  $\beta,\gamma$ -methyleneadenosine 5'triphosphate (AMPPCP) and 5' adenylymidodiphosphate (AMPPNP), and the non-reactive Fru-6P analog arabinose 5-phosphate (Ara-5P), were performed on the forward reaction in order to further delineate the kinetic mechanism. As with the reverse reaction, primary



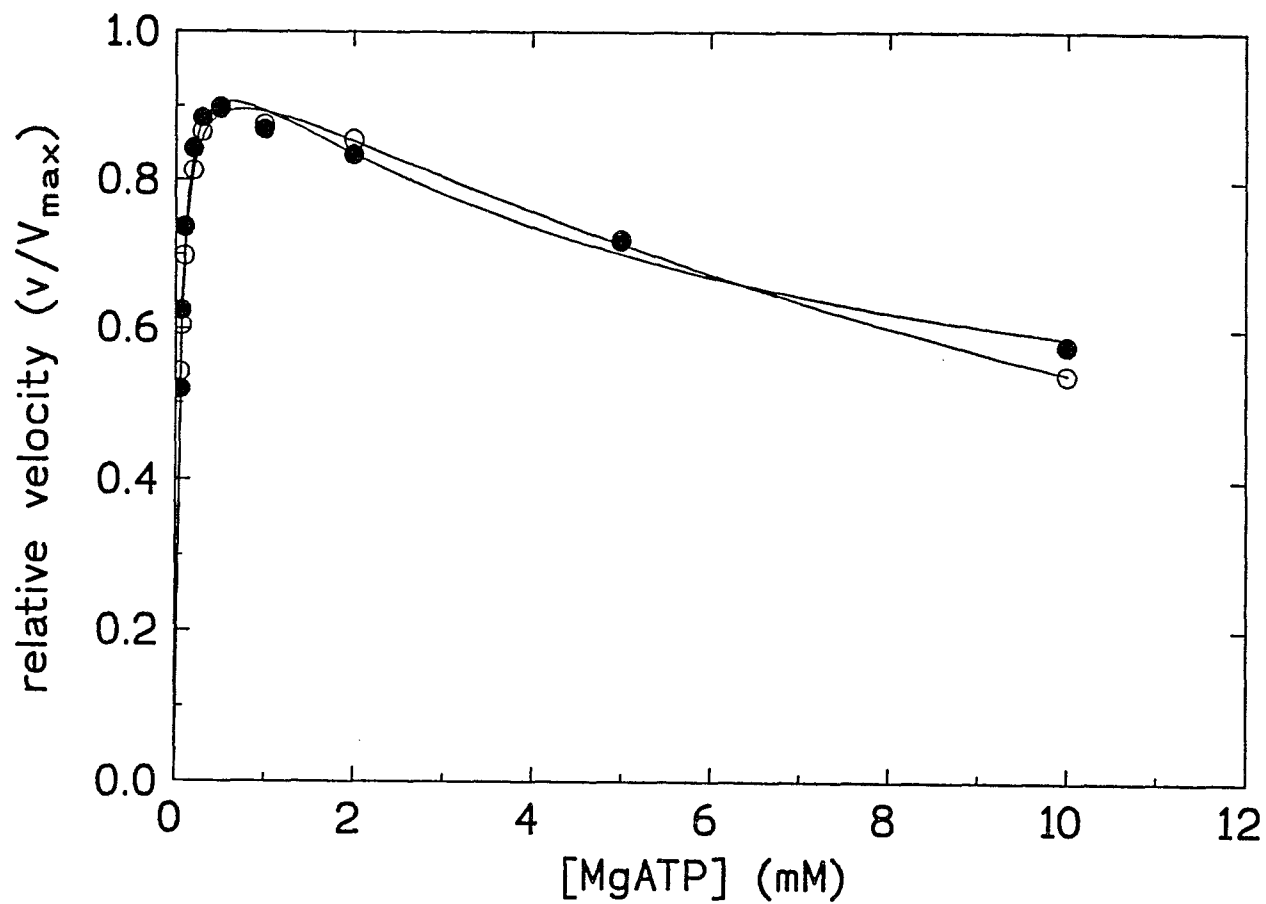


**FIGURE 2.4 . MgATP Inhibition of the Mutant GV212 BsPFK Enzyme.** Initial velocity was measured *versus* MgATP concentration for (●) mutant and (○) wild-type BsPFK in the presence of 0.05 mM Fru-6P. Both curves were generated by curve-fitting to eqn. (9).

**TABLE 2.2**  
*Alternative Nucleoside Triphosphate (NTP) Substrates*

NTP	$K_m(\text{NTP})^a$ (mM)	Percent of $k_{cat}(\text{ATP})$	$K_m(\text{Fru-6P})^b$ ( $\mu\text{M}$ )
ATP	$0.07 \pm 0.01$	100	$33 \pm 5$
GTP	$0.18 \pm 0.01$	73	$28 \pm 4$
CTP	$2.6 \pm 0.2$	98	$146 \pm 19$
UTP	$2.8 \pm 0.2$	93	$68 \pm 7$

<sup>a</sup>Fru-6P concentration was kept fixed at 1.0 mM (saturating) for these determinations. <sup>b</sup>NTP concentration was kept fixed at 5 x  $K_m(\text{NTP})$ . In each assay,  $\text{Mg}^{++}$  was present in excess of the NTP concentration.

double-reciprocal plots were constructed to determine the nature of the inhibition, and the saturation data were fit directly to equations for linear competitive, linear noncompetitive, and linear uncompetitive inhibition. The patterns obtained in the plots and the parameters obtained from curve-fitting are shown in Table 2.3.

The product and dead-end inhibition results for the forward reaction are somewhat more difficult to interpret than are the product inhibition results for the reverse reaction. The double-reciprocal plots for inhibition by both Fru-1,6BP and Ara-5P with respect to MgATP (up to 1 mM) yield nearly parallel yet divergent lines (Table 2.3). In both of these inhibition studies, when the MgATP concentration is extended to 10 mM, the plots bend upward as they approach the  $1/v$  axis, indicating substrate inhibition at high (>2 mM) MgATP concentration. Because of the curvature, it is not possible from these plots alone to establish whether the inhibition is uncompetitive (parallel lines) or noncompetitive (convergent lines). An uncompetitive inhibition pattern would be expected in these studies if the kinetic mechanism were ordered with MgATP binding first, whereas a noncompetitive pattern would be expected if the mechanism were random. However, the ordered mechanism under consideration here is incompatible with the competitive nature of the inhibition by MgATP with respect to Fru-6P seen in Fig. 2.2A. Competitive substrate inhibition by MgATP would be possible for an ordered mechanism only when Fru-6P is the first substrate to bind to the enzyme; it is not possible for an ordered mechanism in which MgATP binds first to the enzyme (Segel, 1975a). On the other hand, competitive substrate inhibition by MgATP with respect to Fru-6P is consistent with a random mechanism. In this case, inhibition can occur in several ways, including the two being proposed here: (1) abortive binding of MgATP in the Fru-6P site, and (2) reaction flux through a kinetically-disfavored substrate binding pathway (see below). Thus, taking the substrate inhibition into account, the most likely interpretation of the product and dead-end inhibition results is that Fru-6P and MgATP bind to the enzyme in random order.

**TABLE 2.3**  
*Product and Dead-end Inhibition Patterns for the Forward Reaction*

**A. Product Inhibition Patterns.**

[Fru-6P] (mM)	[MgATP] (mM)	product inhibitor	pattern <sup>a</sup>	K <sub>is</sub> (mM)	K <sub>ij</sub> (mM)
0.2	varied	MgADP	C	0.50 ± 0.01	N.A.
varied	0.87	MgADP <sup>b</sup>	NC	22 ± 2	3.92 ± 0.05
1.0	varied	Fru-1,6BP <sup>c</sup>	UC (NC) <sup>d</sup>	N.A.	14 ± 2

**B. Dead-end Inhibition Patterns.<sup>b</sup>**

[Fru-6P] (mM)	[MgATP] (mM)	dead-end inhibitor	pattern	K <sub>is</sub> (mM)	K <sub>ij</sub> (mM)
0.20	varied	AMPPCP	C	1.12 ± 0.04	N.A.
varied	0.87	AMPPCP	NC	10.2 ± 0.9	9.8 ± 0.8
0.20	varied	AMPPNP	C (or NC)	0.05 ± 0.02	1.56 ± 0.81
varied	0.87	AMPPNP	NC	0.29 ± 0.09	0.40 ± 0.12
varied	0.87	Ara-5P	C	1.2 ± 0.2	N.A.
0.20	varied	Ara-5P	UC (NC) <sup>d</sup>	N.A.	6.2 ± 0.5

<sup>a</sup>NC=noncompetitive; C=competitive; and UC=uncompetitive. <sup>b</sup>The Fru-1,6BP-coupled assay was used for these studies. <sup>c</sup>When Fru-1,6BP was the product inhibitor, the ADP-coupled assay system was used. Fru-1,6BP inhibition with respect to Fru-6P could not be determined since the phospho(enol)pyruvate required for the assay is an allosteric inhibitor of BsPFK at low Fru-6P concentration. <sup>d</sup>Parallel lines were observed in the double-reciprocal plots. See the text for further discussion. The pattern in parentheses is that expected in the absence of substrate inhibition. N.A., not applicable.

An examination of the AMPPCP and AMPPNP inhibition patterns (Table 2.3) sheds light on the mechanism by which ATP inhibits BsPFK. Although AMPPCP inhibition with respect to ATP is purely competitive, AMPPNP inhibition with respect to ATP, though mostly competitive, nevertheless has some noncompetitive character. In the latter case, the lines in the double-reciprocal plot (Fig. 2.5A) clearly converge just to the left of the  $1/v$  axis. The simplest interpretation of this result is that AMPPNP (and presumably ATP) binds abortively in the Fru-6P site, forming a dead-end E-MgATP-AMPPNP [or E-(MgATP)<sub>2</sub>] complex. Further evidence for the formation of this complex is seen in the double-reciprocal plot for AMPPNP inhibition with respect to Fru-6P (Fig. 2.5B), which gives an essentially noncompetitive (mixed-type) pattern composed of lines that intersect progressively closer to the  $1/v$  axis as AMPPNP concentration is increased. This effect is not seen for AMPPCP. AMPPCP apparently does not bind abortively as does AMPPNP, most likely because the orientation of its  $\gamma$ -phosphate group is quite different from that of AMPPNP, which is similar to that of ATP (Yount *et al.*, 1971; Larsen *et al.*, 1969). These results suggest that ATP binds in the Fru-6P site via its  $\gamma$ -phosphate group. Thus, abortive binding at least partially explains the inhibition seen at high MgATP concentration.

### Discussion

The intersecting patterns of lines obtained in the double-reciprocal initial velocity plots for the reverse reaction indicate that the kinetic mechanism is sequential rather than ping-pong. Further, the patterns of lines obtained in the reverse reaction product inhibition (Table 2.1) and mixed alternate substrate (GDP) studies indicate that the kinetic mechanism of the reverse reaction is rapid equilibrium random. The results of product inhibition and dead-end inhibition studies of the forward reaction (Table 2.3) are also consistent with a random mechanism, after taking into account the effect of substrate inhibition by MgATP. The binding of MgATP to the enzyme was found to be rate-limiting when its concentration is low. Thus, the kinetic mechanism of BsPFK in

A

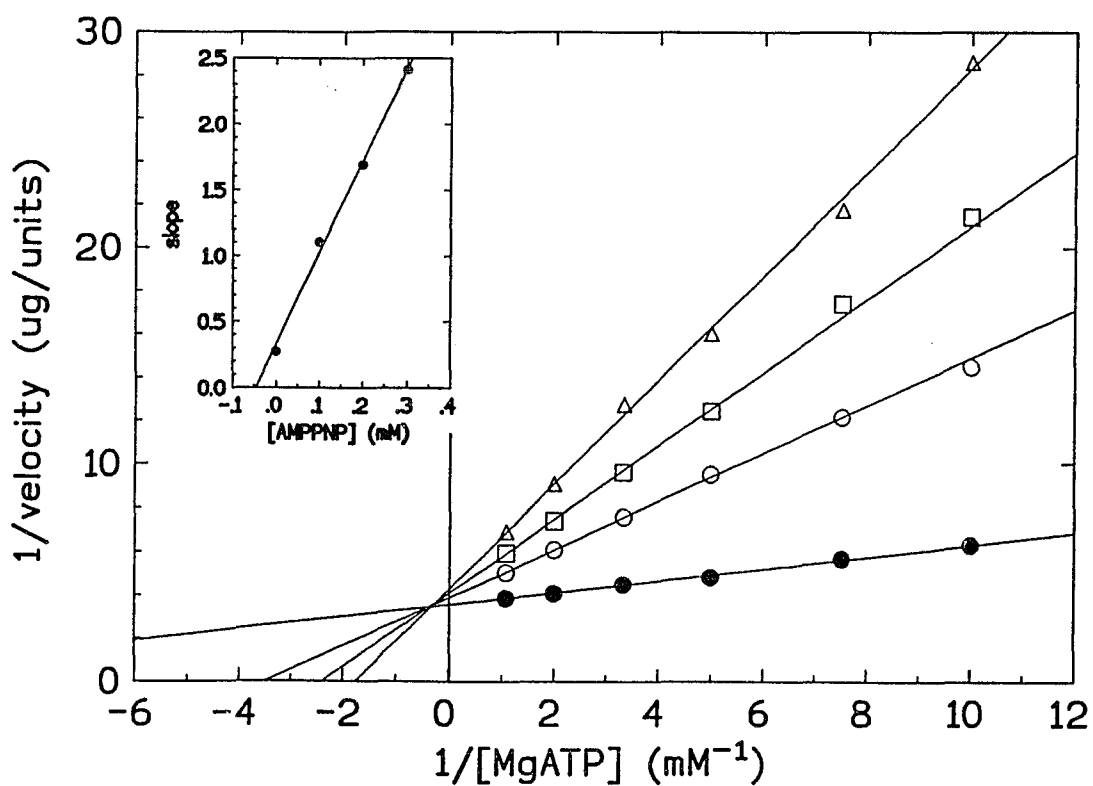
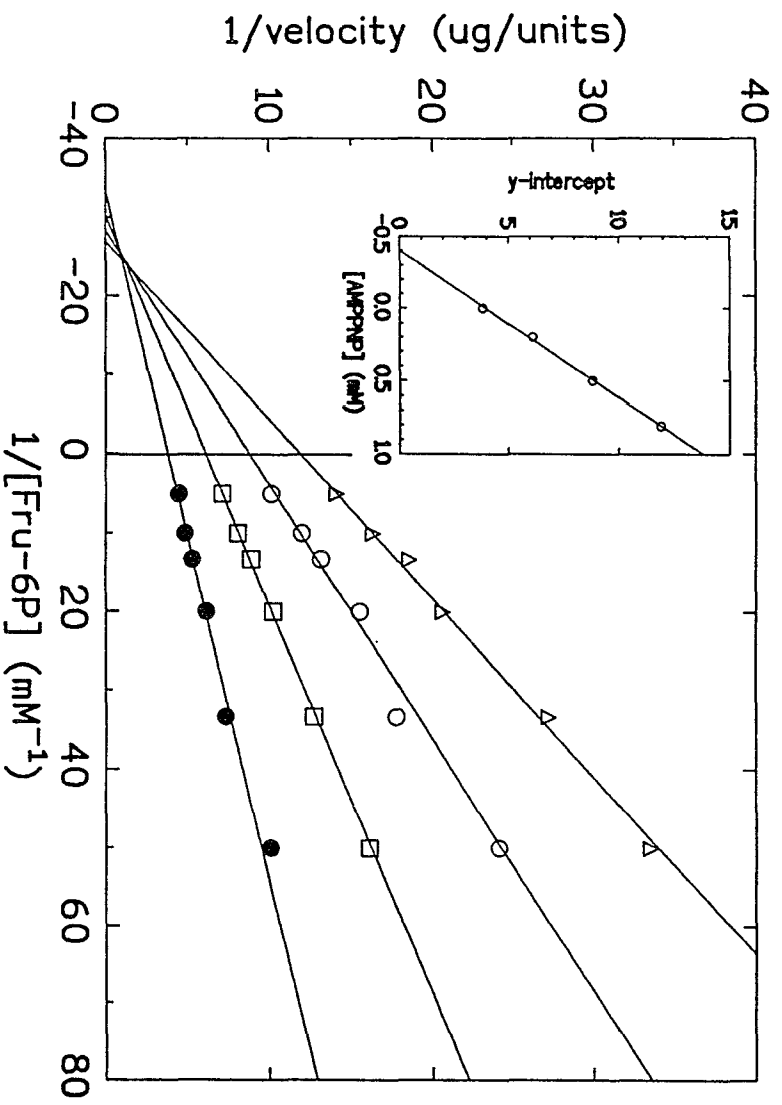
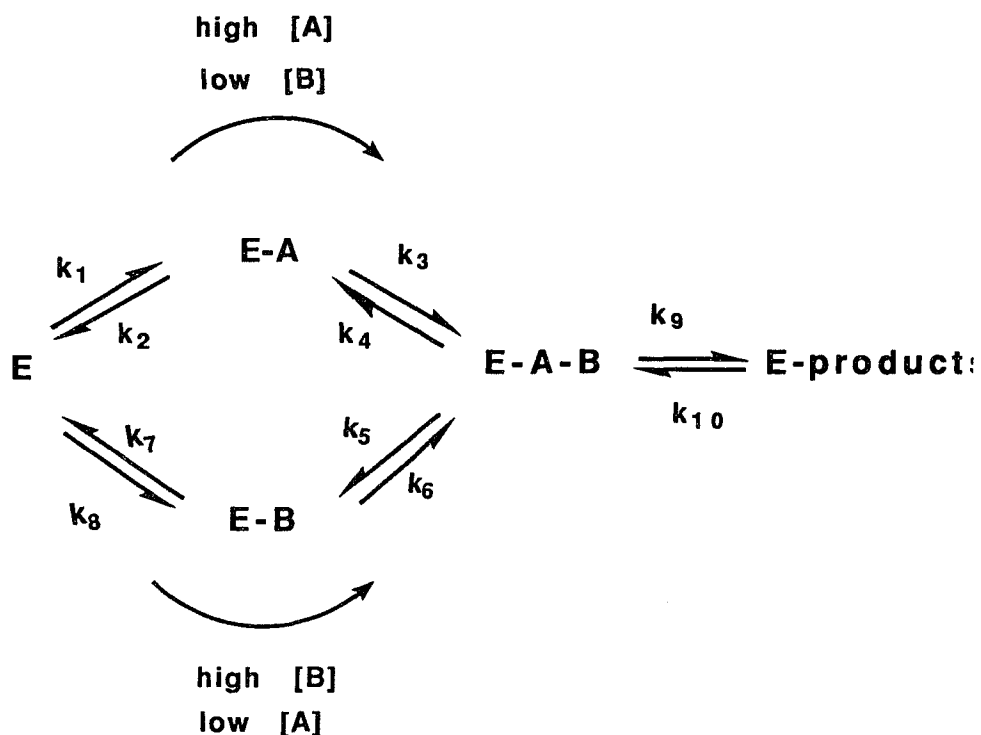


**FIGURE 2.5. AMPPNP Inhibition Patterns.** (A) Plot of the reciprocal of initial velocity *versus* the reciprocal of MgATP concentration in the presence of 0.2 mM Fru-6P and (●) 0 mM, (○) 0.1 mM, (□) 0.2 mM, or (Δ) 0.3 mM AMPPNP. (inset) Slope replot. (B) Plot of the reciprocal of initial velocity *versus* the reciprocal of Fru-6P concentration in the presence of 0.87 mM MgATP and (●) 0 mM, (□) 0.2 mM, (○) 0.5 mM, or (Δ) 0.81 mM AMPPNP. (inset) Intercept replot. Initial velocities (units/ug) were measured using the Fru-1,6BP-coupled assay.

**B**



the forward direction can best be described as sequential random with binding of MgATP being rate-limiting, *i.e.*, the rate of its binding is lower than the catalytic rate.



**SCHEME I**

The kinetic mechanism in the forward direction is depicted in Scheme I, where E is free enzyme, A and B are substrates MgATP and Fru-6P, respectively, E-A and E-B are their binary complexes, and E-A-B is the reactive, ternary complex. The constants  $k_1$  through  $k_{10}$  are rate constants for the steps indicated. It is assumed that the binding of MgATP is slow relative to the catalytic step, *i.e.*,  $k_1, k_6 \ll k_9$ . The curved arrows in Scheme I indicate that different substrate binding pathways are followed in the presence of different relative amounts of the substrates, assuming non rapid-equilibrium conditions.

The MgATP saturation results for the mutant GV212 enzyme (Fig. 2.4) indicate that the substrate inhibition observed is not due to MgATP binding in the effector site. Thus, inhibition by MgATP occurs as a result of its binding in the active site. Within



this context, there are several possible mechanisms by which MgATP inhibition can occur: (1) binding of MgATP to the binary product complex E-Fru-1,6BP to form a dead-end ternary complex E-Fru-1,6BP-MgATP, from which Fru-1,6BP dissociates more slowly than it does from the normal product ternary complex. [Inhibition of liver alcohol dehydrogenase by ethanol occurs *via* a similar mechanism (Dalziel and Dickinson, 1966)]. (2) abortive binding of MgATP in the Fru-6P site (linear substrate inhibition; Cleland, 1979), or (3) the existence of two alternative pathways to the reactive ternary complex, with one pathway kinetically-favored (Dalziel, 1957; Ferdinand, 1966). In this last mechanism, inhibition by MgATP would result from the binding of substrates *via* the disfavored pathway.

A mechanism for MgATP inhibition that involves formation of a dead-end complex E-Fru-1,6BP-MgATP is shown to be unlikely from the results of product inhibition studies. Specifically, inhibition by MgATP with respect to Fru-1,6BP in the reverse direction (Table 2.1), indicates that the complex E-Fru-1,6BP-MgATP does not form readily.

The results of the dead-end inhibition studies in the forward direction using AMPPNP (Table 2.3 and Fig. 2.5) give evidence for abortive binding of AMPPNP, and presumably ATP, in the Fru-6P site via their  $\gamma$ -phosphate groups. Such abortive binding at least partially explains the observed inhibition by MgATP. However, the experimental evidence suggests that this is not the only mechanism involved.

Dalziel (1957) has shown that substrate inhibition (and activation) are inherent in an alternative-pathways mechanism when the binding or release of substrates is rate-limiting and the rate constants for the steps involved are such that one of the two pathways is kinetically-disfavored. Ferdinand (1966) presented the theoretical basis (eqn. 9) for this mechanism, which can give rise to a variety of non-hyperbolic initial velocity curves (Segel, 1975b), the shapes of which depend on the relative magnitudes of the rate constants for the steps of the mechanism. There is evidence that BsPFK

obeys such a mechanism: (1) The binding of MgATP is clearly rate-limiting when its concentration is low, *i.e.*, when it is less than about three times the Fru-6P concentration. This indicates that catalysis is fast relative to the rate of MgATP binding. (2) The observed substrate inhibition by MgATP when its concentration is greater than 10-fold the Fru-6P concentration (Fig. 2.2B and Fig. 2.3) is consistent with the binding of substrates through a kinetically-disfavored pathway when MgATP concentration is relatively high. Thus, the upper binding pathway in Scheme I, with MgATP binding first and Fru-6P binding second, is the disfavored pathway for BsPFK. (3) The initial velocity equation for the alternative-pathways mechanism (eqn. 2.4) fits the Fru-6P saturation data well ( $R^2$  is 1.000 for the upper curve in Fig. 2.2A) with the assumption that  $i_m=j_l$  and  $k_i<m_j$ , and it fits the MgATP saturation data well ( $R^2$ -values are 0.998 and 0.984 for the curves in Fig. 2.3) with the assumption that  $i_m<j_l$  and  $k_i<m_j$ . Thus, a steady-state alternative-pathways mechanism is consistent with not only the observed substrate inhibition by MgATP, but also with other aspects of BsPFK kinetic behavior in the forward direction.

Substrate activation can be observed in a steady-state alternative-pathways mechanism. Typically, this activation is evident as sigmoidicity in saturation curves with respect to the first substrate to bind the enzyme in the kinetically-favored pathway. However, whether or not activation (hence, sigmoidicity) is observed depends on the various rate constants involved, and the extent to which one pathway is kinetically-favored (or disfavored). Thus, the reason sigmoidicity is not observed in the Fru-6P saturation curve for BsPFK is probably because the extent to which the lower pathway in Scheme I is favored (or the upper pathway is disfavored) is not great.

Altogether, the results discussed above provide evidence that BsPFK in the reverse direction obeys a rapid-equilibrium random mechanism. In the forward direction, it obeys an alternative-pathways kinetic mechanism that involves (1) non rapid-equilibrium binding of MgATP ( $k_1, k_6 \ll k_9$  in Scheme I), evident when MgATP

concentration is low, and (2) substrate binding through a kinetically-disfavored pathway (the upper pathway in Scheme I) evident when MgATP concentration is high. In addition, abortive binding of the  $\gamma$ -phosphate of ATP in the Fru-6P site contributes to some extent to the inhibition seen at high MgATP concentration. As such, the kinetic mechanism of BsPFK shares features in common with the kinetic mechanisms of other PFKs, including those from rabbit muscle, *Ascaris suum*, and *E. coli*. Using initial velocity, product inhibition and dead-end inhibition studies, Bar-Tana and Cleland (1974a,b) have shown that the kinetic mechanism of rabbit muscle PFK is sequential random, being rapid-equilibrium in the reverse direction but not in the forward direction, where the rate constants for the release of substrates are lower than the catalytic constant. Although the kinetic mechanism of *Ascaris suum* PFK in the forward direction is predominantly steady-state ordered (Rao *et al.*, 1987), it nevertheless involves some randomness in the order of substrate binding. In the reverse direction, the mechanism is essentially rapid-equilibrium random.

Studies by Deville-Bonne *et al.* (1991a) have indicated that the kinetic mechanism of EcPFK is sequential random, and that the binding of one substrate antagonizes the binding of the other. Johnson and Reinhart (1992) have further studied the interactions between MgATP and Fru-6P in the active site of EcPFK by thermodynamic linked-function analysis. Their results indicate that all the observed features of substrate interaction can be explained by two independent couplings: an antagonistic MgATP/Fru-6P coupling extending between active sites, and a MgATP-induced Fru-6P/Fru-6P coupling. Zheng and Kemp (1992) have recently proposed that ATP inhibition of EcPFK involves substrate antagonism coupled with a steady-state random mechanism in which the rate of catalysis is too high to permit rapid equilibration of substrates. It is interesting to note that the kinetic behavior of 3-deoxy-D-arabino-heptulosonate 7-phosphate synthetase from *Rhodospirillum rubrum*,

which is proposed to follow an alternative-pathways mechanism (Jensen and Trentini, 1970), closely resembles that of EcPFK (Zheng and Kemp, 1992).

Despite similarities between the kinetic mechanisms of EcPFK and BsPFK, the mechanisms by which MgATP inhibits the two enzymes are clearly different. Specifically, MgATP inhibition appears to be allosteric for EcPFK (Berger and Evans, 1991) but not for BsPFK. The reason for this difference has only recently begun to be understood. Steady-state fluorescence studies show that MgATP and Fru-6P each bind to EcPFK non-cooperatively in the absence of the other (Deville-Bonne and Garel, 1992). In these studies, cooperative Fru-6P binding was induced by the presence of AMPPCP (and presumably ATP), although the Hill coefficient for the cooperative binding was not as high as that observed in steady-state kinetic measurements (2.0 *versus* 3.8-4.0). Based on studies showing that both  $k_{cat}$  and  $n$  (the Hill coefficient) vary with pH, Deville-Bonne *et al.* (1991b) have suggested that catalysis and cooperativity are linked in EcPFK. Thus, it is the superimposition of (1) “kinetic cooperativity” resulting from non-equilibrium conditions and (2) concerted binding cooperativity (Monod *et al.*, 1965) that fully explains the allosteric behavior of EcPFK.

The lack of allosteric regulation of BsPFK by MgATP suggests that, unlike EcPFK, catalysis and cooperative Fru-6P binding are not linked. Cooperative binding of Fru-6P does occur, but only in the presence of PEP. The data presented in this paper indicate that MgATP inhibition of BsPFK occurs entirely within the active site by means of (1) abortive MgATP binding and (2) reaction flux through the kinetically-disfavored substrate binding pathway. Thus, inhibition of BsPFK by MgATP is a process distinct from allosteric inhibition by PEP.

Finally, the nature of the regulation by MgATP and PEP of BsPFK is compatible with the thermostability of the enzyme. Large conformational changes, which could lead to structural destabilization, are apparently not part of the response of the enzyme to inhibitors. The allosteric transition (Schirmer and Evans, 1990) involves minimal

movement: a rotation by  $7^\circ$  of one pair of rigid dimers relative to the other, along with a coordinated back-and-forth movement of a pair of loops (the 8H and 6F loops) across the dimer-dimer interface. Likewise, inhibition by ATP apparently involves little if any conformational change.

## **Chapter 3**

### **A Chimeric Bacterial Phosphofructokinase Exhibits Cooperativity in the Absence of Heterotropic Regulation**

Phosphofructokinase (PFK, EC 2.7.1.11) catalyzes the transfer of the  $\gamma$ -phosphate from MgATP to fructose-6-phosphate (Fru-6P) in the first committed step of glycolysis. In bacteria, PFK is regulated heterotropically by the activator ADP (or GDP) and the inhibitor phosphoenolpyruvate (PEP). The PFKs from the bacteria *Escherichia coli* and *Bacillus stearothermophilus* are remarkably similar in structure (Evans *et al.*, 1981; Shirakihara & Evans, 1988). The enzymes are both tetramers of identical subunits, their subunit  $\alpha$ -carbon traces are nearly superimposable, and they share 55% amino acid identity. They can be viewed as dimers of rigid dimers. In each enzyme, the subunit is divided into a large and a small domain, with the active site located in a cleft between the two domains. There are thus four active sites. There are also four effector sites into which PEP and ADP (or GDP) bind; these are located in deep clefts between subunits of the rigid dimer. Within the active site, the amino acid residues that bind ATP are almost entirely from the large domain, while those that bind Fru-6P are mostly from the small domain, but include two arginines (arginines 162 and 243) from across the dimer-dimer interface. Coordination of the Mg<sup>++</sup> ion as well as transfer of the  $\gamma$ -phosphate of ATP involves residues from both domains.

Despite the remarkable structural similarity between *E. coli* PFK (EcPFK) and *B. stearothermophilus* PFK (BsPFK), there is a significant kinetic and allosteric difference between them. Whereas Fru-6P saturation of BsPFK is hyperbolic in the presence of saturating MgATP levels (Valdez *et al.*, 1989), Fru-6P saturation of EcPFK is highly cooperative (Hill number around 4.0) under the same conditions (Blangy *et al.*, 1968). ATP has been termed an "allosteric" inhibitor of EcPFK (Evans, 1992) because of its ability to profoundly inhibit the enzyme at low Fru-6P concentration (Kundrot & Evans, 1990). On the other hand, ATP only slightly inhibits BsPFK, and the inhibition is clearly non-allosteric. Blangy *et al.* (1968) have shown that EcPFK obeys the Monod-Wyman-Changeux (MWC) model of allosteric behavior (Monod *et al.*, 1965), in which the protein exists in an equilibrium involving two conformational states, a

low-activity T-state and a high-activity R-state. The allosteric behavior of EcPFK has been explained in terms of this model. Recent studies, however, suggest that the MWC model cannot fully account for the cooperativity of EcPFK (Deville-Bonne *et al.*, 1991a; Berger & Evans, 1992).

X-ray diffraction studies indicate that two different subunit structures are present in the EcPFK tetramer: "open" and "closed" (Shirakihara & Evans, 1988). Therefore, an open-to-closed transition may be taking place within the EcPFK subunit. A comparison between the  $\alpha$ -carbon traces of the open and closed subunit structures reveals that most of the movement occurs within a region of the large (ATP-binding) domain. The transition apparently does not occur within the large domain of BsPFK (Schirmer & Evans, 1990).

We have constructed and studied a chimeric PFK, composed of parts of BsPFK and EcPFK, in order to investigate the structural basis for their different regulation by ATP. The chimeric enzyme (ChiPFK) contains a portion of the "rigid" large domain of BsPFK (the ATP-binding domain) grafted in-frame onto the remainder of the EcPFK subunit. The active site of ChiPFK is thus composite: residues that bind ATP are from BsPFK while those that bind Fru-6P are from EcPFK. Steady-state kinetics and fluorescence studies were performed on the chimeric PFK and the two native enzymes. The results indicate that active site of ChiPFK is locked in an "open" conformation that resembles that of the activated form of EcPFK. Nevertheless, the enzyme displays sigmoidal Fru-6P saturation kinetics (Hill number  $1.7 \pm 0.2$ ). The absence of regulation by PEP despite its ability to bind in the effector site indicates that the structural pathways of allosteric PEP inhibition are different between the two native enzymes. In many respects, ChiPFK resembles a proteolyzed derivative of EcPFK (Le Bras & Garel, 1982) that is cooperative yet insensitive to allosteric effectors. The possible origins of ChiPFK sigmoidal saturation kinetics are discussed.



## Materials and Methods

*Enzymes, Chemicals and Oligonucleotides*—Restriction endonucleases, T4 DNA ligase and T4 polynucleotide kinase were either from New England Biolabs, Inc. (Beverly, MA) or U. S. Biochemical (Cleveland, OH). NADH, NAD<sup>+</sup>, Fru-6P, ATP (and other NTPs), GDP, PEP, AMPPNP, and the auxiliary enzymes aldolase, triosephosphate isomerase and  $\alpha$ -glycerophosphate dehydrogenase were all from Sigma Chemical Co. (St. Louis, MO), as was the Cibacron Blue 3GA-agarose resin (type 3000-CL-L). Oligonucleotides were either purchased from DNA International, Inc. (Lake Oswego, OR) or synthesized on an Applied Biosystems 380A DNA Synthesizer.

*Construction of the Chimeric Gene: PCR, Cloning and Sequencing*—The chimeric gene was constructed by ligating together two polymerase chain reaction (PCR) amplification products: one from *bspfk*, the other from *ecpfk*. The two PFK genes (French & Chang, 1987; Hellinga & Evans, 1985) had previously been cloned into pUC18 plasmids, and were oriented in opposite directions. Three oligonucleotide primers were used in the PCR amplification:

<u>Primer</u>	<u>Sequence</u>
1	5'AGGAAACAGCTATGACCATGATTAC <sup>3'</sup>
2	5'CGTCCCCGGGGCCCCGACGCACG <sup>3'</sup>
3	5'CGTGCATCGGGGCCCCGGGCACTATC <sup>3'</sup>

Primer 1 was designed to hybridize to pUC18 itself just beyond the Eco RI cloning site, which is located upstream of the *bspfk* promoter in recombinant *bspfk/pUC18*, and located downstream of the *ecpfk* termination sequence in recombinant *ecpfk/pUC18*. In both cases, primer 1 points into the *pfk* insert. Primer 2 was designed to hybridize to the *bspfk* coding strand with its 3' end located at the codon for Pro 118, pointing upstream. Primer 2 contains an internal Apa I restriction site (underlined above) that also causes the mutation Val 122  $\rightarrow$  Ala. (It was reasoned that this mutation would not significantly alter the properties of the chimeric enzyme since (1) the amino acid change

is not a drastic one, and (2) there is already a degree of variation between the native enzymes at this position, i.e., valine *versus* leucine). Primer 3 was designed to hybridize to the *ecpfk* complementary strand with its 3' end located at the codon for Ile 126, pointing downstream. Like primer 2, it contains an internal Apa I site. PCR using primers 1 and 2 amplifies a region of *bspfk* stretching from beyond its promoter to codon 125. PCR using primers 1 and 3 results amplifies a region of *ecpfk* stretching from codon 118 to beyond its termination sequence. PCR was performed using a Perkin Elmer-Cetus (Norwalk, CT) DNA thermal cycler, a GeneAmp™ PCR kit, and *AmpliTaq*™ DNA polymerase. The procedure suggested in the kit was followed.

The chimeric gene was created by digesting the two PCR products with Apa I, then ligating the fragments together with T4 DNA ligase. In this way, the BsPFK gene up to codon 122 was grafted in-frame onto the EcPFK gene beginning at codon 123. The chimeric gene was cloned into pUC18 *via* its Hind III and Eco RI restriction sites. The integrity of the chimeric gene was verified by directly sequencing the entire coding region using a Sequenase™ kit (U. S. Biochemical, Inc., Cleveland, OH). No unintentional mutations were found.

*Expression and Purification of PFKs*—Both the chimeric PFK and the two native PFKs were expressed in PFK-deficient *E. coli* cells (DF1020 cells) that had been transformed with recombinant pUC18 plasmids containing the PFK genes. BsPFK was purified as described by Valdez *et al.* (1989), and EcPFK was purified as described by Kundrot & Evans (1991), but on a 40-fold larger scale. The enzymes were shown to be pure by electrophoresis on a 12% SDS-polyacrylamide gel (see Fig. 3.2A) using the method of Laemmli (1970).

Expression of ChiPFK was performed as follows: recombinant *chipfk*/pUC18 plasmid DNA was transformed into competent DF1020 cells. The cells were plated onto Luria broth (LB) agar containing 50 µg/ml ampicillin, and the plates were incubated overnight at 30°C. Six transformants were picked, directly inoculated into

3-ml volumes of LB-ampicillin (50  $\mu\text{g/ml}$ ) medium, and grown at 30°C with agitation. The cultures reached stationary phase after about 60 hours. A 1-ml aliquot of the culture having the highest PFK activity was inoculated into 500 ml of LB-ampicillin (50  $\mu\text{g/ml}$ ). This large culture was grown at 30°C, reaching stationary phase after about 24 hrs. The cells were harvested by centrifugation at 4°C. Cell pellets were brought up in buffer A (50 mM Tris-Cl, pH 7.9, 1 mM EDTA and 8 mM DTT) containing 1 mM phenylmethyl sulfonyl fluoride (PMSF), frozen in liquid nitrogen, and stored at -20°C until ready for use.

The frozen cell suspension was thawed, then sonicated and centrifuged. The resulting clear supernatant was loaded onto a Cibacron Blue 3GA-agarose column that had been equilibrated with buffer A. The loaded column was washed with 10 volumes of buffer A, and ChiPFK was then eluted with 2 mM ATP/10 mM  $\text{MgCl}_2$  in buffer A. (The column was not washed with salt prior to elution with ATP because NaCl concentrations as low as 100 mM caused elution of ChiPFK). The most active fractions were pooled and dialyzed against buffer A to remove the ATP and  $\text{Mg}^{++}$ . SDS-PAGE analysis of the PFK preparation at this point revealed the presence of several contaminating bands. The column was regenerated by washing it first with several volumes of 1.5 M NaCl, then extensively with buffer A. The dialyzed pool containing PFK activity was re-loaded, the column was washed with 5 volumes of buffer A, and ChiPFK was then eluted with 0.5 mM Fru-6P in buffer A. PFK activity came off in a broad peak. Fractions having the highest activity were pooled. The enzyme was shown to be pure by electrophoresis on a 12% SDS-polyacrylamide gel (Fig. 3.2A) using the Laemmli method (1970). Half of the pool was concentrated using an Amicon (Beverly, MA) pressure cell, then stored at 4°C as a 55% ammonium sulfate suspension. The other half was first dialyzed in buffer A to remove the Fru-6P, then concentrated in 50% glycerol/50% buffer A containing 2 mM ATP/10 mM  $\text{MgCl}_2$ , and stored at -20°C.

*Sedimentation Studies*—Sucrose gradient sedimentation was performed according to the method of Martin & Ames (1961). Each 5 to 20% sucrose gradient was buffered with 100 mM Tris-Cl, pH 8.2, containing 10 mM MgCl<sub>2</sub>, 5 mM NH<sub>4</sub>Cl, 0.25 mM EDTA, 2.0 mM DTT, and 0.5 mM Fru-6P (buffer B). An aliquot of a stock solution of PFK containing 2 to 5 µg was dialyzed at 4°C against buffer B containing 2% sucrose, combined with a similarly-dialyzed solution of yeast alcohol dehydrogenase (ADH; 10 µg), then layered between the gradient (about 4 ml) and a volume of buffer B (about 1.4 ml) placed over the gradient just prior to sample layering. The ADH was used as an internal reference standard for determining the molecular weight of the sedimenting PFK species. Sedimentation was performed at 4°C in a Beckman SW 50.1 rotor spun at 44,000 rpm for 13 hours. After sedimentation, fractions were collected by puncturing the bottom of the tube, then analyzed for PFK activity as described below. Fractions were analyzed for ADH activity by measuring the increase in absorbance at 340 nm in 1-ml assays that contained 100 mM Tris-Cl, pH 8.6, 1 mM NAD<sup>+</sup>, and 8.4 µmoles (50 µl) of ethanol.

*Enzyme Activity Assays*—Initial velocities were measured at 30°C in 100 mM Tris-Cl, pH 8.2, containing 10 mM MgCl<sub>2</sub> and 5 mM NH<sub>4</sub>Cl by coupling the production of fructose 1,6-bisphosphate to the oxidation of NADH (0.2 mM). The coupled assay (Kotlarz & Buc, 1982) utilized the auxiliary enzymes aldolase (20 µg/ml), triosephosphate isomerase (10 µg/ml) and α-glycerophosphate dehydrogenase (10 µg/ml). Auxiliary enzymes were dialyzed at 4°C against 100 mM Tris-Cl, pH 8.2, prior to use. ADP produced in the EcPFK-catalyzed reaction was regenerated to ATP using creatine phosphate (1 mM) and creatine kinase (10 µg/ml). However, this regenerating system was found to be unnecessary for the BsPFK- and ChiPFK-catalyzed reactions. In all assays, the free Mg<sup>++</sup> concentration was kept 5 to 10 mM in excess of the ATP concentration to avoid inhibition by free ATP. Assays were initiated by addition of PFK. The change in absorbance at 340 nm was measured for at least one

minute following an initial nonlinear phase. A thermostatted Hitachi UV-2000 spectrophotometer was used for the measurements.

*Fluorescence Measurements*—The binding of various substrates or effectors can either enhance or quench the intrinsic fluorescence of the single tryptophan, Trp 311, of EcPFK (Berger & Evans, 1991). Trp 311 is located near the C-terminus of the EcPFK subunit within the large subunit-subunit interface of the rigid dimer. ChiPFK also has a tryptophan at position 311. (The intrinsic fluorescence of the single tryptophan of BsPFK, Trp 179, is largely insensitive to ligand binding (Kim *et al.*, 1993)).

Steady-state fluorescence measurements were made at 25°C using either a SPEX 1680 or an SLM 8000C fluorescence spectrometer. The excitation source was a Xenon arc lamp. Intrinsic fluorescence emission due to the single tryptophan, Trp 311, of EcPFK or ChiPFK was measured at 340 nm following excitation at 295 nm. Slit widths were set at 8 nm. Protein concentrations were 5 to 25 µg/ml (below 1 µM), which is low enough to avoid the inner-filter effect. The enzyme was buffered in 100 mM Tris-Cl, pH 8.2, containing 10 mM MgCl<sub>2</sub>, 5 mM NH<sub>4</sub>Cl, 0.25 mM EDTA, and 2 mM DTT. Two types of experiments were performed: (1) addition of a saturating amount of ligand, and (2) addition of increments of ligand to the enzyme solution. Corrections were made to compensate for volume change, enzyme dilution, and nonspecific quenching. This was done by performing parallel experiments in which phosphate of the same concentration was added to the enzyme.

*Data Analysis*—Parameters were obtained from steady-state kinetic or fluorescence studies by fitting the substrate saturation data to either the Michaelis-Menten equation for hyperbolic kinetics or the Hill equation for sigmoidal kinetics. Kinetic data for MgATP saturation at low Fru-6P concentration (Figure 3.4B) were fit to the initial velocity equation for a sequential random kinetic mechanism assuming non rapid-equilibrium conditions (Segel, 1975; Ferdinand, 1966). The GDP and AMPPNP inhibition data were analyzed as follows: first, the inhibition pattern was

identified (competitive, noncompetitive, etc.). Based on this identification, the inhibition data were fit, using nonlinear regression analysis, to the equation for either competitive or noncompetitive inhibition (Cleland, 1979). The parameters generated were used to construct linear equations for the double-reciprocal plots. Finally, slopes and/or intercepts of the inhibition lines were plotted against inhibitor concentration to determine the values for  $K_{is}$  and/or  $K_{ij}$ . All inhibition data were corrected for loss of activity due to enzyme instability. Curve-fitting was performed using the program INPLOT (GraphPad, Inc., San Diego, CA).

## Results

*The Chimeric Subunit*—X-ray crystallography has revealed that the amino acid residues that bind Fru-6P are the same between the active sites of the two native enzymes (Evans *et al.*, 1981; Shirakihara & Evans, 1988). Three of the residues that bind ATP are different between the two active sites. They are, for BsPFK *versus* EcPFK: Cys instead of Phe 73, Lys instead of Arg 77, and Gln instead of Met 107. In the chimeric subunit (Fig. 3.1), the BsPFK/EcPFK junction is at residue 122. The residues that bind ATP are from the BsPFK portion of the subunit, while those that bind Fru-6P are from the EcPFK portion. Since residues 118 to 130 (except residue 122) are conserved between BsPFK and EcPFK, Thr 125, Asp 127, and Asp 129 can be considered as being from either enzyme portion. The region of the ATP-binding domain of EcPFK that moves (residues 71-95 and 101-118) during the open-to-closed transition (Shirakihara & Evans, 1988) has been replaced with the corresponding "rigid" region of BsPFK (Schirmer & Evans, 1990).

The residues that comprise the effector sites of the two native enzymes differ at several positions: Val instead of Arg 54, Gly instead of Tyr 55, Gly instead of Ser 58, Arg instead of Lys 211, and Ile 320 instead of Tyr 319 for BsPFK *versus* EcPFK, respectively. Because of these differences, the effector site of the chimeric enzyme is different from that of either native enzyme. In EcPFK, there are five positively-charged

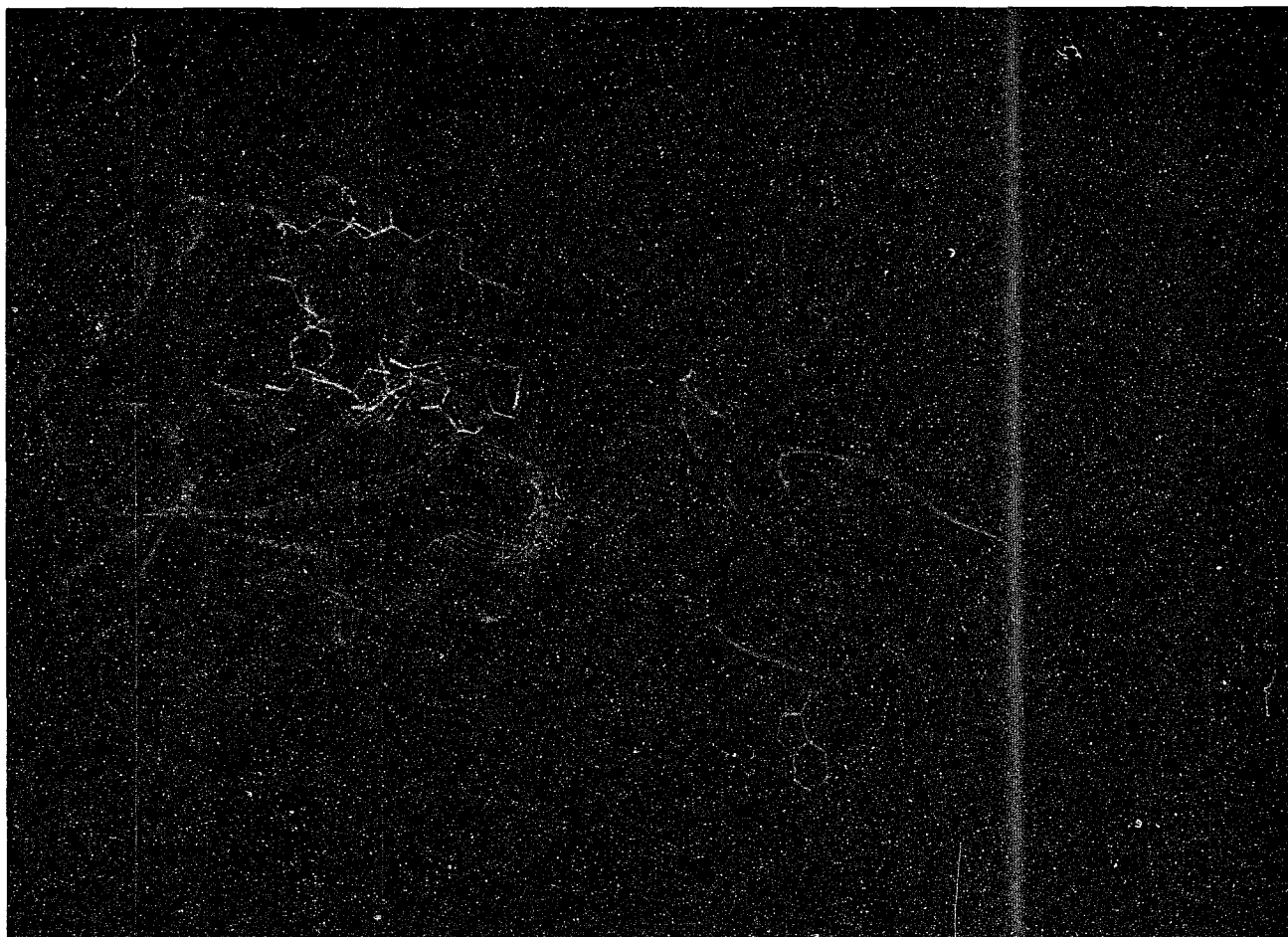


**FIGURE 3.1. Molecular Graphics Image of the Chimeric Subunit.** The portion of the subunit in *blue* is from *B. stearothermophilus* PFK, while the portion in *purple* is from *E. coli* PFK. ATP and Fru-6P molecules are in *red*. Amino acid residues that bind ATP are in *yellow*, while those that bind Fru-6P are in *green*. The lone tryptophan, Trp 311, is in *yellow-orange*. The image was generated from *B. stearothermophilus* PFK atomic coordinates using SYBYL (Tripos Associates, St. Louis, MO) on an Evans and Sutherland ps390 graphics terminal.

residues that bind the phosphate groups of GDP and PEP: Args 21, 25, 54, 154 and Lys 213 (Shirakihara & Evans, 1988; Lau & Fersht, 1989). In BsPFK, these residues are Arg's 21, 25, 211, 154 and Lys 213 (Evans *et al.*, 1981; Valdez *et al.*, 1988). Thus, in BsPFK, Arg 211 substitutes for Arg 54. In ChiPFK, however, neither Arg 54 nor Arg 211 is present. The presence of only three arginines in the ChiPFK effector site may explain its lower affinity for GDP (see below).

*Structural Properties*—It is important to know something about the structural properties of the chimeric enzyme before investigating its kinetic and allosteric properties. SDS-PAGE analysis (Fig. 3.2A) indicates that the subunit molecular weights of the three enzymes are similar, being  $36,000 \pm 1,000$  daltons. The results of a sucrose gradient sedimentation study (Fig. 3.2B) show that ChiPFK exists as a tetramer 137,000 daltons in size. Sedimentation experiments performed under the same conditions for BsPFK and EcPFK give similar molecular weights of 139,000 and 136,000, respectively. Thus, the three enzymes exist as tetramers similar in size. Analysis of the ChiPFK sucrose gradient fractions by SDS-PAGE followed by silver staining (not shown) reveals that no dimers or monomers were present within the gradient. About 75% of the total enzyme activity loaded was recovered from the fractions collected in the sedimentation study.

*Stability*—The chimeric enzyme, once diluted to a concentration appropriate for activity assays, began to lose activity over time. Specifically, about 15% of its original activity was lost over a period of 2 hours. The instability is an intrinsic property of ChiPFK since the diluted enzyme was unstable under a variety of buffer and temperature conditions. Instability was also observed in the fluorescence experiments in which Trp 311 fluorescence was titrated by incremental addition of ligand solution. A saturable quenching of fluorescence was observed in these experiments regardless of whether ligand or buffer was added. Even MgATP, which caused an increase in fluorescence when added in saturating amounts, caused a saturable decrease in



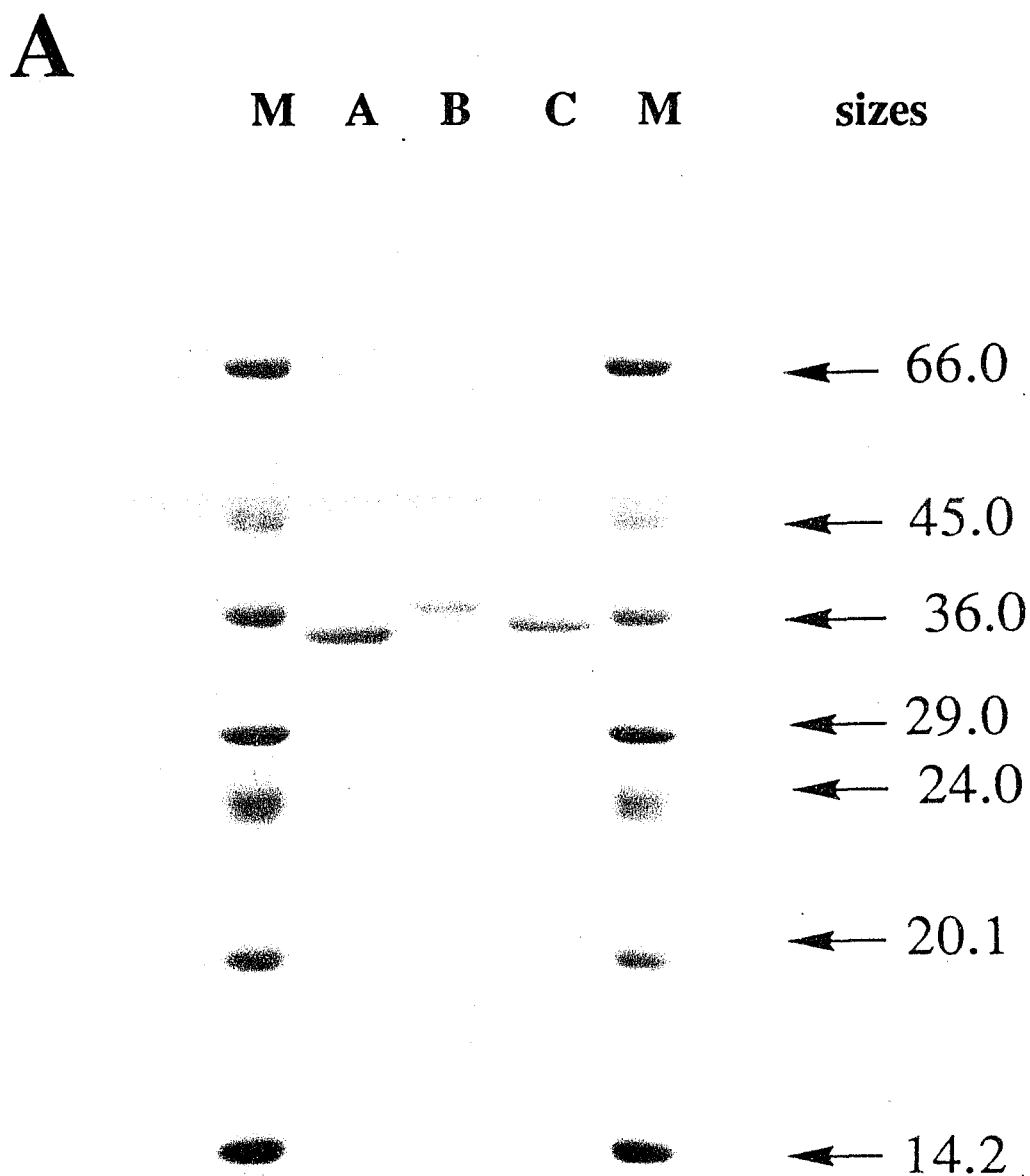
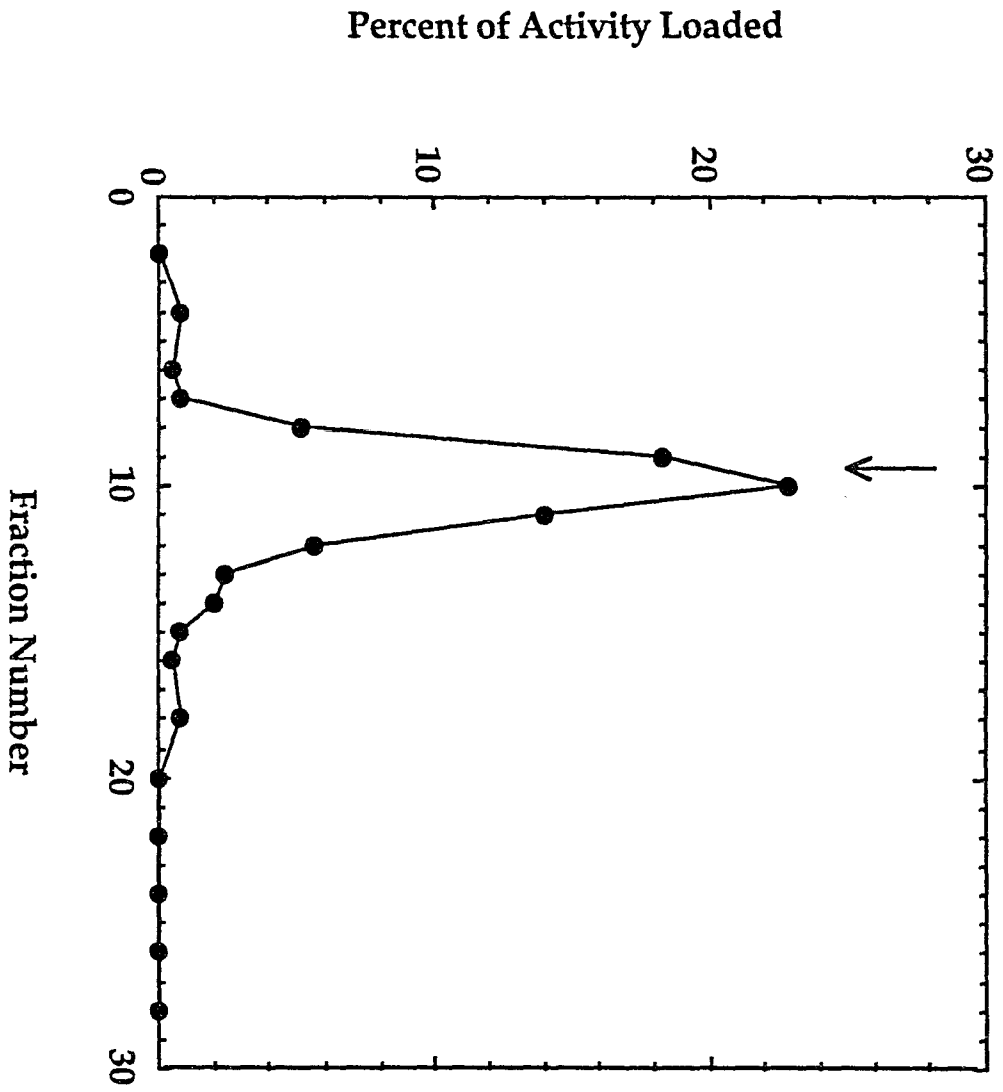


**FIGURE 3.2. Structural Properties of the Chimeric PFK.** (A) SDS-PAGE Analysis. M, molecular mass markers; A, native *B. stearothermophilus* PFK; B, the chimeric PFK; C, native *E. coli* PFK. Marker sizes are indicated in kilodaltons. (B) Sucrose Gradient Sedimentation. Plot of Percent of PFK Activity Loaded *versus* Fraction Number. The position of the yeast ADH marker (144,000 daltons) is indicated with a *downward arrow*. The sedimentation origin was at fraction 29.

**B**



fluorescence in titration experiments. Thus, both activity and fluorescence measurements gave evidence that ChiPFK is somewhat unstable.

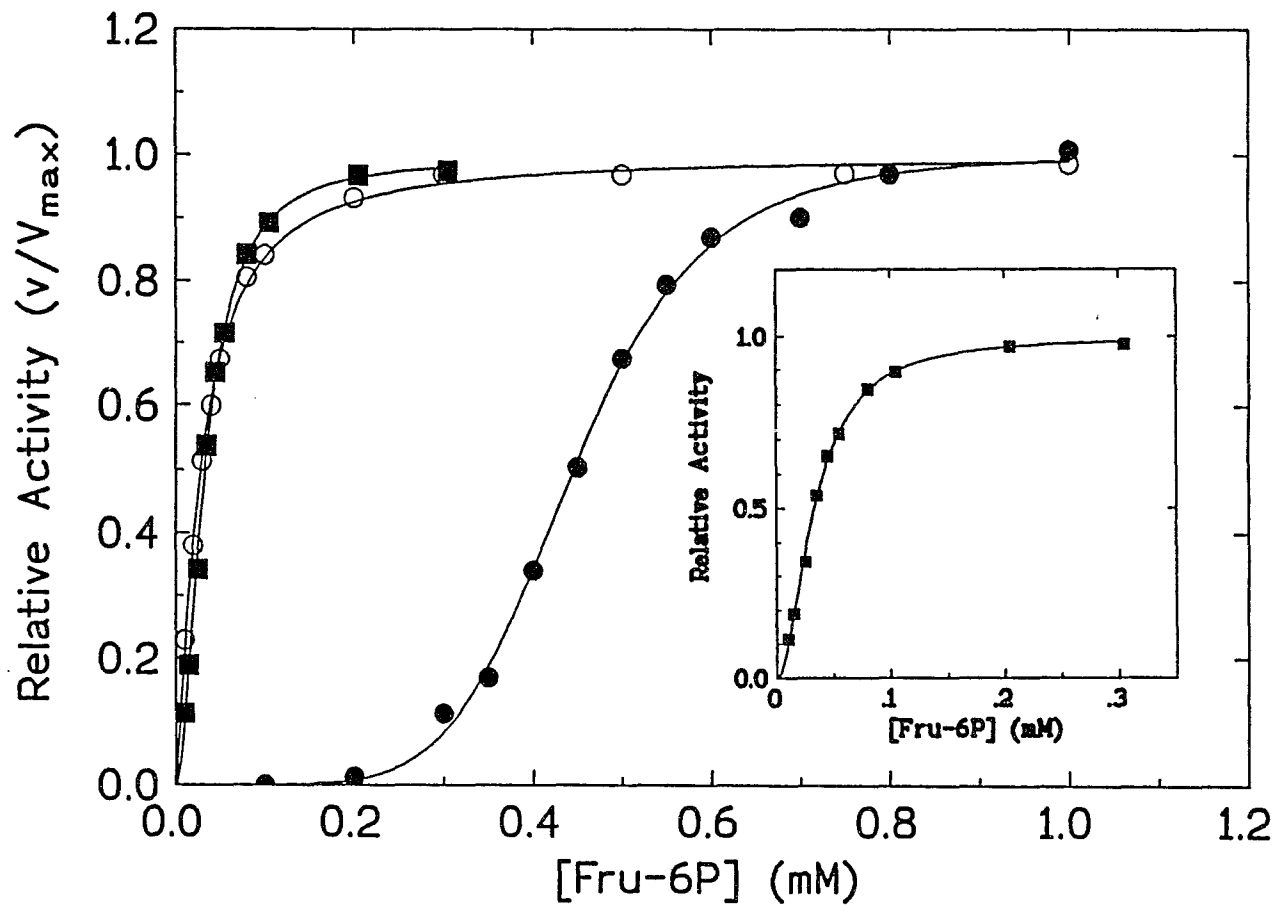
*Kinetic Parameters*—The chimeric enzyme was studied using steady-state kinetics, and the kinetic parameters obtained were compared to those for the two native enzymes. The results (Table 3.1) indicate that the chimeric enzyme is two-fold less catalytically active than either of the native enzymes. However, its affinity for ATP as measured by  $K_m^{\text{ATP}}$  is similar. The larger value of  $K_m^{\text{ATP}}$  for EcPFK (103  $\mu\text{M}$ ) is most likely the result of substrate antagonism between MgATP and Fru-6P in the active site (Deville-Bonne *et al.*, 1991b) since, when Fru-6P concentration is 50  $\mu\text{M}$  instead of 1.5 mM,  $K_m^{\text{ATP}}$  drops to 70  $\mu\text{M}$ . The Fru-6P saturation curves in the presence of saturating MgATP concentration vary in degree of sigmoidicity among the three enzymes. Whereas Fru-6P saturation of EcPFK is highly sigmoidal ( $n_H$  is 5.8), it is hyperbolic for BsPFK ( $n_H$  is 1.1), and somewhat sigmoidal for ChiPFK ( $n_H$  is 1.7). The  $S_{1/2}^{\text{Fru-6P}}$ -value for ChiPFK is closer to the value for BsPFK than that for EcPFK. However, when EcPFK is activated by GDP (2 mM), the Fru-6P saturation curve becomes hyperbolic and  $S_{1/2}^{\text{Fru-6P}}$  falls to 50  $\mu\text{M}$ , which is close to the value for either BsPFK or ChiPFK. These results show that, in terms of its kinetic parameters, ChiPFK is remarkably similar to BsPFK and the activated form of EcPFK.

*Fru-6P Saturation Kinetics*—Figure 3.3 displays more clearly the differences among the three enzymes in terms of their saturation by Fru-6P in the presence of 1.0 mM MgATP. Whereas saturation of EcPFK is highly sigmoidal, saturation of ChiPFK is nearly hyperbolic. Thus, cooperativity has been largely destroyed in ChiPFK. Some remains, however ( $n_H$  is 1.7; Fig. 3.3, *inset*). The residual cooperativity persists ( $n_H$  is 1.8) even for Fru-6P saturation of ChiPFK in the presence of less-than-saturating MgATP concentration (50  $\mu\text{M}$ ; not shown). It is also present ( $n_H$  is 1.5) when other nucleoside triphosphates (NTPs) such as GTP or CTP serve as the phosphate donor. Together, these results suggest that ChiPFK cooperative behavior is independent of the

**TABLE 3.1**  
*Kinetic Parameters for ChiPFK and the Native Enzymes*

<b>Enzyme</b>	<b><math>k_{\text{cat}}</math> (<math>\text{s}^{-1}</math>)</b>	<b><math>K_{\text{m}}^{\text{ATP}}</math> (<math>\mu\text{M}</math>)</b>	<b><math>S_{1/2}^{\text{Fru-6P}}</math> (<math>\mu\text{M}</math>)</b>	<b><math>n_{\text{H}}</math></b>
ChiPFK	$60 \pm 2$	$85 \pm 2$	$34 \pm 1$	$1.7 \pm 0.2$
BsPFK	$139 \pm 24$	$70 \pm 3$	$28 \pm 7$	$1.1 \pm 0.1$
EcPFK	$127 \pm 5$	$103 \pm 2$	$445 \pm 3$	$5.8 \pm 0.2$

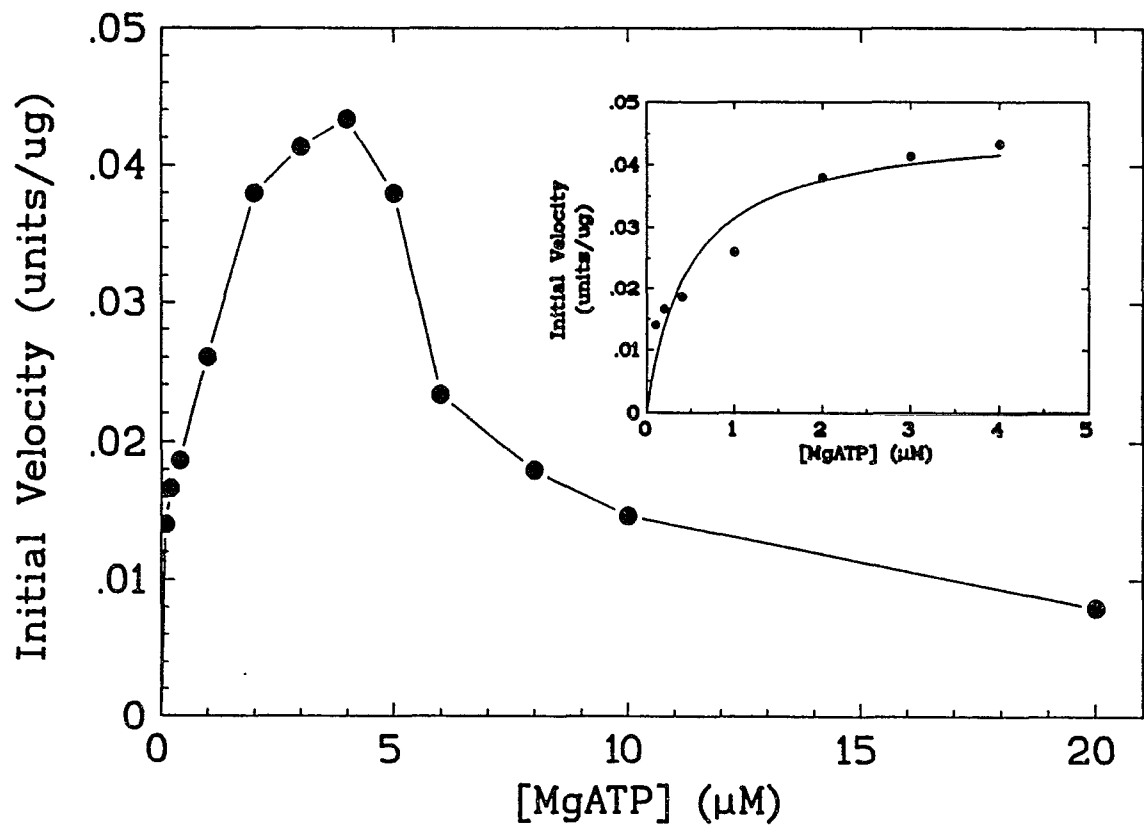
The conditions for the assays are described under "Materials and Methods."  $k_{\text{cat}}$ , the catalytic rate constant;  $K_{\text{m}}^{\text{ATP}}$ , the MgATP concentration at half-maximal velocity;  $S_{1/2}^{\text{Fru-6P}}$ , the Fru-6P concentration at half-maximal velocity; and  $n_{\text{H}}$ , the Hill number. In determining  $K_{\text{m}}^{\text{ATP}}$ , the Fru-6P concentration was 0.3 mM for BsPFK and ChiPFK, and 1.5 mM for EcPFK. In determining  $S_{1/2}^{\text{Fru-6P}}$  and  $n_{\text{H}}$ , the MgATP concentration was 1.0 mM.



**FIGURE 3.3.** Dependence of PFK Activity on Fru-6P Concentration. (○), native *B. stearothermophilus* PFK; (●), native *E. coli* PFK; (■), chimeric PFK. The inset shows the chimeric PFK plot on an expanded x-axis. [MgATP] was saturating at 1.0 mM.

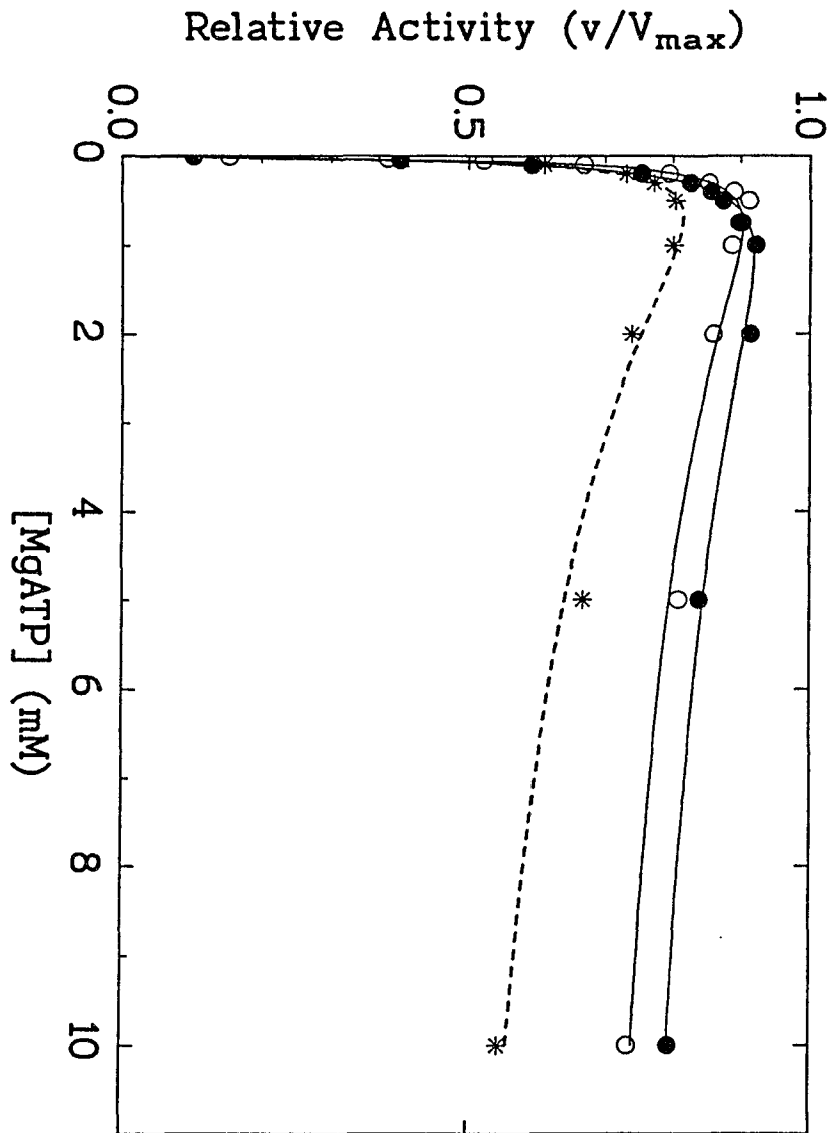
absolute amount of ATP present and the identity of the NTP. What appears to be important is the amount of MgATP (or other NTP) relative to the amount of Fru-6P present. When MgATP concentration was low (50  $\mu\text{M}$ ), ChiPFK activity did not increase with Fru-6P concentration beyond 50  $\mu\text{M}$ . This result indicates that MgATP binding and/or release is not a rapid-equilibrium process for ChiPFK. Similar results showing non rapid-equilibrium binding and/or release of MgATP were obtained for BsPFK and the activated form of EcPFK.

*MgATP Saturation in the Presence of Low Fru-6P Concentration*— MgATP saturation curves for ChiPFK and the two native enzymes obtained in the presence of saturating Fru-6P concentration are hyperbolic and yield similar  $K_m^{\text{ATP}}$ -values (Table 3.1). However, when Fru-6P concentration is low (50  $\mu\text{M}$ ), differences become apparent between the MgATP saturation curves of EcPFK and ChiPFK (Figs. 3.4A & B). Under these conditions, significant substrate inhibition of EcPFK by MgATP is evident (Fig. 3.4A; Kundrot & Evans, 1991; Johnson & Reinhart, 1992). The left-most portion of the curve in Fig. 3.4A can be fit to the Michaelis-Menten equation (*inset*), yielding a  $K_m^{\text{ATP}}$  of  $0.5 \pm 0.1 \mu\text{M}$ . As shown in Fig. 3.4B, MgATP also inhibits ChiPFK at low Fru-6P concentration (*open circles*), but the inhibition is much less severe. Furthermore, the data for ChiPFK can be fit to the equation for a steady-state random Bi Bi kinetic mechanism (Segel, 1975b) but those for unactivated-EcPFK (Fig. 3.4A) cannot. The results suggest that the mechanisms of ATP inhibition of ChiPFK and unactivated-EcPFK are different. However, whereas MgATP saturation curves at low Fru-6P concentration for ChiPFK and unactivated-EcPFK are dramatically different, those for ChiPFK and EcPFK activated by 2 mM GDP (Fig. 3.4B, *closed circles*) are similar. Their profiles, and the extent of inhibition relative to  $V_{\text{max}}$  at 10 mM MgATP—25% for ChiPFK and 20% for activated-EcPFK—are similar. These results suggest that the ChiPFK subunit is locked in a conformation that resembles the activated EcPFK subunit.

**A**

**FIGURE 3.4. Dependence of PFK Activity on MgATP Concentration when Fru-6P Concentration is Low (50 μM).** (A) Initial Velocity (units/ug) versus MgATP concentration for native EcPFK in the absence of activator GDP. The *inset* shows the data between 0.1 and 4 μM MgATP fit to the Michaelis-Menten equation. (B) Relative Activity ( $v/V_{max}$ ) versus MgATP concentration for (●), native *E. coli* PFK fully activated with 2 mM GDP and (○), chimeric PFK (no GDP present). The curve for BsPFK (*dashed line*) is included for comparison. The data were fit to the equation for a steady-state random kinetic mechanism (Ferdinand, 1966).

**B**

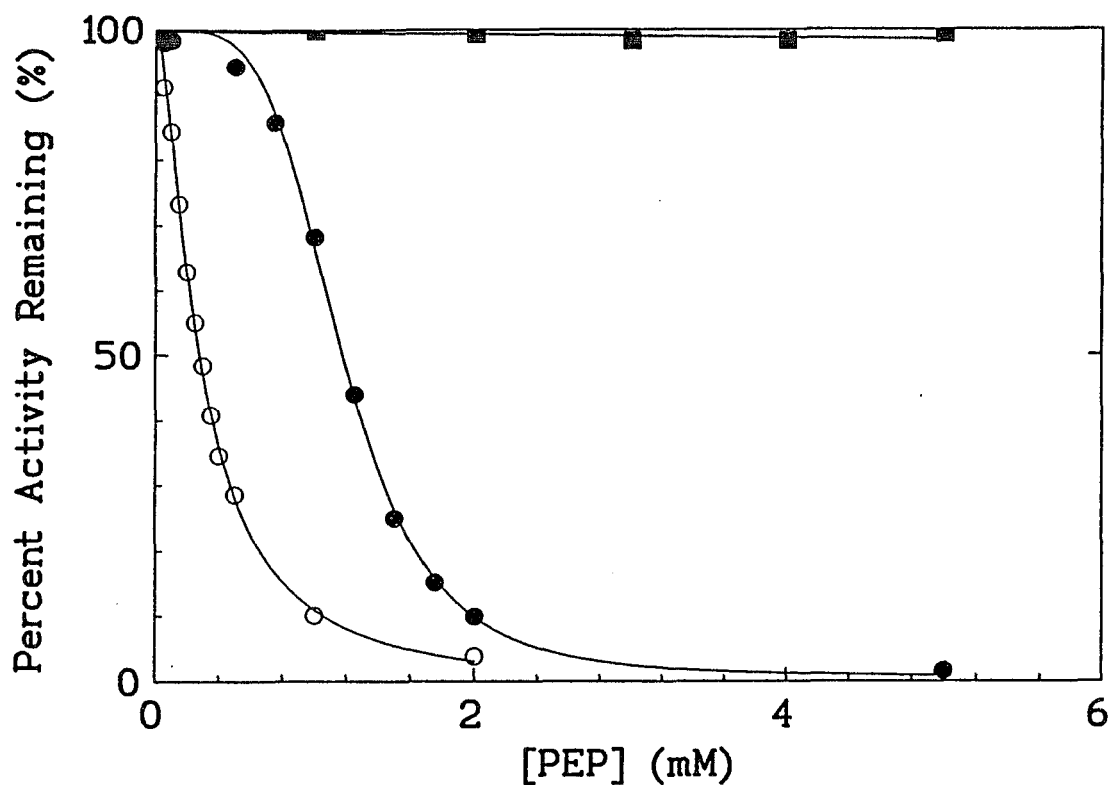




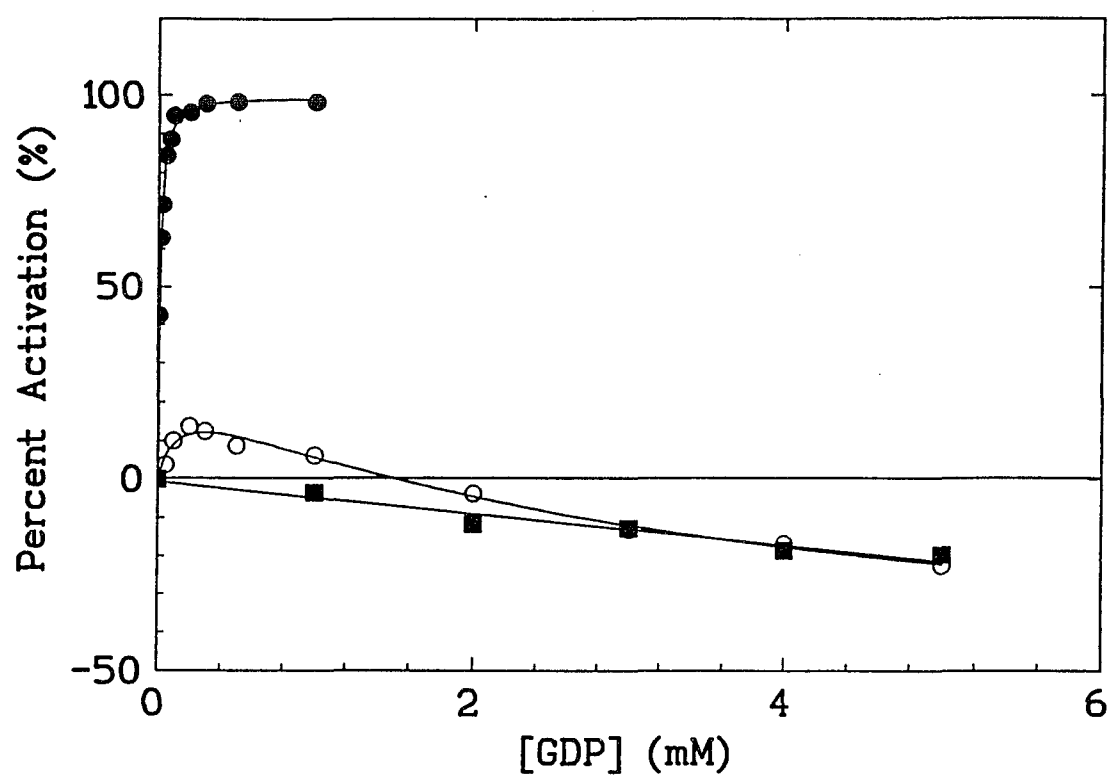
*Heterotropic Regulation*—The abilities of PEP to allosterically inhibit, and GDP to allosterically activate ChiPFK were investigated using steady-state kinetics. The results obtained indicate that ChiPFK activity is insensitive to regulation by either effector. Fig. 3.5A shows that both native enzymes are inhibited by PEP, although the sensitivity and cooperativity of their responses differ. The inhibition profile for EcPFK is highly sigmoidal with a Hill number of 4.3 ( $I_{1/2}$  is  $1.17 \pm 0.01$  mM), while the profile for BsPFK is much less sigmoidal with a Hill number of 1.6 ( $I_{1/2}$  is  $0.28 \pm 0.01$ ). However, PEP has essentially no effect on the chimeric enzyme. ChiPFK likewise cannot be activated by GDP. As shown in Fig. 3.5B, GDP strongly activates EcPFK when MgATP concentration is saturating and the Fru-6P concentration is equal to the  $S_{1/2}$ -value (0.45 mM). The  $K_{act}^{GDP}$  for the activation, which is hyperbolic, is  $13 \pm 0.4$   $\mu$ M. On the other hand, GDP can either activate or inhibit BsPFK, depending on the concentration of GDP. In the presence of Fru-6P at a concentration equal to the  $S_{1/2}$ -value (30  $\mu$ M), as GDP concentration increases, it first activates BsPFK weakly to about 20% ( $K_{act}^{GDP}$  is  $90 \pm 10$   $\mu$ M), then begins to inhibit (Fig. 3.5B). Since the inhibition by GDP is competitive with respect to MgATP ( $K_{iS} = 1.5 \pm 0.2$  mM; not shown), it is due to binding in the active site. The chimeric enzyme cannot be activated by GDP but, like BsPFK, is inhibited by it. However, the inhibition pattern is mixed-type noncompetitive with respect to MgATP ( $K_{iS} = 4.3 \pm 0.9$  mM;  $K_{ij} = 26 \pm 6$  mM) rather than competitive. The origin of the inhibition is not clear.

*Thermal Inactivation Studies*—A possible explanation for the lack of heterotropic regulation of ChiPFK by PEP and GDP is that these ligands cannot bind the effector site of the enzyme. To address this possibility, thermal inactivation experiments were performed in which ChiPFK was heated in the absence or presence of ligand. The results show that both Fru-6P and MgGDP protect native EcPFK against thermal inactivation at 60°C (Fig. 3.6A). PEP also protects EcPFK, but the protection is partial, with 68% of activity remaining after 1 hour. Similar experiments were

A



**FIGURE 3.5. Effect of PEP and GDP on PFK Activity.** (○), *B. stearotherophilus* PFK; (●), *E. coli* PFK; (■), chimeric PFK. (A), Effect of PEP. Percent Activity Remaining versus PEP Concentration. [MgATP] was saturating at 1.0 mM. [Fru-6P] was 0.3 mM for BsPFK and ChiPFK, and 1.5 mM for EcPFK. (B), Effect of GDP. Percent Activation versus GDP Concentration. [MgATP] was saturating at 1.0 mM. [Fru-6P] was equal to the  $S_{1/2}$ -value, which was 0.03 mM for ChiPFK and BsPFK, and 0.45 mM for EcPFK.

**B**

A

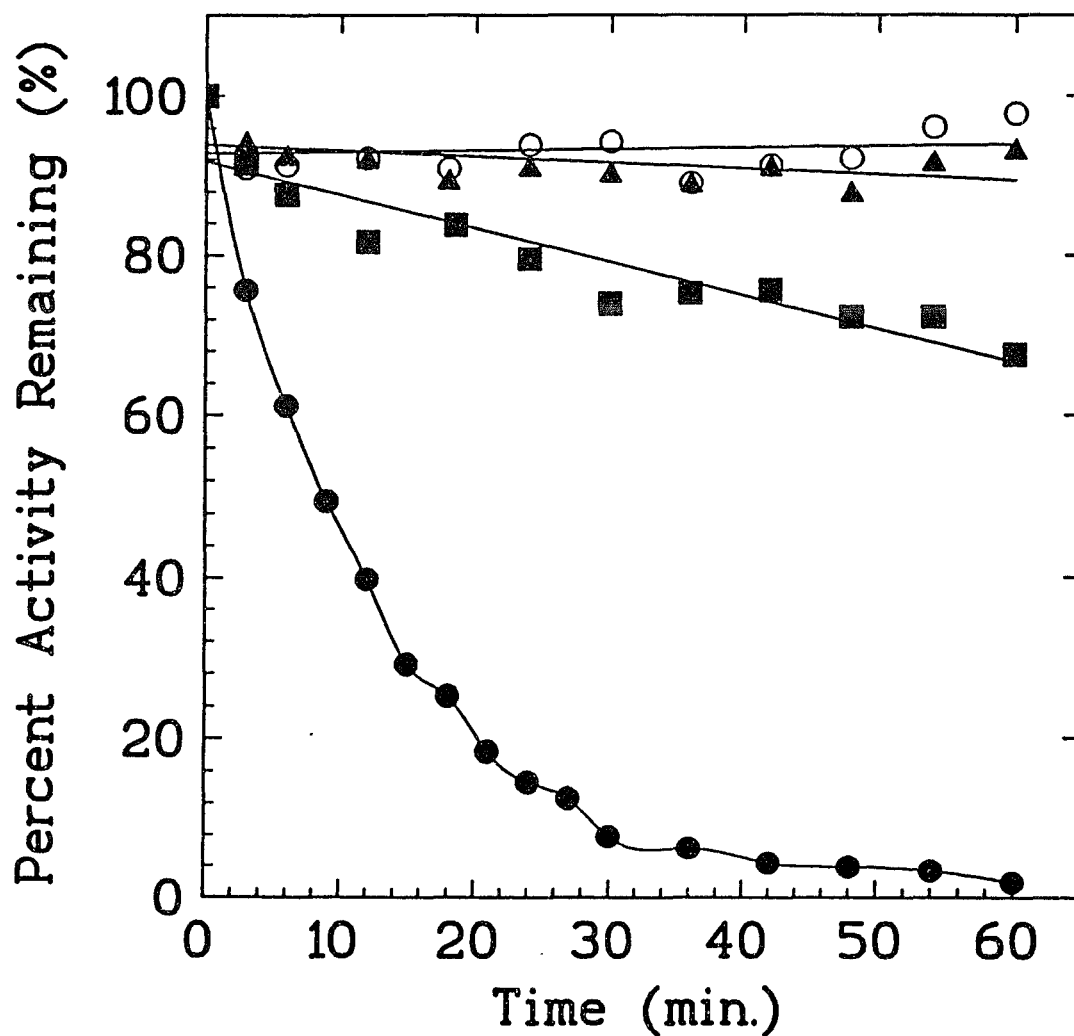
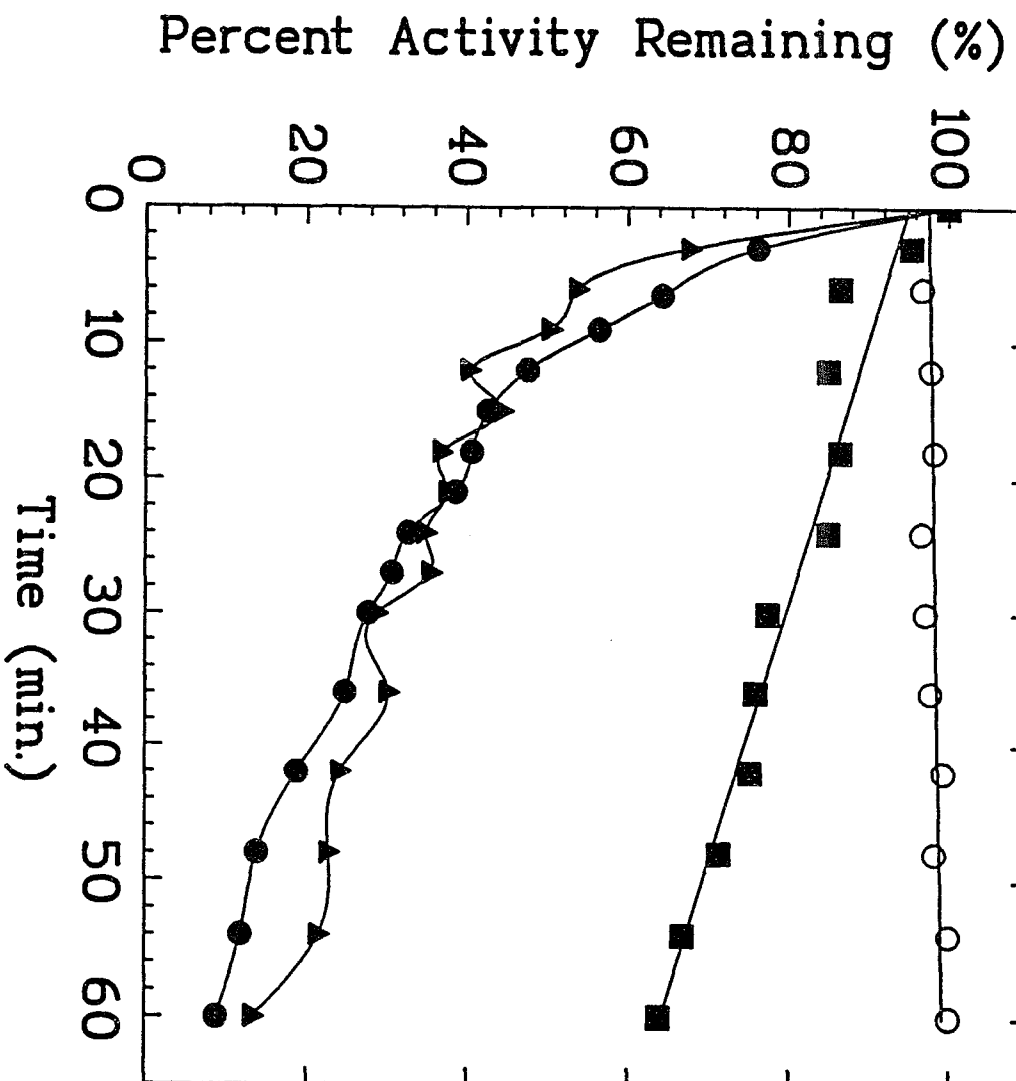


**FIGURE 3.6. Protection of (A) Native *E. coli* PFK and (B) Chimeric PFK Against Thermal Inactivation.** Enzymes were incubated in 100 mM Tris-Cl, pH 8.2, containing 10 mM MgCl<sub>2</sub> and 2 mM DTT (at 60°C and 50°C for EcPFK and ChiPFK, respectively) in the presence of (●), no ligand; (○), 5 mM Fru-6P; (■), 10 mM PEP; or (▲), 5 mM GDP for the indicated time period. An aliquot was then removed and assayed for PFK activity. MgATP and Fru-6P concentrations were both 1.0 mM in the activity assays.

**B**



performed on ChiPFK. (50°C was used instead of 60°C because of the lower stability of ChiPFK). As shown in Fig. 3.6B, Fru-6P at 5 mM protects ChiPFK against thermal inactivation. This result contrasts with the inability of a 10-fold lower concentration of Fru-6P to stabilize ChiPFK diluted for activity assays (above). It suggests that ChiPFK dissociates along its "active" interface, and that Fru-6P prevents dissociation by interacting with Arg 162 and Arg 243 across it (Teschner *et al.*, 1990). PEP also protects ChiPFK to about the same extent it protects native EcPFK (64% *versus* 68% for EcPFK). Thus, PEP binds as well to ChiPFK as it does to EcPFK. In contrast, MgGDP offers little protection. Only 15% of activity remains after a 1-hour incubation, compared to 9% in the absence of ligand (Fig. 3.6B). The simplest interpretation of this result is that MgGDP binds poorly in the effector site of ChiPFK. The structural basis for poor binding could be the presence of three rather than four arginine residues in the effector site.

*AMPPNP Inhibition Studies*—Inhibition of both activated-EcPFK and ChiPFK by AMPPNP with respect to MgATP was competitive ( $K_{is} = 24 \pm 2$  and  $20 \pm 2$   $\mu\text{M}$ , respectively), as was AMPPNP inhibition of BsPFK with respect to MgATP ( $K_{is}$  of  $50 \pm 20$   $\mu\text{M}$ ; Byrnes *et al.*, 1994). Thus, as expected, AMPPNP competes with MgATP for binding in the active site. Interestingly, AMPPNP inhibition of both activated-EcPFK and ChiPFK with respect to Fru-6P gave similar competitive-like patterns of lines that intersected just to the right of the 1/velocity axis in double-reciprocal plots. ( $K_{is}$ -values of  $7 \pm 7$  and  $9 \pm 6$   $\mu\text{M}$  were obtained for activated-EcPFK and ChiPFK, respectively.) In contrast, AMPPNP inhibition of BsPFK with respect to Fru-6P is noncompetitive ( $K_{is} = 0.29 \pm 0.09$  mM and  $K_{ii} = 0.40 \pm 0.12$  mM; Byrnes *et al.*, 1994). Thus, AMPPNP binding to activated-EcPFK and ChiPFK is different from its binding to BsPFK. The competitive-like inhibition with respect to Fru-6P could be due to antagonism of Fru-6P binding by AMPPNP in the active site (ATP shows a similar effect that is less pronounced). In addition, as shown in Figure 3.7, the Hill number for

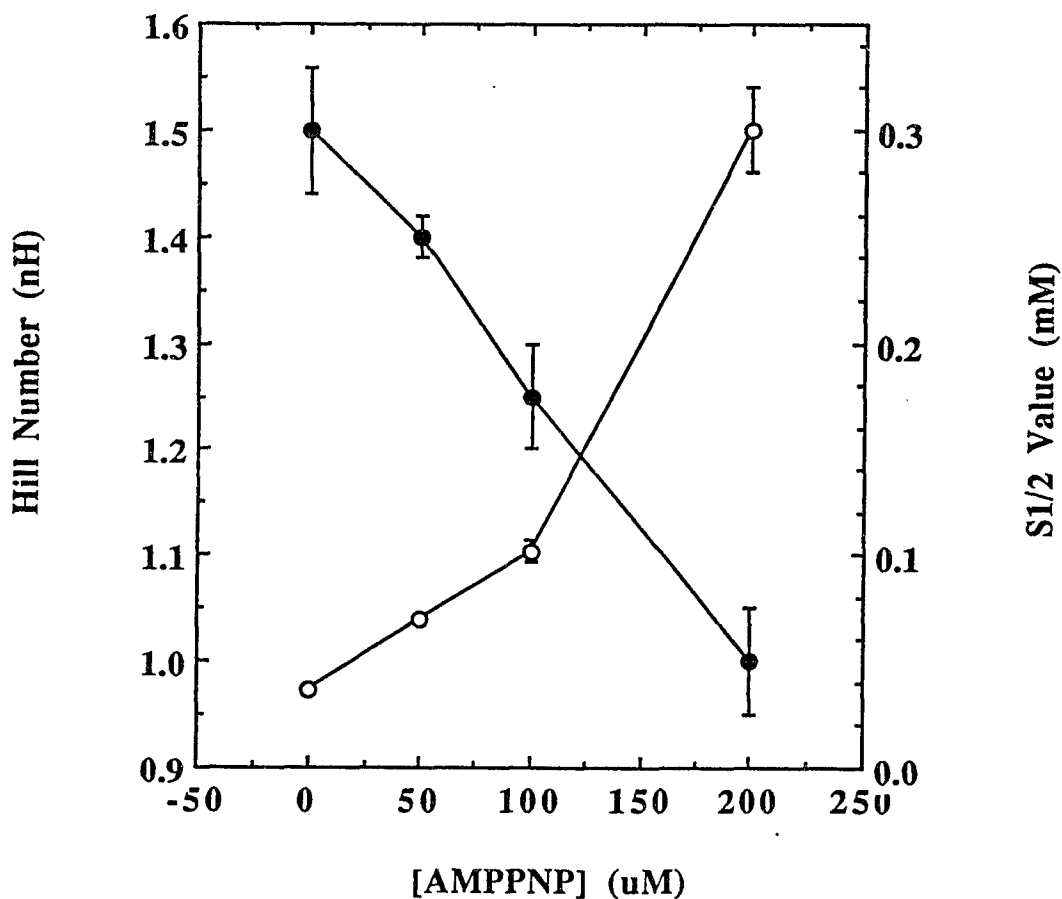


**FIGURE 3.7. Effect of AMPPNP on the Fru-6P-Dependent Cooperative Behavior of Chimeric PFK.** Plot of Hill Number (●) or  $S_{1/2}$ -value (○) versus AMPPNP Concentration. The Hill numbers and  $S_{1/2}$ -values were obtained by fitting Fru-6P saturation data, collected in the presence of 0.93 mM MgATP and the indicated [AMPPNP], to the Hill equation. Error bars represent standard errors.

the Fru-6P saturation curve obtained in the presence of AMPPNP decreases with increasing AMPPNP concentration until it reaches 1.0 at 200  $\mu\text{M}$  AMPPNP. Thus, AMPPNP abolishes the sigmoidicity of the Fru-6P saturation curve of ChiPFK.

*Effect of Ligand Binding on Trp 311 Intrinsic Fluorescence*—Two types of steady-state fluorescence experiments were performed. In the first type, the intrinsic fluorescence of EcPFK was titrated by addition of small volumes of ligand to the enzyme solution. (These experiments could not be done on ChiPFK because of its instability). The results are presented in Table 3.2. In the second type of experiment, a saturating amount of ligand was added to the enzyme solution, and the change in fluorescence intensity measured (Table 3.3). Titration of EcPFK fluorescence with Fru-6P, with AMPPNP, and with AMPPNP after incubation in the presence of Fru-6P (Table 3.2) gave results similar to those previously reported (Deville-Bonne & Garel, 1992; Johnson & Reinhart, 1992). The results in Table 3.3 show that AMPPNP (or ATP) binding cause the same fluorescence increase (12%) in both ChiPFK and EcPFK, but the fluorescence decrease induced in ChiPFK upon Fru-6P binding (8%) was less than that induced in EcPFK (19%). ChiPFK can thus exist in two conformational states: a high fluorescence state and a low fluorescence state. Addition of Fru-6P to EcPFK incubated in the presence of AMPPNP at concentrations as low as 5  $\mu\text{M}$  resulted in no fluorescence change (Table 3.3; AMPPNP concentrations below 2  $\mu\text{M}$  did allow Fru-6P (500  $\mu\text{M}$ ) to bind, however). This dramatic blockage of Fru-6P binding by AMPPNP, which may indicate closure of the EcPFK active site upon AMPPNP binding, was not seen in ChiPFK (Table 3.3). Finally, in order to investigate the effect of interactions between Fru-6P and AMPPNP on the fluorescence of ChiPFK, experiments were done in which a saturating amount of one ligand was added to the enzyme in the presence of increasing amounts of the other. Fig. 3.8A shows that Fru-6P (500  $\mu\text{M}$ ) cannot bring ChiPFK completely to the low-fluorescence state when AMPPNP is present, even at low levels, and Fru-6P is increasingly less effective in bringing ChiPFK to this



**TABLE 3.2**  
*Dissociation Constants and Maximum Fluorescence Changes for Fru-6P and AMPPNP Binding to E. coli PFK*

Ligand	$K_d$ ( $\mu\text{M}$ )	$\Delta F_{\text{max}}$ (%)	$n_H$
Fru-6P	$9.6 \pm 1.2$	$-20 \pm 1$	1.0 (h)
AMPPNP	$0.1 \pm 0.01$	$+16.6 \pm 0.3$	1.0 (h)
AMPPNP/Fru-6P	$0.20 \pm 0.03$	$+35.6 \pm 1.0$	$1.9 \pm 0.1$

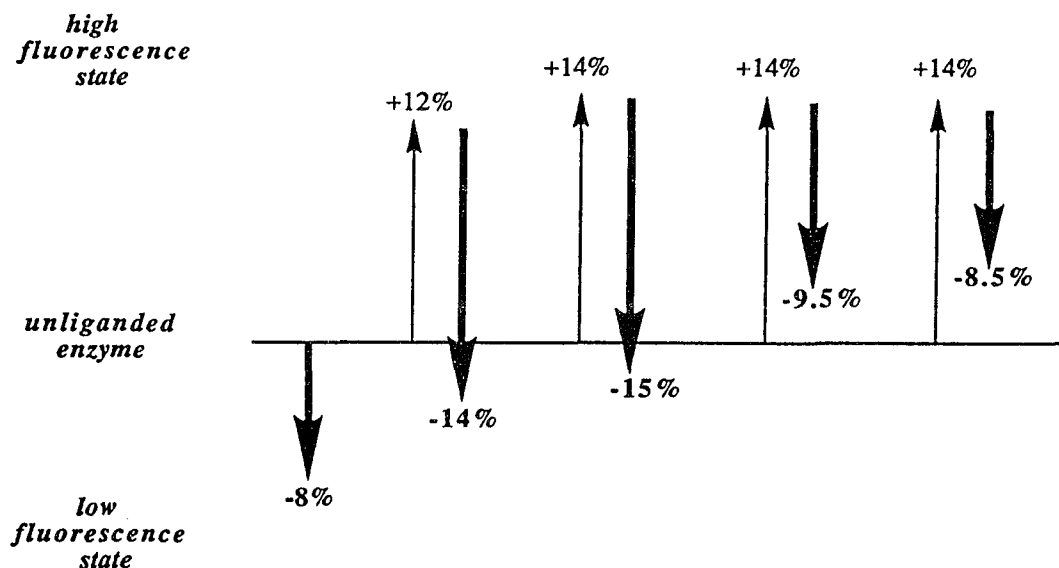
Small increments of the indicated ligand were added to the enzyme solution, and the changes in fluorescence measured. After correction, the fluorescence change was plotted against ligand concentration. The resulting curves were fit to either the Michaelis-Menten equation or the Hill equation.  $K_d$ , equilibrium dissociation constant;  $\Delta F_{\text{max}}$ , maximum fluorescence change;  $n_H$ , Hill number; h, hyperbolic. AMPPNP/Fru-6P indicates incremental addition of AMPPNP to EcPFK in the presence of Fru-6P (100  $\mu\text{M}$ ).

**TABLE 3.3**  
*Changes in Intrinsic Fluorescence Induced by Ligand Binding to E. coli PFK and the Chimeric PFK*

Enzyme	Ligand Added						
	Fru-6P (500 $\mu$ M)	Fru-6P after AMPPNP <sup>a</sup> (500 $\mu$ M)	ATP (20 $\mu$ M)	AMPPNP (20 $\mu$ M)	AMPPNP after Fru-6P <sup>b</sup> (20 $\mu$ M)	ADP (100 $\mu$ M)	PEP (2 mM)
EcPFK	-18.8 $\pm$ 0.5	no change	+11.6 $\pm$ 0.5	+12.2 $\pm$ 0.3	+35.5 $\pm$ 4.8	-13.9 $\pm$ 0.1	+3.6 $\pm$ 0.2
ChiPFK	-8.4 $\pm$ 0.6	-9.5 $\pm$ 0.8	+11.5 $\pm$ 2.5	+13.4 $\pm$ 1.0	+6.3 $\pm$ 0.5	no change	no change

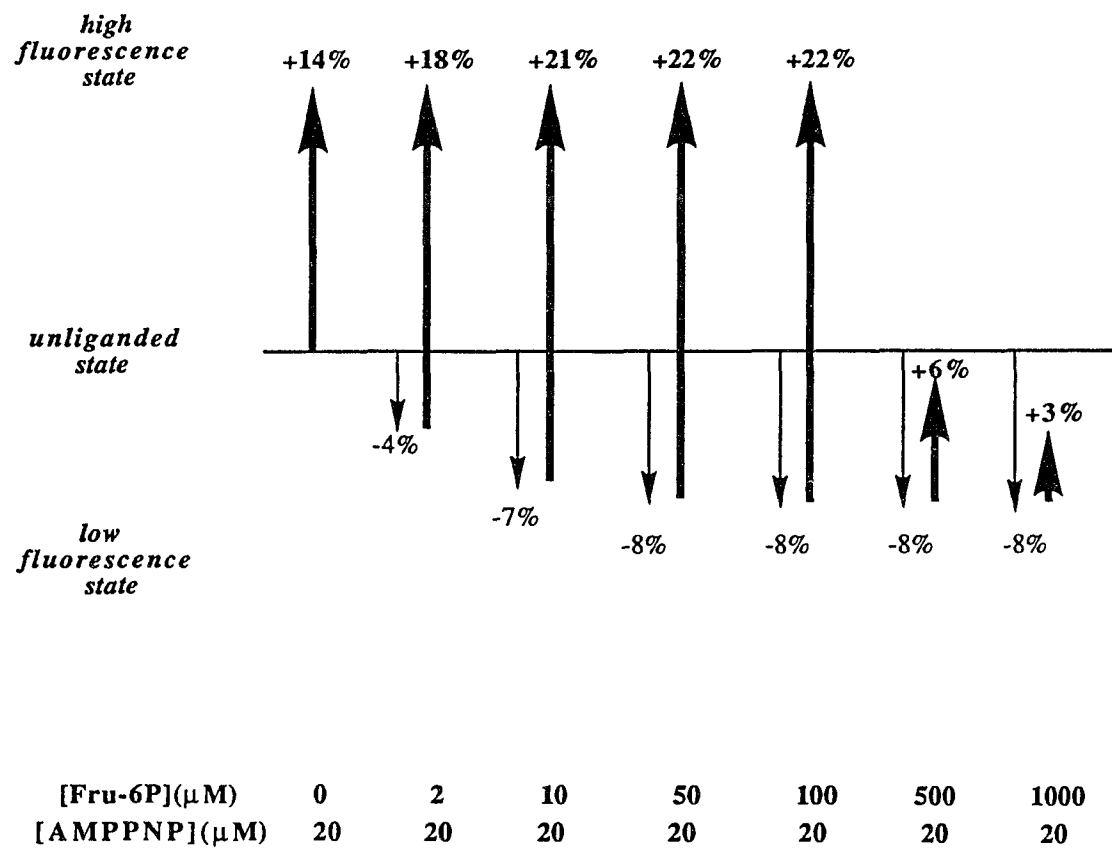
The change in steady-state fluorescence was measured upon addition of the indicated ligand at the indicated concentration, as described under "Materials and Methods". Each value is the average of two measurements. Based on the dissociation constants in Table 3.2, concentrations of 500  $\mu$ M and 20  $\mu$ M were assumed to be saturating for Fru-6P and AMPPNP, respectively. <sup>a</sup>The enzyme was incubated with AMPPNP (20  $\mu$ M), then Fru-6P (500  $\mu$ M) was added. <sup>b</sup>The enzyme was incubated with Fru-6P (500  $\mu$ M), then AMPPNP (20  $\mu$ M) was added.

A



[AMPPNP] (uM)	0	1	5	20	50
[Fru-6P] (uM)	500	500	500	500	500

**FIGURE 3.8. Combined Effects of Fru-6P and AMPPNP on Intrinsic Fluorescence of the Chimeric PFK.** (A) Effect of Adding a Saturating Amount of Fru-6P (500  $\mu\text{M}$ ) to ChiPFK Incubated with Increasing Amounts of AMPPNP. The *thin arrows* show the initial effect of AMPPNP on the fluorescence, and the *thick arrows* show the subsequent effect of Fru-6P. AMPPNP places ChiPFK in a high-fluorescence state, Fru-6P a low-fluorescence state. (B) Effect of Adding a Saturating Amount of AMPPNP (20  $\mu\text{M}$ ) to ChiPFK Incubated with Increasing Amounts of Fru-6P. The *thin arrows* show the initial effect of Fru-6P on the fluorescence, and the *thick arrows* show the subsequent effect of AMPPNP. The *number* at each arrowhead is the overall percent change in fluorescence represented by the arrow it accompanies. Each number is the average of two measurements. The concentrations of AMPPNP and Fru-6P are indicated.

**B**

conformational state as AMPPNP levels increase. Fig. 3.8B shows that AMPPNP (20  $\mu$ M) can bring ChiPFK to the high-fluorescence state when Fru-6P levels are low to moderate, but is less effective in doing so at high Fru-6P levels.

## Discussion

Here we report studies on a chimeric bacterial phosphofructokinase (ChiPFK), which has been successfully purified after high-level expression in PFK-deficient *E. coli* cells. ChiPFK exists as an active tetramer similar in size to tetramers of the native enzymes from which it is derived. Its catalytic rate constant is about half that of either of the two native enzymes. Its affinities for substrates, as measured by the  $K_m^{\text{ATP}}$ - and  $S_{1/2}^{\text{Fru-6P}}$ -values, are similar to those of BsPFK and the activated form of EcPFK. Although hybrid EcPFK tetramers have been studied before (Lau & Fersht, 1989), this is the first time a chimeric PFK, containing parts of two different PFKs grafted together, has been constructed and studied. Our results attest to the great structural and functional similarity between BsPFK and EcPFK, especially at their active sites. However, the results also emphasize differences in their mechanisms of heterotropic regulation.

Though stable as a tetramer in the sucrose gradient sedimentation experiment, ChiPFK is somewhat unstable under the conditions of the activity assay. The two native enzymes are stable under these conditions. The loss of ChiPFK activity over time is paralleled by a quenching of its Trp 311 fluorescence in titration experiments. The fact that similar quenching profiles were observed in the titration experiments irrespective of the ligand added suggests that the effect is time-dependent rather than ligand-dependent. It most likely reflects dissociation of the active tetramer when present in dilute solutions. This dissociation is to monomers rather than dimers since quenching of Trp 311 fluorescence occurs when the EcPFK tetramer dissociates into monomers, but not dimers (Deville-Bonne *et al.*, 1989; LeBras *et al.*, 1989).

Phosphoenolpyruvate does not inhibit ChiPFK. PEP binds to the enzyme, but the binding causes no measurable change in Trp 311 intrinsic fluorescence. This

suggests that conformational changes normally associated with allosteric inhibition are absent in ChiPFK. The observation that GDP inhibits ChiPFK noncompetitively with respect to MgATP indicates that GDP binds to ChiPFK. This binding may occur in both the active and effector sites. The inability of GDP to protect ChiPFK against thermal inactivation suggests that GDP does not bind the effector site. However, GDP binding in the active site of BsPFK has been shown to destabilize BsPFK in thermal inactivation experiments (Zhu *et al.*, manuscript in preparation). Thus, such binding in the active site of ChiPFK could destabilize the enzyme and mask the stabilization offered by its binding in the effector site. The inability of GDP to induce a fluorescence decrease in ChiPFK could thus be due either to poor binding in the effector site or to an inability of the ChiPFK tetramer to transmit allosteric changes. A third possibility is that the ChiPFK tetramer is already locked in an activated state and cannot be further activated by GDP.

The active site of EcPFK appears to close when AMPPNP binds to it, while the active site of ChiPFK is locked in an "open" conformation. EcPFK bound tightly to the Cibacron Blue affinity column during purification, and AMPPNP strongly inhibited subsequent Fru-6P binding to EcPFK in fluorescence studies. The latter result suggests that closure of the active site when AMPPNP binds in the absence of Fru-6P blocks subsequent binding of Fru-6P. Unlike EcPFK, ChiPFK associated loosely with the column during purification, and Fru-6P could bind to and cause a fluorescence decrease in ChiPFK after the enzyme had bound AMPPNP (20  $\mu$ M). The active site of ChiPFK is thus locked open. Our results also suggest that the ChiPFK active site resembles that of the activated form of EcPFK. This is shown by similarities between ChiPFK and activated-EcPFK in their kinetic parameters (Table 3.1), their saturation by MgATP in the presence of low Fru-6P (Fig. 3.4B), and their AMPPNP *versus* Fru-6P inhibition patterns. Thus, the active site of ChiPFK is locked in an open structure similar to that of the activated form of EcPFK.

The results in Table 3.3 indicate that ChiPFK can exist in two conformational states: a high-fluorescence state induced by the binding of ATP or AMPPNP, and a low-fluorescence state induced by Fru-6P binding. The smaller fluorescence decrease seen when Fru-6P binds to ChiPFK compared to EcPFK ( 8% *versus* 19%, respectively) suggests that the conformational change is less, and perhaps different, in ChiPFK. As revealed in Figs. 3.8A & B, the balance between high- and low-fluorescence conformational states depends on the relative amounts of AMPPNP and Fru-6P present. Furthermore, AMPPNP is more potent than Fru-6P in its ability to reverse the fluorescence state (low *versus* high) of the ChiPFK molecule. These binding results parallel the kinetic results showing that the relative amounts of Fru-6P and ATP present determine the reaction rate.

There are at least three possible explanations for the sigmoidal Fru-6P saturation kinetics of ChiPFK: (1) the sigmoidicity is due to apparent cooperativity arising from the kinetic mechanism. Both of the native enzymes from which ChiPFK is derived obey a steady-state random Bi Bi kinetic mechanism (Byrnes *et al.*, 1994; Zheng & Kemp, 1992). This mechanism can allow two kinetically-distinct pathways, and sigmoidal saturation curves (Ferdinand, 1966). Although we have not rigorously determined the kinetic mechanism of ChiPFK, our results suggest that ChiPFK also obeys a steady-state random mechanism. (2) a slow isomerization occurs in the active site when Fru-6P binds in the presence of ATP. If the isomerization is slower than the catalytic rate, cooperativity can result (Ainslie *et al.*, 1972). (3) only two of the four active sites of ChiPFK are allosterically-linked by a cooperative structural transition (Monod *et al.*, 1965) that is triggered by interactions between ATP and Fru-6P in the active site.

The fact that two conformational states exist for ChiPFK casts doubt on the notion that its cooperativity is entirely kinetic in origin. Presumably, the ChiPFK molecule goes through a conformational transition as it moves from one state to the

other according to the balance of substrate concentrations. Regarding this transition, the questions are: (1) is it a rapid and concerted one, involving more than one active site? or (2) is it slow relative to catalysis? Although one would expect homotropic linkage to be absent in ChiPFK since it is not heterotropically-regulated, this may not be the case. Indeed, a mutant EcPFK enzyme (Leu 178—>Trp) has been reported to exhibit a highly sigmoidal Fru-6P saturation profile in the absence of heterotropic regulation (Serre *et al.*, 1990). A determination of whether the conformational transition is fast or slow relative to catalysis will have to await stopped-flow fluorescence measurements.

The mechanism by which AMPPNP abolishes the cooperativity of ChiPFK (Fig. 3.7) is not known. However, it could be related to an interaction between the imidophosphate group of AMPPNP and Arg 72, an active site residue important in the cooperative behavior of EcPFK (Berger & Evans, 1990). Arg 72 is involved in neutralizing the negative charge on the transferred  $\gamma$ -phosphate of ATP in the transition state of EcPFK (Zheng & Kemp, 1994). The imidophosphate group of AMPPNP is less acidic than the  $\gamma$ -phosphate of ATP (Yount *et al.*, 1971). As a result, at pH 8.2 the Arg 72-imidophosphate interaction may be weakened relative to the Arg 72-phosphate interaction. A strengthening of the interaction with Arg 72 has been proposed to occur when the ATP analog adenosine 5'-[ $\gamma$ -thio]triphosphate (ATP- $\gamma$ -S) is used instead of ATP, in this case by perturbation of an interaction with Thr 125 (Auzat *et al.*, 1994). Whether the conformational transition associated with ChiPFK cooperativity is concerted or involves slow isomerization, the altered interaction with Arg 72 could be important in explaining the effect of AMPPNP on ChiPFK cooperative behavior.

In conclusion, we have found that the active site of the the chimeric enzyme is locked in an "open" conformation similar to that of the activated form of *E. coli* PFK. Presumably, a conformational change responsible for closure of the active site has been disrupted in the chimeric enzyme, whose ATP-binding domain is from BsPFK. Yet, despite the "openness" of its active site, ChiPFK exhibits sigmoidal kinetics with respect



to Fru-6P. We propose that the lower cooperativity of the chimeric PFK is related to its inability to undergo the open-to-closed transition involving its ATP-binding domain. Furthermore, the fact that some cooperativity remains in ChiPFK suggests that mechanisms in addition to one involving closure and opening of the active site are important for *E. coli* PFK cooperative behavior. Indeed, the complete mechanism for allosteric regulation of *E. coli* PFK is probably complex, involving binding cooperativity (Blangy *et al.*, 1968), cooperativity due to slow transitions (Deville-Bonne *et al.*, 1991a), and kinetic cooperativity arising from the kinetic mechanism (Zheng & Kemp, 1992).

## **Chapter 4**

### **The Role of Residue 161 in the Allosteric Transitions of Two Bacterial Phosphofructokinases**

Phosphofructokinase (PFK, EC 2.7.1.11) catalyzes the first committed step of glycolysis, the transfer of the  $\gamma$ -phosphate of ATP to fructose 6-phosphate (Fru-6P) to produce ADP and fructose 1,6-bisphosphate. A divalent  $Mg^{++}$  ion, as well as a monovalent  $NH_4^+$  or  $K^+$  ion, is required for catalysis. In bacteria, PFK is allosterically inhibited by phosphoenolpyruvate (PEP) and activated by ADP (or GDP). Bacterial PFK is a tetramer of identical subunits each 36,000 daltons in size. There are four active sites, and four effector sites into which both PEP and ADP (or GDP) bind.

The PFKs from the two bacteria *Escherichia coli* and *Bacillus stearothermophilus* are remarkably similar in structure (Evans *et al.*, 1981; Shirakihara & Evans, 1988): their subunits have all the same secondary structural elements, their subunit  $\alpha$ -carbon traces are nearly superimposable, and they share 55% amino acid identity. Nevertheless, PEP and GDP regulate the two enzymes somewhat differently. For example, the PEP inhibition profile for EcPFK is highly sigmoidal, while the profile for BsPFK is only slightly sigmoidal. In addition, whereas GDP strongly activates EcPFK in the presence of saturating MgATP and a Fru-6P concentration equal to the  $S_{1/2}$ -value, it weakly activates BsPFK under these conditions (Byrnes *et al.*, manuscript submitted). This difference is related to the fact that MgATP "allosterically" inhibits EcPFK (Evans, 1992), but not BsPFK, at low Fru-6P concentration (Byrnes *et al.*, 1994). However, GDP strongly activates BsPFK when the enzyme is inhibited by PEP (Valdez *et al.*, 1989). Finally, GDP can super-activate EcPFK in the presence of saturating Fru-6P levels, raising the  $k_{cat}$  10-20% higher than its value without GDP (Deville-Bonne *et al.*, 1991a), but it cannot super-activate BsPFK.

The heterotropic regulation of EcPFK by PEP and GDP has been explained in terms of the concerted two-state model of Monod, Wyman, and Changeux (MWC model, Monod *et al.*, 1965), in which the protein molecule exists in equilibrium between two states: a low-activity tense (T) state that binds PEP, and a high-activity relaxed (R) state that binds GDP (Blangy *et al.*, 1968). We will assume that BsPFK

also obeys the MWC model, although recent evidence suggests it does not (Zhu *et al.*, manuscript submitted). Schirmer & Evans (1990) have uncovered the structural basis for the allosteric transition of BsPFK by comparing crystal structures of the enzyme obtained in the presence of inhibiting *versus* activating conditions. The BsPFK tetramer can be viewed as a dimer of rigid dimers. During the transition from the T- to the R-state, the rigid dimers rotate 7° relative to each other. This rotation is coupled with a coordinated movement of two loops, the 8H and 6F loops, located between the effector and active sites. At the effector site, the major movement involves a change in the position of the 8H loop, which lines one edge of the effector cleft. In the absence of effector, the cleft is open. Binding of the smaller molecule PEP closes the cleft, shifting the enzyme to its T-state. On the other hand, binding of the larger ADP (or GDP) molecule pushes the 8H loop away from the effector site, causing it to contact the 6F loop which transmits a structural change to the active site. This structural change involves reorganization of the 6F loop, which is composed of residues Thr 156 to Arg 162 (Fig. 4.1). Arg 162, which points away from the active site in the T-state, swings back into the active site during the T-to-R transition, and binds the phosphate group of Fru-6P in the R-state. At the same time, Glu 161 which projects across the dimer-dimer interface into the active site in the T-state, has rotated away in the R-state. The 6F loop and residues Arg 162 and Glu 161 within it are thus proposed to be important in the allosteric transition of BsPFK. Most of the residues within the 6F loop, including Arg 162, are conserved between BsPFK and EcPFK (French & Chang, 1987; Hellings & Evans, 1985), but Glu 161 is not. In EcPFK, residue 161 is a glutamine (Fig. 4.2).

How important is Glu 161 for PEP inhibition and GDP activation of BsPFK? Does Gln 161 of EcPFK play a role in its regulation by either PEP or GDP? Can any differences between the two enzymes be traced to the difference at position 161, i.e., Glu *versus* Gln? To answer these questions, we have constructed a set of mutants of both BsPFK and EcPFK with changes at position 161. Glu 161 of BsPFK has been

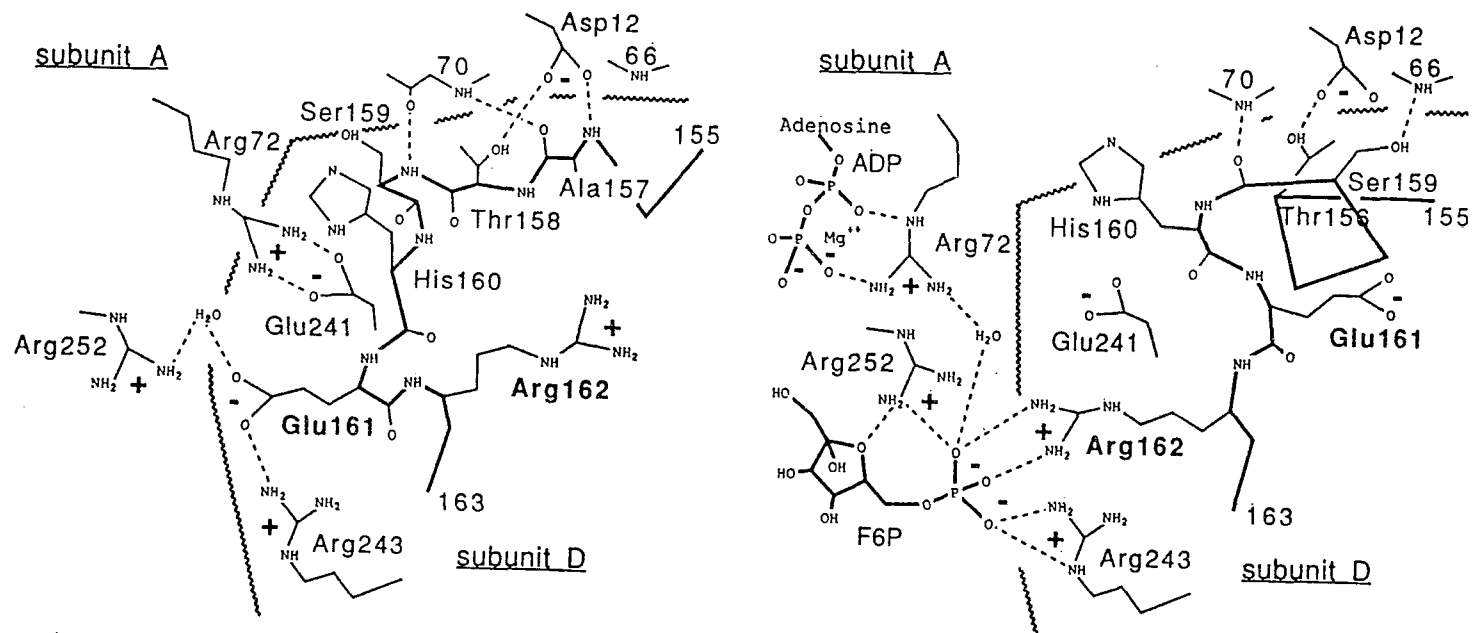


**FIGURE 4.1.** Reorganization of the 6F Loop (156-162) of *B. stearotherophilus* PFK. The wavy line represents the boundary between dimers. (A) T-state structure, showing Glu 161 in the Fru-6P site. (B) R-state structure, showing the phosphate of Fru-6P bound by Arg 162 and Arg 243. (Taken with permission from Schirmer, T., & Evans, P. R. (1990) *Nature* 343, 140-145. Copyright 1990 Macmillan Magazines, Limited).

	161
<i>B. stearrowthermophilus</i>	T A T S H <b>E</b> R
E161Q	T A T S H <b>Q</b> R
E161A	T A T S H <b>A</b> R
<i>E. coli</i>	T S S S H <b>Q</b> R
Q161E	T S S S H <b>E</b> R
Q161R	T S S S H <b>R</b> R
Q161A	T S S S H <b>A</b> R

**FIGURE 4.2.** The Amino Acid Sequences of the 6F Loops of *B. stearrowthermophilus* PFK, *E. coli* PFK, and the Five Mutant Enzymes. Residue 161 is shown in enlarged, bold print.

changed to glutamine, and to alanine which lacks hydrogen bonding ability and is smaller. Gln 161 of EcPFK has been changed to glutamate, to alanine, and to arginine in order to have a positively-charged residue at position 161. The abilities of PEP and GDP to inhibit and activate, respectively, the five mutant and the two wild-type enzymes were studied using steady-state kinetics. The results of these studies are presented.

### Materials and Methods

*Enzymes, Chemicals, and Oligonucleotides*—Restriction endonucleases, T4 DNA Ligase, DNA Polymerase (Klenow fragment), T4 Polynucleotide Kinase, and other enzymes used for cloning or *in vitro* mutagenesis were from New England Biolabs (Beverly, MA), Gibco-BRL (Grand Island, NY), or United States Biochemical (Cleveland, OH). X-gal and IPTG were from Gibco-BRL. The auxiliary enzymes aldolase,  $\alpha$ -glycerophosphate dehydrogenase, and triosephosphate isomerase were from Sigma Chemical Co. (St. Louis, MO). Substrates ATP and Fru-6P, and effectors PEP and GDP, as well as the Cibacron Blue 3GA agarose (type 3000-CL-L) were also from Sigma. The mutagenic oligonucleotides and the sequencing primers were synthesized on an Applied Biosystems 380A DNA Synthesizer. All oligonucleotides were purified in a two-step procedure involving (1) reverse-phase chromatography on an Oligo-Pak<sup>TM</sup> (Millipore, Milford, MA) purification column and (2) preparative 20% polyacrylamide gel electrophoresis. The purity and length of each oligonucleotide was verified by first 5' end-labeling the oligo using [<sup>32</sup>P]  $\gamma$ -ATP and T4 polynucleotide kinase, then subjecting it to electrophoresis on an analytical 20% polyacrylamide gel and autoradiography.

*Site-directed Mutagenesis*—The EcPFK gene was excised from a recombinant *ecpfk*/pUC18 plasmid (Hellenga & Evans, 1985), and subcloned into M13mp19 *via* its Nar I and Kpn I restriction sites. Similarly, the BsPFK gene contained within a 2.5 kilobase EcoR I/ Cla I fragment that had been cloned into pBR322 (French & Chang,

1987) was subcloned into M13mp18 *via* its EcoR I and Acc I sites. The single-stranded DNA produced from either M13 vector contained the coding strand of the *pfk* gene.

Competent DH5 $\alpha$ F' *E. coli* cells (Gibco-BRL) were transformed with the recombinant M13 RF DNA, then plated by the top-agar method onto YT (yeast extract/tryptone) agar plates containing X-gal and IPTG, which allow blue/white color selection. After overnight incubation at 37°C, a clear (turbid) plaque harboring the *ecpfk* or *bspfk* insert was picked and used to infect DH5 $\alpha$ F' cells. The infected cells were grown in liquid YT medium for 6 hours at 37°C. After centrifugation, the supernatant of the cell culture, which contained M13 phage particles, was used to infect fresh *E. coli* BW313 cells. (BW313 cells are *dur<sup>-</sup> ung<sup>-</sup>*). The infected BW313 cells were grown overnight at 37°C in YT containing uridine at 25  $\mu$ g/ml. Uracil-containing single-stranded DNA was then prepared from the supernatant of the infected cell culture (Kunkel *et al.*, 1987), and used as a template for *in vitro* mutagenesis as described by Zoller & Smith (1983). The mutagenic oligonucleotides were designed to change codon 161 in *bspfk* from that for a glutamate (GAG) to that for either a glutamine (CAG) or an alanine (GCG). In *ecpfk*, the mutagenic oligos were designed to change codon 161 from that for a glutamine (CAG) to that for a glutamate (GAA), an arginine (CGT), and an alanine (GCT). Table 4.1 lists the oligos and their sequences. After mutagenesis, competent DH5 $\alpha$ F' cells were transformed with the reaction mixture containing the mutated DNA, then plated onto YT agar plates. Transformants were screened for the mutation by (1) plaque hybridization using the mutagenic oligonucleotide labeled with <sup>32</sup>P as a probe (Seong & RajBhandary, 1987), and (2) partial sequencing of the single-stranded DNA from positives identified in the plaque hybridization. A single positive transformant was then selected, single stranded DNA was prepared from it, and the entire coding region of the mutated gene was sequenced by the dideoxy method (Sanger, 1977) using a Sequenase<sup>TM</sup> kit (United States Biochemical) and a battery of



**TABLE 4.1**  
*Mutagenic Oligonucleotides*

Oligo Designation	Position of 3' End (codon number)	Sequence (5'→3')
Bs E161Q	157	CGTACGTCCG <u>CT</u> GGTGCACGTCGC *
Bs E161A	157	CGTACGTCCG <u>GCG</u> GTGCACGTCGC *
Ec Q161E	156	CGGAAATACG <u>TTC</u> GTGAGAAGAAGAGG * *
Ec Q161R	156	CGGAAATACG <u>ACG</u> GTGAGAAGAAGAGG * *
Ec Q161A	156	CGGAAATACG <u>GCG</u> GTGAGAAGAAGAGG * * *

Bs, *B. stearothermophilus*; Ec, *E. coli*. The mutagenic oligonucleotides are complementary to the *bspfk* or *ecpfk* coding strands. Oligos Bs E161Q and E161A are designed to change the codon for glutamate 161 of *bspfk* (GAA) to those for a glutamine (CAG) and an alanine (GCG), while oligos Ec Q161E, Q161R, and Q161A are designed to change the codon for glutamine 161 of *ecpfk* (CAG) to those for a glutamate (GAA), an arginine (CGT), and an alanine (GCT). The *underlined* nucleotides are those complementary to codon 161. The nucleotides with *asterisks* above them are the ones that are different in the mutated gene.

intragenic primers to verify that no unintentional mutations had been introduced. This was done for all five mutated genes.

*Expression and Purification of PFKs*—The mutated BsPFK genes were excised from M13mp18 and inserted into the EcoR I/ Hind III sites of the plasmid pUC18. Similarly, the mutated EcPFK genes were excised from M13mp19 and inserted into the Hind III site of pUC18. The recombinant pUC18 plasmids were then transformed into competent cells of a PFK-deficient *E. coli* strain (DF 1020) for expression. The transformed DF 1020 cells were grown to stationary phase in Luria Broth containing ampicillin (50 µg/ml) and the cells were pelleted, resuspended in 50 mM Tris-Cl, pH 7.4, 1 mM DTT, 1 mM EDTA, and 1 mM phenylmethylsulfonyl fluoride (Buffer A), and sonicated. The procedures used to purify BsPFK and EcPFK were somewhat different. BsPFK and its mutants were purified from the crude extract in a two-step procedure that involved heat-treatment at 70°C followed by affinity chromatography on a Cibacron Blue 3GA agarose column (Valdez *et al.*, 1989). The wild-type and two mutant BsPFK enzymes were eluted from the column with a 0.25 to 1.5 M NaCl gradient; all three eluted at approximately 1.1 M NaCl. Like wild-type BsPFK, the EQ161 and EA161 mutant enzymes were both stable when incubated at 70°C during the heat step. Heat-treatment was not used in purifying the wild-type and mutant EcPFK enzymes since they are not thermostable. Rather, the crude extract obtained after sonication was loaded directly onto a Cibacron Blue 3GA agarose column and purified essentially as described (Hellings & Evans, 1987). The column was washed with 1 M NaCl, then with Buffer A, and the native or modified EcPFK was eluted with 2 mM ATP/ 10 mM MgCl<sub>2</sub> in Buffer A. For all enzymes, column fractions having the highest PFK activity were pooled. Each enzyme preparation was shown to be pure by the presence of a single band on a 12% SDS-polyacrylamide gel stained with Coomassie Brilliant Blue. Purified wild-type or mutant BsPFK enzymes were concentrated by dialysis against 50% glycerol in Buffer A at 4°C. Purified wild-type or mutant EcPFK

enzymes, on the other hand, were concentrated by either (1) dialysis at 4°C against 50% glycerol in Buffer A containing 2 mM ATP/10 mM MgCl<sub>2</sub>, or (2) ultrafiltration in an Amicon cell (Beverly, MA). The enzymes concentrated in 50% glycerol were stored at -20°C, and the enzymes concentrated by ultrafiltration were precipitated with 55% ammonium sulfate, then stored at 4°C.

*Activity Assays*—PFK activity was measured at 30°C using an assay system (Kotlarz & Buc, 1982) that coupled the production of fructose 1,6-bisphosphate to the oxidation of NADH. The assay solution contained 100 mM Tris-Cl, pH 8.2, 10 mM MgCl<sub>2</sub>, 5 mM NH<sub>4</sub>Cl, 0.20 mM NADH, and the coupling enzymes aldolase (20 µg/ml), triosephosphate isomerase (10 µg/ml) and α-glycerophosphate dehydrogenase (10 µg/ml). An ATP-regenerating system that utilizes creatine phosphate (1 mM) and creatine phosphokinase (10 µg/ml) was used in all EcPFK-catalyzed reactions to prevent activation by ADP produced in the reaction. When studying GDP-activation, the regenerating system was not used. It was found to be unnecessary for BsPFK and its mutants since they are not activated to any significant degree by GDP except in the presence of PEP. For each assay, the change in absorbance at 340 nm was measured for at least 1-minute using an Hitachi UV-2000 spectrophotometer. Reactions were initiated by addition of PFK. One initial velocity unit is defined as the number of µmoles of fructose 1,6-bisphosphate formed per minute; there are 12.4 initial velocity units per ΔA<sub>340</sub>/min. unit. In order to obtain kinetic parameters, initial velocity data were fit to either the Michaelis-Menten equation for hyperbolic kinetics, or the Hill equation for sigmoidal kinetics. All curve-fitting was performed by nonlinear regression analysis using the program INPLOT (GraphPad, Inc., San Diego, CA).

## Results

*Steady-state Kinetic Parameters*—Substrate saturation of the wild-type and mutant enzymes was studied using steady-state kinetics. Fig. 4.3 shows that the two wild-type enzymes have different Fru-6P saturation curves: whereas the curve for

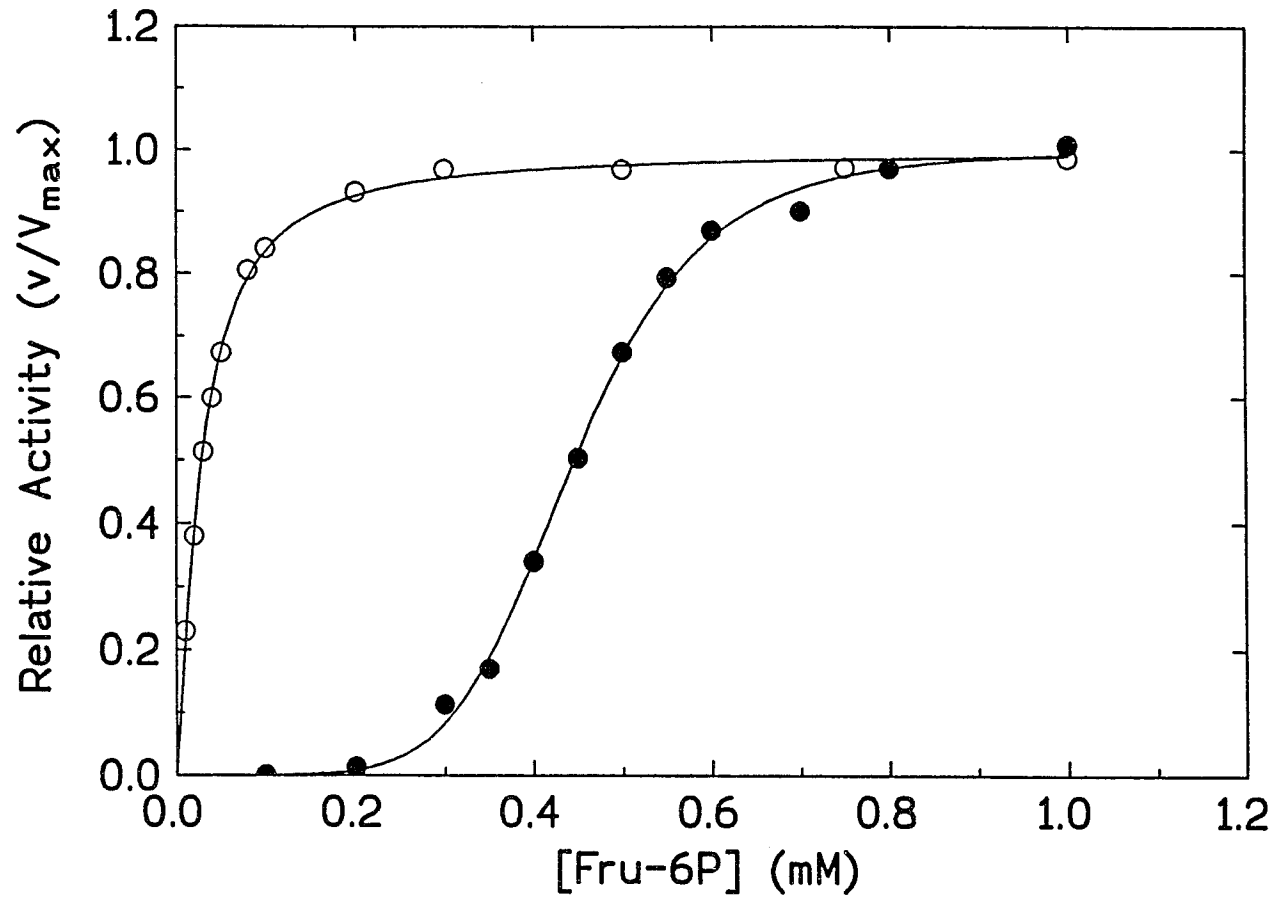


**FIGURE 4.3. Fructose 6-phosphate Saturation Curves for *B. stearothermophilus* PFK (○) and *E. coli* PFK (●). The MgATP concentration was saturating at 1.0 mM.**

EcPFK is highly sigmoidal (Hill number 5.6) in the presence of saturating MgATP concentration, the curve for BsPFK is essentially hyperbolic (Valdez *et al.*, 1989), though not perfectly so (Byrnes *et al.*, 1994). Table 4.2 presents the kinetic parameters for the five mutant PFKs as well as the two wild-type enzymes. The  $k_{cat}$ ,  $K_m^{ATP}$ , and  $K_m^{Fru-6P}$  values for the two BsPFK mutants (EQ161 and EQ161) are similar to the values for wild-type BsPFK. The three EcPFK mutants (QE161, QR161, and QA161) have kinetic parameters similar to those for wild-type EcPFK, but show some variation in the sensitivity and cooperativity of their responses to Fru-6P (Table 4.2). These differences between the mutants and the wild-type enzyme are not great, however. Thus, alteration of residue 161 does not significantly affect the response of either BsPFK or EcPFK to substrates Fru-6P and MgATP, indicating that this residue is not involved in substrate binding and catalysis.

*PEP Inhibition*—Fig. 4.4 shows that both EcPFK and BsPFK are subject to inhibition by PEP. However, the sensitivity and cooperativity of their responses differ. EcPFK is both less sensitive ( $I_{1/2}^{PEP}$  is 1.17 mM) and more cooperative ( $n$  is 4.3) in its response to increasing PEP concentration than is BsPFK ( $I_{1/2}^{PEP}$  is 0.28 and  $n$  is 1.6). Table 4.3, which presents the values for  $I_{1/2}^{PEP}$  and  $n$  for the five mutant enzymes as well as the wild-type ones, shows that mutation of Glu 161 in BsPFK to either Gln or Ala decreases the sensitivity and increases the cooperativity of the response to PEP. These changes, though significant, are not drastic. They suggest that residue 161 is involved in PEP inhibition of BsPFK, but neither its hydrogen-bonding ability nor its size is critical. Mutation of Gln 161 in EcPFK to either Glu or Arg decreases the sensitivity and also decreases the cooperativity of the response. It is interesting that mutants EQ161 of BsPFK and QE161 of EcPFK, in which residue 161 of one enzyme has been replaced with that of the other, have similar responses to PEP: both are less sensitive to PEP than their respective wild-type enzymes, and both display similar cooperative responses to PEP that are in-between those of the two wild-type enzymes,

**TABLE 4.2**  
*Steady-state Kinetic Parameters for Wild-type and Mutant PFKs*

Enzyme	$k_{\text{cat}}$ (s <sup>-1</sup> ) <sup>a</sup>	$K_{\text{m}}^{\text{ATP}}$ (μM)	$K_{\text{m}}^{\text{Fru-6P}}$ (μM) <sup>b</sup>	$S_{1/2}^{\text{Fru-6P}}$ (mM) <sup>c</sup>	n
WT BsPFK	206	70 ± 3	36 ± 2	N.A.	h
Bs EQ161	208	112 ± 8	35 ± 3	N. A.	h
Bs EA161	168	123 ± 6	41 ± 3	N. A.	h
WT EcPFK	127	103 ± 2	N. A.	0.48 ± 0.01	5.8 ± 0.2
Ec QE161	126	77 ± 4	N. A.	1.87 ± 0.04	5.6 ± 0.2
Ec QR161	133	47 ± 4	N. A.	0.91 ± 0.03	5.0 ± 0.4
Ec QA161	134	55 ± 3	N. A.	0.92 ± 0.02	4.4 ± 0.3

The kinetic parameters were obtained by fitting substrate saturation data to either the Michaelis-Menten equation or the Hill equation.  $k_{\text{cat}}$ , the catalytic rate constant;  $K_{\text{m}}^{\text{ATP}}$ , the ATP concentration at half-maximal velocity;  $K_{\text{m}}^{\text{Fru-6P}}$  and  $S_{1/2}^{\text{Fru-6P}}$ , the Fru-6P concentration at half-maximal velocity for Fru-6P saturation data fit to the Michaelis-Menten and Hill equations, respectively; n, the Hill coefficient; N.A., not applicable; h, hyperbolic.  $K_{\text{m}}^{\text{ATP}}$  was obtained in the presence of saturating Fru-6P concentration, and  $K_{\text{m}}^{\text{Fru-6P}}$  was obtained in the presence of saturating MgATP concentration. <sup>a</sup>The  $k_{\text{cat}}$ -values for BsPFK and its mutants appear to be higher than the values for EcPFK and its mutants, but this is a function of their different Fru-6P saturation profiles, *i.e.*, hyperbolic *versus* sigmoidal. In the presence of GDP, their  $k_{\text{cat}}$  values are similar. <sup>b</sup> $K_{\text{m}}^{\text{Fru-6P}}$  is appropriate only for BsPFK and its mutants, which follow Michaelis-Menten Fru-6P saturation kinetics. <sup>c</sup> $S_{1/2}^{\text{Fru-6P}}$  is appropriate only for EcPFK and its mutants.

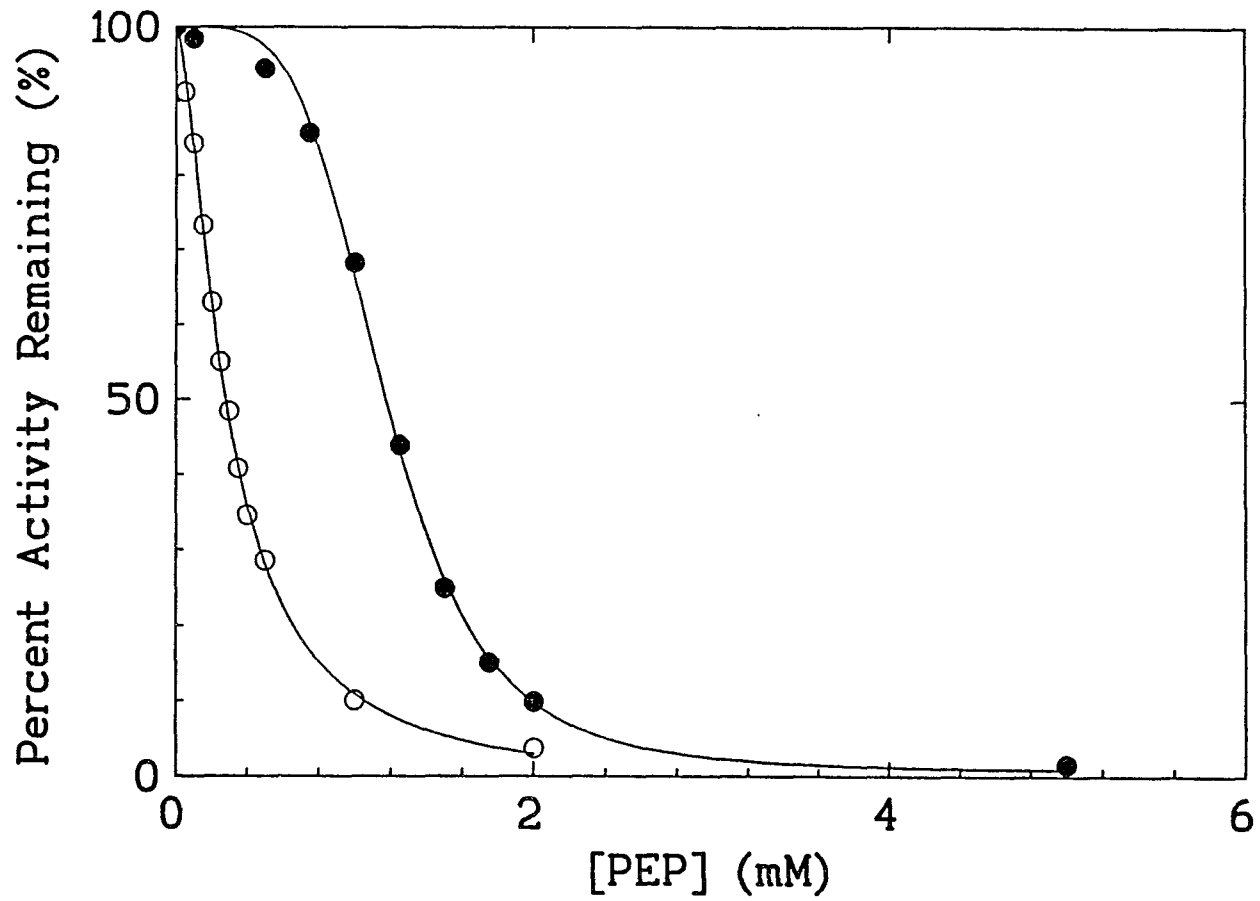


**FIGURE 4.4.** PEP Inhibition of *B. stearotherophilus* PFK (○) and *E. coli* PFK (●). The Fru-6P concentration was 0.3 mM for BsPFK, and 1.5 mM for EcPFK. The MgATP concentration was 1.0 mM for both.

**TABLE 4.3**  
*PEP Inhibition of Wild-type and Mutant PFKs*

Enzyme	[Fru-6P] (mM) <sup>a</sup>	I <sub>1/2</sub> <sup>PEP</sup> (mM)	n
WT BsPFK	0.3	0.28 ± 0.01	1.6 ± 0.1
Bs EQ161	0.3	3.9 ± 0.1	3.0 ± 0.2
Bs EA161	0.3	0.70 ± 0.01	2.6 ± 0.1
WT EcPFK	1.5	1.17 ± 0.01	4.3 ± 0.2
Ec QE161	5.0	6.3 ± 0.6	2.4 ± 0.5
Ec QR161	2.5	9.8 ± 0.2	3.7 ± 0.2
Ec QA161	5.0	NO INHIBITION	

Bs, *B. stearothermophilus*; Ec, *E. coli*; WT, wild-type; I<sub>1/2</sub><sup>PEP</sup>, the PEP concentration at half-maximal (50%) inhibition; n, the Hill coefficient. The values for I<sub>1/2</sub><sup>PEP</sup> and n were obtained by fitting data from Activity *versus* PEP Concentration plots to the Hill equation. <sup>a</sup>The Fru-6P concentration used was a saturating amount chosen by inspection of individual Activity *versus* Fru-6P Concentration plots. The MgATP concentration was 1 mM for all assays.



*i.e.*, the Hill coefficients are between 1.6 and 4.3. Most importantly, Table 4.3 shows that mutation of Gln 161 to Ala completely abolishes PEP inhibition of EcPFK. This indicates that the hydrogen-bonding ability of residue 161 is required for the inhibition. The fact that the hydrogen-binding ability of residue 161 is crucial for PEP inhibition of EcPFK but not BsPFK suggests that the mechanisms by which PEP inhibits the two enzymes are somewhat different.

*GDP Activation of EcPFK and Its Mutants*—GDP activation of EcPFK and its mutants was studied in two different ways: (1) by examining the ability of GDP to "super-activate" the enzymes, *i.e.*, by comparing Fru-6P saturation curves in the absence and presence of 2 mM GDP, and (2) by looking at GDP activation of the ATP-inhibited enzymes, *i.e.*, by plotting activity *versus* GDP concentration for the enzymes in the presence of saturating MgATP, and a Fru-6P concentration equal to  $S_{1/2}^{\text{Fru-6P}}$ . Fig. 4.5 and its *inset* show GDP activation of EcPFK analyzed in these two ways. From plots such as those in Fig. 4.5, one can obtain the extent to which GDP increases the  $k_{\text{cat}}$  beyond its value in the absence of GDP, *i.e.*, the extent to which it super-activates. For wild-type EcPFK, the super-activation is 11% . On the other hand, from activation profiles such as the one in the *inset* of Fig. 4.5, which is hyperbolic, one can obtain the GDP concentration at half-maximal activation,  $K_{\text{act}}^{\text{GDP}}$ . For wild-type EcPFK, the value is  $13 \pm 4 \mu\text{M}$ . Table 4.4 presents the results of GDP activation studies of the three mutant enzymes QE161, QR161, and QA161, as well as wild-type EcPFK, analyzed in the two ways described above. All three mutant enzymes were super-activated by GDP to an extent similar to wild-type EcPFK, but their sensitivities to GDP activation, as measured by  $K_{\text{act}}^{\text{GDP}}$ , were lower.

*Activation of BsPFK and Its Mutants by GDP and Fru-6P*—Unlike EcPFK, BsPFK is not subject to GDP activation to any significant extent unless the enzyme is already inhibited by PEP. Furthermore, GDP does not super-activate BsPFK. Therefore, GDP activation of BsPFK was analyzed differently. BsPFK and its mutants

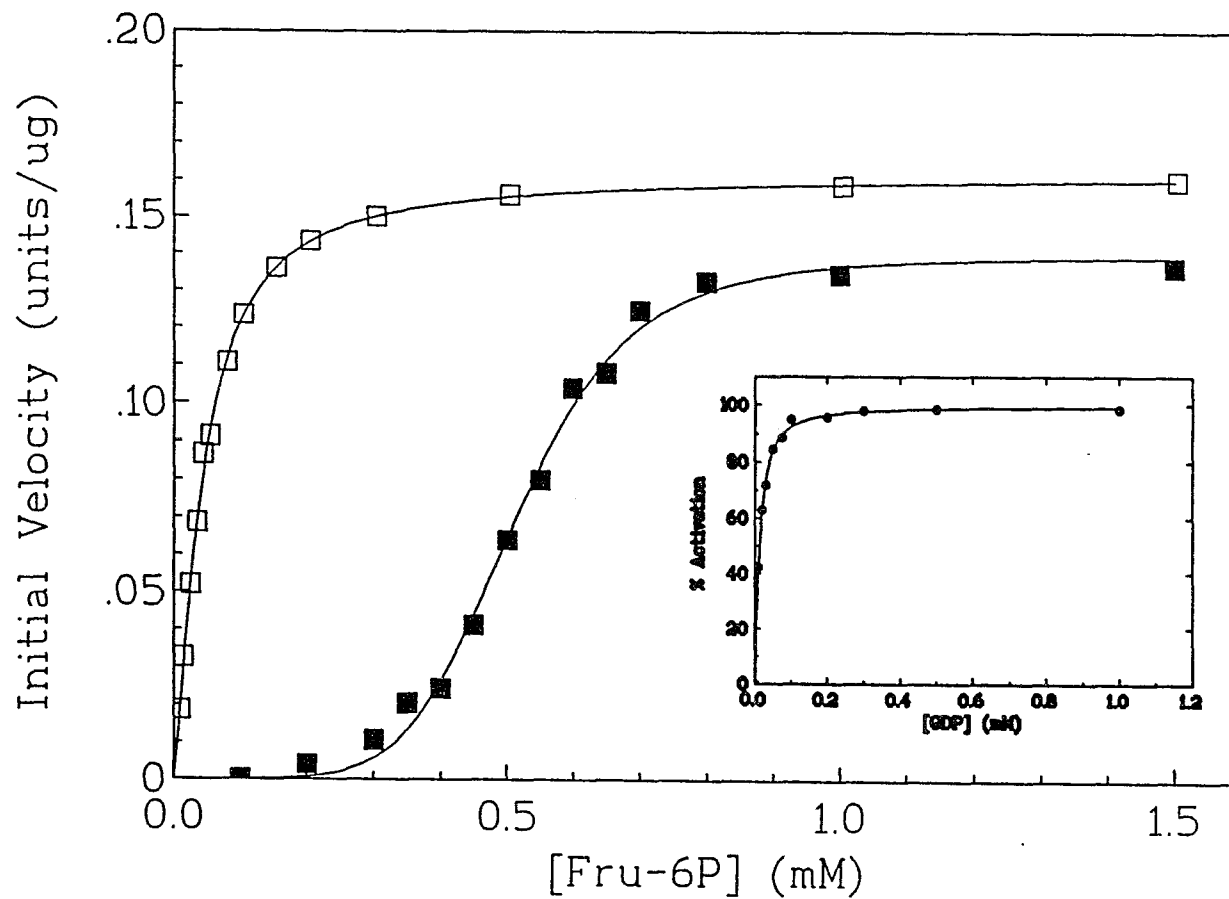


**FIGURE 4.5. GDP Activation of *E. coli* PFK.** Fru-6P saturation curves in the absence (■) or presence (□) of 2 mM GDP, showing super-activation by GDP. The MgATP concentration was 1.0 mM. *Inset*, % activation versus GDP concentration for EcPFK inhibited by MgATP. The Fru-6P concentration was equal to  $S_{1/2}^{\text{Fru-6P}}$  (0.5 mM), and the MgATP concentration was saturating at 1.0 mM.

**TABLE 4.4**  
*Activation of EcPFK and Its Mutants by GDP*

Enzyme	$k_{\text{cat}}^{\text{super}}$ (s <sup>-1</sup> )	% Activation	$K_{\text{act}}^{\text{GDP}}$ (μM)
WT EcPFK	140 (127)	11	13 ± 4
Ec QE161	89 (70)	28	51 ± 12
Ec QR161	147 (133)	10	84 ± 23
Ec QA161	157 (134)	17	95 ± 12

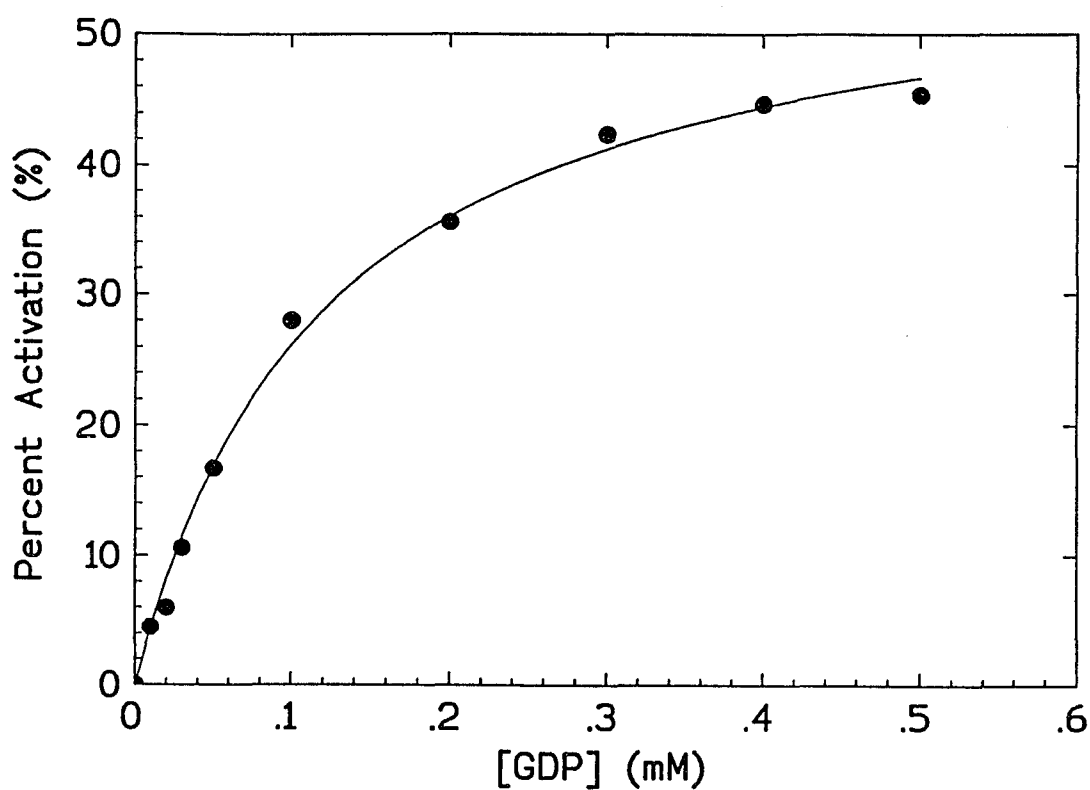
*Ec, E. coli*; WT, wild-type;  $k_{\text{cat}}^{\text{super}}$ , the catalytic rate constant for the enzyme super-activated by 2 mM GDP (the number in parentheses is the  $k_{\text{cat}}$  value for the enzyme in the absence of GDP.);  $K_{\text{act}}^{\text{GDP}}$ , the concentration of GDP at half-maximal activation. The values for  $k_{\text{cat}}^{\text{super}}$  and the % Activation were obtained from plots such as the one in Fig. 4.5.  $K_{\text{act}}^{\text{GDP}}$ -values were obtained from plots such as the one in Fig. 4.5, *inset*. The MgATP concentration was 1.0 mM in all assays. In determining  $K_{\text{act}}^{\text{GDP}}$ , the Fru-6P concentration was equal to the  $S_{1/2}^{\text{Fru-6P}}$ -value. See the text for further details.

were first inhibited by PEP, then the ability of GDP to activate the PEP-inhibited enzyme was studied. (The PEP concentration was equal to its  $I_{1/2}^{\text{PEP}}$ -value). Fig. 4.6A shows the activation profile obtained for wild-type BsPFK; it is hyperbolic and yields a  $K_{\text{act}}^{\text{GDP}}$  of  $122 \pm 11 \mu\text{M}$ . The activation constants obtained from similar curves for the two mutant enzymes EQ161 and EA161 are presented in Table 4.5. Both are four-fold lower than the value for wild-type BsPFK, indicating that EQ161 and EA161 are more sensitive to GDP activation.

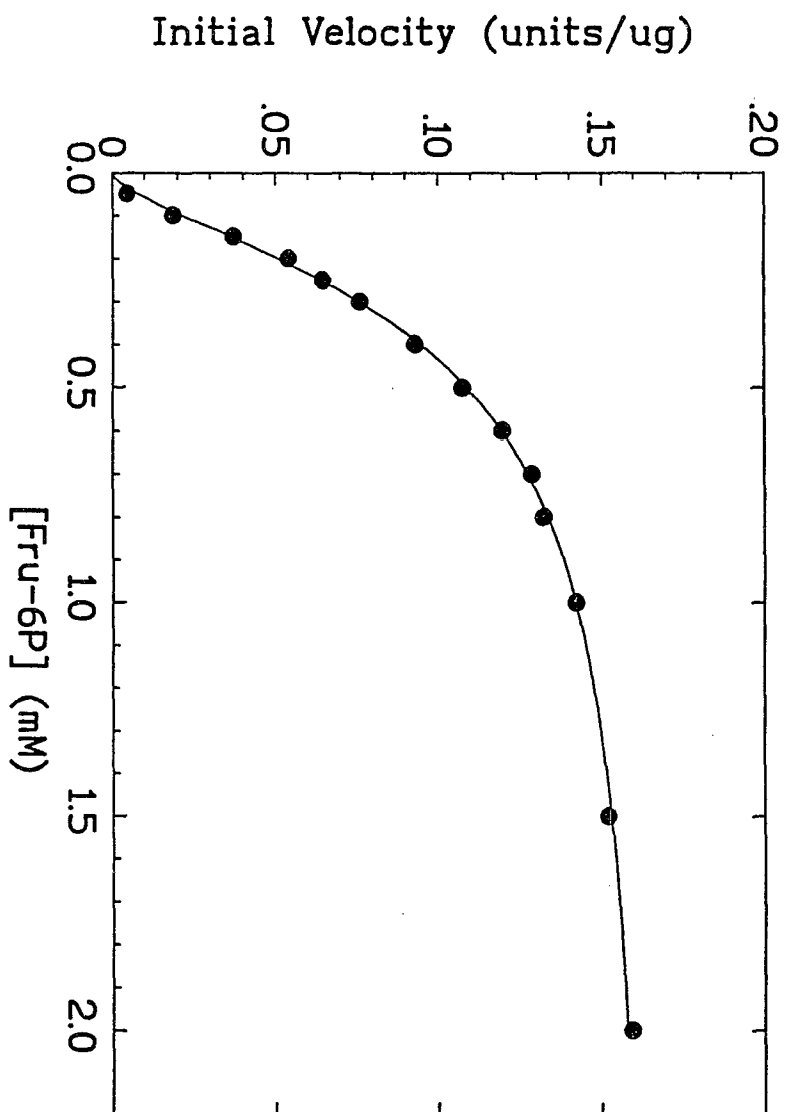
The ability of Fru-6P to activate the PEP-inhibited wild-type and mutant BsPFK enzymes was also investigated. The Fru-6P saturation profile for wild-type BsPFK in the presence of PEP at a concentration equal to its  $I_{1/2}^{\text{PEP}}$  value (Fig. 4.6B) is somewhat cooperative ( $n$  is 1.6), and gives an  $S_{1/2}^{\text{Fru-6P}}$  value of  $0.34 \pm 0.01 \mu\text{M}$ . As shown in Table 4.5, the EQ161 and EA161 mutants are as sensitive as the wild-type enzyme is to Fru-6P, but the cooperativity of their responses are higher. It is interesting that, for each PEP-inhibited enzyme (wild-type, EQ161, and EA161), the cooperativity of its response to Fru-6P matches the cooperativity of its response to PEP (Table 4.3). This symmetry between PEP inhibition and Fru-6P activation for BsPFK and its mutants strongly suggests that the two processes occur through a common structural pathway.

## Discussion

Using steady-state kinetics, we have studied two site-specific mutants of *B. stearothermophilus* PFK (EQ161 and EA161) and three mutants of *E. coli* PFK (QE161, QR161, and QA161) in order to better understand the role of residue 161 in the allosteric regulation of the wild-type enzymes. In the T-state structure of BsPFK, Glu 161 is proposed to form a salt bridge with Arg 243, and to interact with Arg 252 across the dimer-dimer interface through a water molecule (Schirmer & Evans, 1990). The results of the PEP inhibition and GDP activation studies of BsPFK presented here, however, show that neither the negative charge of residue 161 nor its hydrogen-bonding ability is critical for allosteric inhibition and allosteric activation of the enzyme. In view

**A**

**FIGURE 4.6. Activation of PEP-inhibited *B. stearothermophilus* PFK.** The enzyme was inhibited by PEP at a concentration equal to its  $I_{1/2}^{\text{PEP}}$  (0.28 mM). (A) Plot of % Activation versus GDP concentration, showing the ability of GDP to activate the PEP-inhibited enzyme to 100%. The Fru-6P concentration was 0.3 mM. (B) Effect of increasing Fru-6P concentration on the activity of the PEP-inhibited enzyme. The MgATP concentration was 1.0 mM in both (A) and (B).

**B**

**TABLE 4.5**  
*Activation of BsPFK and Its Mutants by GDP and Fru-6P*

Enzyme	$K_{\text{act}}^{\text{GDP}}$ ( $\mu\text{M}$ )	$S_{1/2}^{\text{Fru-6P}}$ (mM)	n
WT BsPFK	122 $\pm$ 11	0.34 $\pm$ 0.01	1.58 $\pm$ 0.05
Bs EQ161	23 $\pm$ 1	0.28 $\pm$ 0.01	3.0 $\pm$ 0.1
Bs EA161	29 $\pm$ 2	0.28 $\pm$ 0.01	2.8 $\pm$ 0.2

The kinetic parameters in this table describe the activation of PEP-inhibited BsPFK and its mutants by GDP and Fru-6P. Bs, *B. stearothermophilus*; WT, wild-type;  $K_{\text{act}}^{\text{GDP}}$ , the GDP concentration at half-maximal activation obtained from plots such as the one in Fig. 4.6A;  $S_{1/2}^{\text{Fru-6P}}$ , the Fru-6P concentration at half-maximal velocity obtained from plots such as the one in Fig. 4.6B; n, the Hill coefficient for the Fru-6P saturation curve. The PEP concentration was equal to its  $I_{1/2}^{\text{PEP}}$ -value. The MgATP concentration was 1.0 mM in all assays. In determining  $K_{\text{act}}^{\text{GDP}}$ , the Fru-6P concentration was 0.3 mM.

of these results, we propose that other interactions such as the one between Arg 72 and Glu 241 (Schirmer & Evans, 1990) are important in stabilizing the T-state of BsPFK, and interactions among Arg 162, Arg 243, and Fru-6P are important in stabilizing the R-state. In addition, it is significant that the EQ161 and EA161 mutants of BsPFK were both less sensitive to PEP inhibition and more sensitive to GDP activation. These results indicate that in BsPFK the processes of inhibition and activation are opposed to each other, and proceed through a common structural pathway, i.e., one that involves Glu 161. Our results are thus consistent with the model of Schirmer & Evans (1990).

The kinetic parameters obtained for the mutant enzymes (Table 4.2) are similar to those for their respective wild-type enzymes. Thus, residue 161 is not directly involved in the binding of substrates, or in catalysis. The residue is also not important for homotropic regulation of EcPFK, *i.e.*, it plays no important role in the sigmoidal response of the enzyme to Fru-6P (at saturating MgATP levels). The mechanism by which ATP inhibits EcPFK, causing its Fru-6P saturation kinetics to be sigmoidal, has been investigated (Zheng & Kemp, 1992), but has not been conclusively determined. The mechanism is proposed to involve substrate antagonism between MgATP and Fru-6P in the active site (Zheng & Kemp, 1992; Deville-Bonne, 1991b; Johnson & Reinhart, 1992). There is evidence in the literature that the structural pathways by which ATP and PEP inhibit EcPFK are different. Several modified EcPFK enzymes have been reported to be insensitive to PEP inhibition but nevertheless have sigmoidal Fru-6P saturation kinetics (Le Bras *et al.*, 1982; Serre *et al.*, 1990; Byrnes *et al.*, manuscript submitted). Our results support the proposal that the mechanisms of ATP inhibition and allosteric PEP inhibition are distinct. Specifically, the cooperativity of the EcPFK mutant QA161, which is insensitive to PEP inhibition, was not significantly different from the cooperativity of wild-type EcPFK (Hill numbers 4.4 *versus* 5.6). This indicates that "allosteric" ATP inhibition is not affected by the mutation; therefore, its mechanism is distinct from PEP inhibition. The two processes, inhibition by ATP and



by PEP, most likely occur *via* different structural pathways altogether. (This is not to say that there is no overlap between them. Indeed, both inhibition processes affect catalysis at the active site. Thus, certain residues at the active site, *e.g.*, Arg 72, Arg 162, and Arg 243, may participate in both).

The results above showing that Gln 161 of EcPFK is not important for ATP inhibition of the enzyme are in contrast to those obtained for the PFK from rabbit muscle (Li *et al.*, 1993). Based on the fact that rabbit muscle PFK is about twice the size of bacterial PFK and has clear N- and C-half internal homology, Poorman *et al.* (1984) have proposed that the rabbit muscle PFK gene arose from its procaryotic progenitor by gene duplication and divergence. Mutation of Gln 200 of rabbit muscle PFK, which corresponds to residue 161 of bacterial PFK, showed that Q200 plays an important role in Fru-6P binding and homotropic regulation by ATP, but is less important for heterotropic regulation by the effectors fructose 2,6-bisphosphate and citrate. The effects of the mutation were pH-dependent. Thus, Q200 in rabbit muscle PFK has evolved to play an important role in pH-dependent regulation of the enzyme by ATP. In *E. coli* PFK, on the other hand, the corresponding residue Q161 is important for heterotropic regulation by PEP, but not homotropic regulation by ATP. Regulation by ATP of the larger eucaryotic PFK therefore proceeds *via* a mechanism that is different from, and undoubtedly more complex than, the mechanism by which ATP regulates the simpler procaryotic enzyme.

Our results also suggest that GDP activation of the ATP-inhibited EcPFK enzyme proceeds through a structural pathway different from the one followed when GDP activates the PEP-inhibited enzyme. Like BsPFK, activation of EcPFK from its PEP-inhibited state most likely involves residue 161, and follows a mechanism similar to the one proposed by Schirmer and Evans (1990). However, the observation that the EcPFK mutant QA161 is activated by GDP despite its insensitivity to PEP inhibition indicates that activation of EcPFK from its ATP-inhibited state does not involve residue

161, and proceeds through an entirely different pathway. The structural elements involved in this second pathway of activation are unknown. It is interesting that BsPFK does show a small degree of activation by GDP (20%) in the absence of PEP when Fru-6P is equal to  $S_{1/2}^{\text{Fru-6P}}$  (Byrnes *et al.*, manuscript submitted). This subtle activation of the more "rigid" BsPFK enzyme may be a scaled-down version of the activation observed in the "floppier" EcPFK molecule inhibited by ATP.

Four of the seven residues along the 6F loop of EcPFK, which is comprised of residues Thr 156 to Arg 162, have been previously mutated: Thr 156 has been changed to Gly/Ser, Ser 159 to Asn, His 160 to Asn (Kundrot & Evans, 1991), and Arg 162 to Ser (Berger & Evans, 1990). The mutation of Q161 reported in this work now brings the number of residues mutated to five. Each mutation has had a somewhat different effect on the enzyme. The T(GS)156 and SN159 mutants exhibit severely reduced catalytic rate constants and affinities for Fru-6P, and linear kinetics (up to 100 mM) with respect to Fru-6P. They are insensitive to GDP activation, have dissociation constants for PEP ( $K_T(\text{PEP})$ -values) similar to wild-type, and exhibit hyperbolic responses to PEP. T(GS)156 and SN159 are proposed to be locked in the T-state (Kundrot & Evans, 1991). HN160 has a 10-fold lower affinity for Fru-6P but retains full cooperativity. It has dissociation constants for GDP and PEP ( $K_R(\text{GDP})$  and  $K_T(\text{PEP})$ , respectively) similar to those of wild-type EcPFK, and gives a hyperbolic response to PEP. The RS162 mutant has a dramatically-reduced catalytic rate constant and affinity for Fru-6P, has a two-fold lower cooperativity, and is inhibited by GDP even though GDP abolishes cooperativity. On the other hand, our results show that QA161 has a  $k_{\text{cat}}$  and response to Fru-6P similar to wild-type, is about 7-fold less sensitive to GDP activation, and is completely insensitive to PEP inhibition. It is difficult to correlate our results involving QA161 with those of the other 6F loop mutants, partly because of the different ways PEP inhibition and GDP activation were analyzed. Certainly, the major effect of the Q161→A mutation is to abolish PEP

inhibition. The structural basis for this could be the loss of one or more hydrogen bonds in the vicinity of the active site and along the dimer-dimer interface in the T-state structure of EcPFK.

In conclusion, our results show that the hydrogen-bonding ability of residue 161 is critical for PEP inhibition of EcPFK. The identity of residue 161 is less important for PEP inhibition of BsPFK, and other residues are apparently important for stabilizing its T-state structure. The fact that GDP can activate the Ec QA161 mutant from its ATP-inhibited state, despite the inability of the enzyme to be inhibited by PEP, suggests that a pathway of activation that does not involve residue 161 exists in EcPFK. This second pathway of GDP activation may be the one associated with super-activation. In contrast, the results showing that mutation of residue 161 in BsPFK affects GDP activation as well as PEP inhibition suggests that the same structural elements are utilized in both processes, as suggested by Schirmer & Evans (1990). Finally, it appears that BsPFK, which has evolved to function at temperatures between 65° and 80°C, possesses a mechanism of heterotropic regulation that involves minimal conformational change. Allosteric inhibition and activation utilize the same pathway. On the other hand, EcPFK, which has evolved under less stringent conditions, has a "floppier" structure, and more varied mechanisms of heterotropic regulation. GDP activation and PEP inhibition follow divergent pathways.

**Chapter 5**  
**Conclusions and Future Studies**

The structural basis for kinetic and allosteric differences between the PFKs from *Bacillus stearothermophilus* and *Escherichia coli* has been investigated, and partially uncovered, in the studies presented in this dissertation. An analysis of the results in the context of the existing literature suggests that many of the differences between the two PFKs can be attributed to differences in their conformational flexibility. *E. coli* PFK has a more "floppy" structure, while *B. stearothermophilus* PFK is more "rigid." The reasons for this are undoubtedly evolutionary. The bacteria from which the enzymes are isolated have evolved to live in very different ecological niches: thermophilic *B. stearothermophilus* in hot springs where temperatures are around 70°C, and mesophilic *E. coli* in the mammalian gut, where temperature is constant at 37°C. One would expect that the enzyme from a thermophilic organism would be much more conformationally conservative in its response to regulatory effectors than one from a mesophilic organism. Why?—because large conformational changes would be more apt to destabilize it. Indeed, BsPFK is conformationally conservative. The allosteric transition involves little movement: a rotation of two rigid dimers by 7° relative to each other, a slight opening of the dimer-dimer interface, and the concerted movement of two loops positioned between the effector and active sites (Schirmer & Evans, 1990).

On the other hand, EcPFK is more conformationally flexible than BsPFK despite the fact that the two enzymes are structurally nearly identical. Support for this conclusion comes from two lines of evidence. First, EcPFK is allosterically inhibited by ATP, and the inhibition appears to be associated with closure of the active site. The subunit of the chimeric PFK (ChiPFK), which contains the rigid large domain of BsPFK grafted onto the remainder of the EcPFK subunit (chapter 3), is locked in an open conformation. Correspondingly, ATP does not inhibit ChiPFK in the same manner it inhibits EcPFK: the inhibition is much less severe, and is more like that of BsPFK. Thus, in EcPFK, there appears to be an association between closure of the active site—presumably *via* the open-to-closed transition discovered by Shirakihara & Evans

(1988)—and allosteric ATP inhibition. This association is absent in BsPFK, which apparently does not undergo the open-to-closed transition. ATP inhibition of BsPFK occurs by a different mechanism. The inhibition is non-allosteric, is much less pronounced, and arises out of the enzyme's steady-state alternative pathways kinetic mechanism (chapter 2). Thus, a conformational change that occurs in EcPFK apparently does not occur in BsPFK.

A second line of evidence indicating that EcPFK is more conformationally flexible comes from the fact that GDP can activate the enzyme through more than one structural pathway. GDP activates BsPFK through only one pathway, the one proposed by Schirmer & Evans (1990). Both PEP inhibition and GDP activation are affected by mutation of residue 161 of BsPFK (chapter 4), indicating that the structural pathways for the two processes overlap. In contrast, there appear to be two pathways by which GDP can activate EcPFK: one similar to that of BsPFK which overlaps with the pathway of PEP inhibition, plus a second one. Evidence for the existence of a second pathway comes from studies of the QA161 mutant (chapter 4). QA161 is activated normally by GDP, but is completely insensitive to PEP inhibition. This suggests that PEP inhibition and GDP activation of the ATP-inhibited enzyme proceed through different structural routes. The presence in EcPFK of a pathway of GDP activation that is absent in BsPFK highlights the greater conformational flexibility of EcPFK compared to BsPFK. Thus, EcPFK can be thought of as being more "conformationally liberal."

In conclusion, it appears that there are structural pathways of inhibition (by ATP) and activation (by GDP) present in EcPFK that are absent in BsPFK. These processes may involve large conformational changes that cause cracking of crystals grown for the purposes of X-ray crystallography. Indeed, cracking appears to have been a problem for Evans and co-workers, who have been unable to obtain a "T" state structure of EcPFK (Evans, 1992).

*B. stearothermophilus* PFK and *E. coli* PFK, once thought to be functionally indistinguishable because of their similar structures, are now known to be quite different in their mechanisms of regulation. The challenge at this point is to use structure-function studies to further uncover the structural basis for these differences. In order to do this, attention will need to be focused in particular on EcPFK, on the mechanisms by which ATP allosterically inhibits the enzyme and GDP activates the ATP-inhibited enzyme. Studies of site-specific mutants as well as of chimeric Bs/Ec PFK mutants will most likely play an important role in these future efforts.

In the following discussion, a collection of possible future experiments is presented. Some of these involve only BsPFK, some only EcPFK, and some both (chimeric PFKs). They are presented in order of increasing time investment needed. Hopefully, they will stimulate future research on bacterial PFK.

1. Perform a pH study of ChiPFK in an effort to determine the mechanism by which AMPPNP abolishes ChiPFK cooperativity (chapter 3). What effect does AMPPNP have on the sigmoidality of the Fru-6P saturation curve of ChiPFK at different pHs, i.e., at pH 7.2 to pH 8.9? How does the  $k_{cat}$  of ChiPFK vary with pH? Does AMPPCP have an effect similar to that of AMPPNP?

2. Could a high rate of ATP hydrolysis be present in the active site of ChiPFK because of its openness? Is inorganic phosphate ( $P_i$ ) produced by ATP hydrolysis, i.e., the reaction  $ATP \longrightarrow ADP + P_i$ , responsible for the quenching observed when ChiPFK is titrated with ATP? Note that both  $P_i$  and Fru-6P bind Arg 162 and Arg 243 (Evans *et al.*, 1986), and Fru-6P binding to EcPFK causes quenching of fluorescence. Could  $P_i$  also be causing quenching of fluorescence by specifically binding in the Fru-6P site after being produced by ATP hydrolysis? This question could be answered by studying the rate of ATP hydrolysis in ChiPFK, and correlating the results with those from fluorescence titrations using  $P_i$ .

3. Does PEP promote dissociation of the BsPFK tetramer into dimers, as it does the thermostable PFK from *Thermus thermophilus* (Xu *et al.*, 1990)? Note: as in *B. stearothermophilus* PFK, there is a glutamate at position 161 in *T. thermophilus* PFK. Is the QE161 mutant of EcPFK less stable along its active dimer-dimer interface than wild-type? These questions could be answered by performing sucrose gradient sedimentation or gel permeation HPLC (Xu *et al.*, 1990) studies of BsPFK and QE161 in the absence and presence of PEP. The resulting fractions could be analyzed for the presence of tetramer or dimer using SDS-PAGE and silver staining.

4. Glutamate 241 has not been mutated in either EcPFK or BsPFK. Yet, this residue is very important for stabilizing the low-activity (T-state) forms of the enzymes (see Fig. 1.9). But mutating Glu 241, it may be possible to obtain an altered enzyme that is locked in the "R" state, and is insensitive to PEP inhibition. Moreover, it would be very significant if the results showed that PEP inhibition and ATP inhibition were affected differently. The following mutations would be appropriate: Glu 241 to Ala, to Asp, to Arg, and to Gln.

5. The fluorescence of the unique tryptophan of BsPFK, Trp 179, is not sensitive to ligand binding while that of Trp 311 of EcPFK is. It would be useful to construct a double mutant of BsPFK, WA179/YW311, in order to remove the Trp from position 179 and place it at position 311, which is hopefully the right place for observing fluorescence changes due to conformational changes in the enzyme molecule. Note that the residue at position 179 in EcPFK is an alanine. The single mutants WA179 and YW311 would also have to be made in order to determine the effect that each individual mutation has on BsPFK kinetics and regulation.

6. Valdez *et al.* (1988) constructed a mutant BsPFK enzyme, RA25, that exhibited sigmoidal Fru-6P saturation kinetics ( $n$  was 2.0) in the absence of PEP. This result is very interesting since the wild-type enzyme is cooperative only in the presence of PEP. Arg 25 is proposed to bind the phosphate of PEP and the  $\beta$ -phosphate of ADP



in the effector site. It is located along the regulatory interface. Residue 25 should be further investigated by site-directed mutagenesis. By changing Arg 25 to other residues besides alanine, it may be possible to increase the Hill number beyond 2.0. The following mutations should be attempted: Arg 25—>Gln, —>Glu, and —>Lys.

7. Construct additional chimeric Bs/Ec PFK enzymes. By constructing a series of chimeras, it may be possible to define those regions of EcPFK responsible for its sigmoidal Fru-6P saturation kinetics. This could be done in a systematic way: one could move from the N-terminus to the C-terminus, grafting progressively longer N-terminal BsPFK segments onto the remainder of the EcPFK subunit. Likewise, progressively longer N-terminal EcPFK segments could be grafted onto the BsPFK subunit. Junctions between BsPFK and EcPFK portions of the chimeric subunits could be carefully chosen to fall within loops between  $\alpha$ -helices and  $\beta$ -strands so that the structure of the enzyme is not disrupted. By examining Fru-6P saturation profiles of the resulting chimeric enzymes, those regions responsible for the sigmoidal Fru-6P saturation kinetics could be identified.

8. The regions responsible for sigmoidality in the Fru-6P saturation curve of EcPFK may have already been fortuitously discovered; they may be the two regions that move during the open-to-closed transition. These two regions are: (i) a portion of the large domain (residues 41 to 122; Shirakihara & Evans, 1988), and (ii) the 40-amino acid stretch between residues 280 and 319 near the C-terminus (Serre *et al.*, 1990; Shirakihara & Evans, 1988). With this in mind, two chimeric PFKs can be constructed: (a) one in which the 40 amino acids near the C-terminus are replaced with the corresponding residues from BsPFK. Does the replacement abolish heterotropic regulation? Is homotropic cooperativity ( $n=2$ ) retained? (b) a chimeric Bs/Ec PFK having residues 41 to 122 and 280 to 319 from EcPFK, and the rest from BsPFK. The goal here is to create a mutant BsPFK enzyme with the ability to undergo an open-to-

closed transition. Possibly it will exhibit homotropic cooperativity, *i.e.*, a sigmoidal Fru-6P saturation curve.

9. The JK loop of *E. coli* PFK moves between the unliganded and active site-liganded forms of the enzyme (Rypniewski & Evans, 1989). Upon binding ligands, the JK loop shifts toward the catalytic loop and away from its symmetry-related equivalent across the molecular p axis (see Fig. 1.3). Hydrogen bonds are formed between residues in the JK loop and the catalytic loop during this process. On the other hand, these same hydrogen bonds are broken, and others are formed, when ligands are released from the active site. Movement of the JK loop may be associated with the cooperativity of the enzyme. The hydrogen bonds between residues in the JK and catalytic loops that are formed and broken are between Asn 288 and Asp 134, Glu 286 and Asp 134, and Glu 286 and Thr 133. Therefore, Thr 133, Asp 134, Glu 286 and Asn 288 would all be good candidate residues for site-directed mutagenesis. Mutation of these residues and subsequent kinetic analysis of the mutants may allow one to determine the importance of JK loop movement in EcPFK allosteric behavior.

## Literature Cited

- Ainslie, R. G., Jonathan, P. S., & Neet, K. E. (1972) *J. Biol. Chem.* 247, 7088-7096.
- Atkinson, D. E., & Walton, G. M. (1972) *J. Biol. Chem.* 240, 757-763.
- Auzat, I., & Garel, J.-R. (1992) *Protein Science* 1, 254-258.
- Auzat, I., Le Bras, G., & Garel, J.-R. (1994a) *Proc. Natl. Acad. Sci. USA* 91, 5242-5246.
- Auzat, I., Le Bras, G., Branny, P., De La Torre, B. T., & Garel, J.-R. (1994b) *J. Mol. Biol.* 235, 68-72.
- Babul, J. (1978) *J. Biol. Chem.* 253, 4350-4355.
- Barford, D., & Johnson, L. N. (1989) *Nature* 340, 609-616.
- Bar-Tana, J., & Cleland, W. W. (1974a) *J. Biol. Chem.* 249, 1263-1270.
- Bar-Tana, J., & Cleland, W. W. (1974b) *J. Biol. Chem.* 249, 1271-1276.
- Berger, S. A., & Evans, P. R. (1987) *Nature* 327, 437-439..
- Berger, S. A., & Evans, P. R. (1990) *Nature* 343, 575-576.
- Berger, S. A., & Evans, P. R. (1991) *Biochemistry* 30, 8477-8480.
- Berger, S. A., & Evans, P. R. (1992) *Biochemistry* 31, 9237-9242.
- Byrnes, M., Zhu, X., Younathan, E. S., & Chang, S. H. (1994) *Biochemistry* 33, 3424-3431.
- Blangy, D., Buc, H., & Monod, J. (1968) *J. Mol. Biol.* 31, 13-35.
- Campos, G., Guixe, V., & Babul, J. (1984) *J. Biol. Chem.* 259, 6147-6152.
- Cleland, W. W. (1963) *Biochim. Biophys. Acta* 67, 104-137.
- Cleland, W. W. (1979) *Methods Enzymol.* 63, 103-138.
- Daldal, F. (1984) *Gene* 28, 337-342.
- Daldal, F., Babul, J., Guixe, V., & Fraenkel, D. G. (1982) *Eur. J. Biochem.* 126, 373-379.
- Daldal, F., & Fraenkel, D. G. (1983) *J. Bacteriol.* 153, 390-394.
- Dalziel, K. (1957) *Acta Chem Scand.* 11, 1706-1723.
- Dalziel, K., & Dickinson, F. M. (1966) *Biochem. J.* 100, 491-500.

- Deville-Bonne, D., Le Bras, G., Teschner, W., & Garel, J.-R. (1989) *Biochemistry* 28, 1917-1922.
- Deville-Bonne, D., Bourgain, F., & Garel, J. R. (1991a) *Biochemistry* 30, 5750-5754.
- Deville-Bonne, D., Laine, R., & Garel, J.-R. (1991b) *FEBS Lett.* 290, 173-176.
- Deville-Bonne, D., & Garel, J. R. (1992) *Biochemistry* 31, 1695-1700.
- Dixon, M., & Webb, E. C. (1979) *Enzymes*, 3rd. ed., pp. 105-107, Academic Press, New York.
- Evans, P. R. (1992) *Proc. Robert A. Welch Found. Conf. Chem. Res: Regulation of Proteins by Ligands* 36, 39-56.
- Evans, P. R., Farrants, G. W., & Hudson, P. J. (1981) *Phil. Trans. R. Soc. Lond. B* 293, 53-62.
- Evans, P. R., Farrants, G. W., & Lawrence, M. C. (1986) *J. Mol. Biol.* 191, 713-720.
- Evans, P. R., & Hudson, P. J. (1979) *Nature* 279, 500-504.
- Ferdinand, W. (1966) *Biochem. J.* 98, 278-283.
- French, B. A., & Chang, S. H. (1987) *Gene* 54, 65-71.
- French, B. A., Valdez, B. C., Younathan, E. S., & Chang, S. H. (1987) *Gene* 59, 279-283.
- Frieden, C. (1970) *J. Biol. Chem.* 245, 5788-5799.
- Guixe, V., & Babul, J. (1985) *J. Biol. Chem.* 260, 11001-11005.
- Hanson, R. L., Rudolph, F. B., & Lardy, H. A. (1973) *J. Biol. Chem.* 248, 7852-7859.
- Hellinga, H. W., & Evans, P. R. (1985) *Eur. J. Biochem.* 149, 363-373.
- Hellinga, H. W., & Evans, P. R. (1987) *Nature* 327, 437-439.
- Hill, A. V. (1910) *J. Physiol. (London)* 40, iv.
- Jarvest, R. L., Lowe, G., & Potter, B. V. L. (1981) *Biochem. J.* 199, 427-432.
- Jensen, R. A., & Trentini, W. C. (1970) *J. Biol. Chem.* 245, 2018-2022.
- Johnson, J. L., & Reinhart, G. D. (1992) *Biochemistry* 31, 11510-11518.
- Johnson, J. L. & Reinhart, G. D. (1994) *Biochemistry* 33, 2635-2643.
- Kantrowitz, E. R. & Lipscomb, W. N. (1988) *Science* 241, 669-674.
- Kim, S.-J., Chowdhury, J. N., Stryjowski, W., Younathan, E. S., Russo, P. S., & Barkley, M. D. (1993) *Biophys. J.* 65, 215-226.

- Kolb, E., Hudson, P. J. & Harris, J. I. (1980) *Eur. J. Biochem.* 108, 587-597.
- Kotlarz, D., & Buc, H. (1981) *Eur. J. Biochem.* 117, 569-574.
- Kotlarz, D., & Buc, H. (1982) *Methods Enzymol.* 90, 60-70.
- Kotlarz, D., & Buc, H. (1989)
- Kundrot, C. E., & Evans, P. R. (1991) *Biochemistry* 30, 1478-1484.
- Kunkel, T. A., Roberts, J. D., & Zakour, R. A. (1987) *Methods Enzymol.* 154, 367-382.
- Laemmli, U. K. (1970) *Nature* 227, 680-685.
- Laine, R., Deville-Bonne, D., Auzat, I., & Garel, J.-R. (1992) *Eur. J. Biochem.* 207, 1109-1114.
- Larsen, M., Willett, R., and Yount, R. G. (1969) *Science* 166, 1510-1511.
- Lau, F. T. , & Fersht, A. R. (1987) *Nature* 326, 811-812.
- Lau, F. T., & Fersht, A. R. (1989) *Biochemistry* 28, 6841-6847.
- Lau, F. T., Fersht, A. R., Hellinga, H. W., & Evans, P. R. (1987) *Biochemistry* 26, 4143-4148.
- Le Bras, G., & Garel, J.-R. (1982) *Biochemistry* 21, 6656-6660.
- Le Bras, G., & Garel, J.-R. (1985) *J. Biol. Chem.* 260, 13450-13453.
- Le Bras, G., & Garel, J.-R. (1986) *Biochemistry* 25, 2490-2493.
- Le Bras, G., Teschner, W., Deville-Bonne, D., & Garel, J.-R. (1989) *Biochemistry* 28, 6836-6841.
- Lee, C. P., Kao, M. C., French, B. A., Putney, S. D., & Chang, S. H. (1987) *J. Biol. Chem.* 262, 4195-4199.
- Li, J., Chen, Z., Lu, L., Byrnes, M., & Chang, S. H. (1990) *Bioch. Biophys. Res. Comm.* 170, 1056-1060.
- Li, J., Zhu, X., Byrnes, M., Nelson, J. W., and Chang, S. H. (1993) *J. Biol. Chem.* 268, 24599-24606.
- Martel, A., & Garel, J.-R. (1984) *J. Biol. Chem.* 259, 4917-4921.
- Martin, R. G., & Ames, B. N. (1961) *J. Biol. Chem.* 236, 1372-1379.
- Monod, J., Wyman, J., & Changeux, J. P. (1965) *J. Mol. Biol.* 3, 318-356.
- Martin, R. G., & Ames, B. N. (1961) *J. Biol. Chem.* 236, 1372-1379.
- Neet, K. E., & Ainslie, R. G. (1980) *Methods Enzymol.* 64, 192-226.

- Poorman, R. A., Randolph, A., Kemp, R. G., and Henrikson, R. L. (1984) *Nature* 309, 467-469.
- Rao, G.S.J., Harris, B. G., & Cook, P. F. (1987) *J. Biol. Chem.* 262, 14074-14079.
- Rypniewski, W. R., & Evans, P. R. (1989) *J. Mol. Biol.* 207, 805-821.
- Sanger, F., Nicklen, S., & Coulson, A. R. (1977) *Proc. Natl. Acad. Sci. USA* 74, 5463-5467.
- Schirmer, T., & Evans, P. R. (1990) *Nature* 343, 140-145.
- Segel, I. H. (1975a) *Enzyme Kinetics*, pp. 309-320 and pp. 818-826, John Wiley & Sons, New York.
- Segel, I. H. (1975b) *Enzyme Kinetics*, pp 460-461 and 657-659, John Wiley & Sons, New York.
- Seong, B. L. & RajBhandary, U. L. (1987) *Proc. Natl. Acad. Sci. USA* 84, 334-338.
- Serre, M.-C. , & Garel, J.-R. (1990) *Eur. J. Biochem.* 189, 487-492.
- Serre, M.-C., Teschner, W., & Garel, J.-R. (1990) *J. Biol. Chem.* 265, 12146-12148.
- Shirakihara, Y., & Evans, P. R. (1988) *J. Mol. Biol.* 204, 973-994.
- Simon, W. A., & Hofer, H. W. (1978) *Eur. J. Biochem.* 88, 175-181.
- Sweeny, J. R., & Fisher, J. R. (1968) *Biochemistry* 7, 561-565.
- Teschner, W., Deville-Bonne, D., & Garel, J.-R. (1990) *FEBS Lett.* 267, 96-98.
- Teschner, W., & Garel, J.-R. (1989) *Biochemistry* 28, 1912-1916.
- Torres, J. C., & Babul, J. (1991) *Eur. J. Biochem.* 200, 471-476.
- Uyeda, K. (1979) *Adv. Enzymol. Relat. Areas Mol. Biol.* 48, 193-244.
- Valdez, B. C., Chang, S. H., & Younathan, E. S. (1988) *Bioch. Biophys. Res. Comm.* 156, 537-542.
- Valdez, B. C., French, B. A., Younathan, E. S., & Chang, S. H. (1989) *J. Biol. Chem.* 264, 131-135.
- Xu, J., Oshima, T., & Yoshida, M. (1990) *J. Mol. Biol.* 215, 597-606.
- Yoshida, M. (1972) *Biochemistry* 11, 1087-1093.
- Yount, R. G., Babcock, D., Ballantyne, W., and Ojala, D. (1971) *Biochemistry* 10, 2484- 2489.
- Zheng, R. L., & Kemp, R. G. (1992) *J. Biol. Chem.* 267, 23640-23645.

Zheng, R.-L., & Kemp, R. G. (1994) *J. Biol. Chem.* 269, 18475-18479.

Zoller, M. J., & Smith, M. (1983) *Methods Enzymol.* 100, 468-500.

**Appendix**  
**Permission Letter**





LOUISIANA STATE UNIVERSITY  
AND AGRICULTURAL AND MECHANICAL COLLEGE  
Department of Biochemistry

29 September 1994  
FAX (504) 388-5321

Dr. Gordon G. Hammes  
Editor, *Biochemistry*  
Duke University Medical Center  
P. O. Box 3673  
081 Yellow Zone  
Duke South  
Durham, NC 27710

Dear Dr. Hammes:

I am a graduate student at Louisiana State University. I am currently writing my dissertation for a PhD in Biochemistry. As one of the chapters of my dissertation, I would like to include the manuscript of a paper published in your journal: Byrnes, M., Xhu, X., Younathan, E. S., and Chang, S. H. (1994) *Biochemistry* 33, 3424-3431.

May I have a letter from you stating that I have the journal's permission to include the manuscript in my dissertation? Could you FAX the letter to the number listed in the heading? If there is a problem with my request, please let me know. Thank you.

Sincerely,

W. Malcolm Byrnes  
Dept. of Biochemistry  
LSU

SENT BY: Xerox Telecopier 7020 ; 9-29-94 ; 15:53 ;

2028726060-

504 388 5321;# 2



## American Chemical Society

PUBLICATIONS DIVISION  
COPYRIGHT OFFICE1155 SIXTEENTH STREET, N.W.  
WASHINGTON, D.C. 20036  
Phone (202) 872-4367 or -4388  
Fax (202) 872-6060DATE: September 29, 1994

## MEMORANDUM

TO: W. Malcolm Byrnes  
Department of Biochemistry  
Louisiana State UniversityFROM: C. Arleen Courtney  
Copyright Assistant *C. Arleen Courtney*RE: Your letter dated September 29, 1994

Thank you for your recent letter, regarding your request for permission to include your paper(s), per your attached letter, in your thesis. Please note the following:

- ⇒ \* If your paper has already been published by ACS, I would be happy to grant you this permission royalty free provided that you print the required ACS copyright credit line on the first page of your article: "Reprinted with permission from FULL REFERENCE CITATION. Copyright YEAR American Chemical Society."
- \* If you plan to submit your thesis to UMI, please inform them that permission to include your already published ACS article as part of your thesis is granted for paper and microform copies only; the ACS copyright notice (see above) must appear on the first page of the ACS article.
- \* If your paper has not already been published by ACS, you may include it in your thesis provided that you print the following ACS copyright credit line on the first page of your article: "Reprinted with permission from JOURNAL NAME, in press. Unpublished work copyright CURRENT YEAR American Chemical Society." You may NOT include the ACS paper in the version that you submit to UMI until ACS has published your paper; permission for UMI to use the ACS article as part of your thesis is then limited to microform and paper copies only.
- \* Other: \_\_\_\_\_

Thank you for writing. If you have any questions, please call me at 202/872-4368.

## Vita

Walton Malcolm Byrnes was born on December 7, 1959 in Covington, Louisiana to Mrs. Christine FitzSimons Byrnes and Mr. Vincent Malcolm Byrnes. He attended college at Xavier University of Louisiana in New Orleans, receiving a B.S. in Chemistry with distinction in English (overall g.p.a. 4.0/4.0) in May, 1981. While at Xavier, Malcolm received several awards, including the ACS Analytical Award (1980), the ACS Award (1981), and the Mother Agatha M. Ryan Award (1981), Xavier's second-highest for overall achievement.

After teaching general, analytical, and organic chemistry laboratories at his *alma mater* for a year, Malcolm entered a graduate program in chemistry and biochemistry at the University of Illinois in Champaign-Urbana. However, he left after two years (in May, 1984) to teach chemistry at St. John's College in Belize City, Belize, Central America. After two years at SJC, having successfully prepared his students for their Cambridge O-level and A-level exams, Malcolm left Belize for Washington, D. C., where he taught chemistry and physics at Gonzaga College High School.

Finally, in August, 1988, Malcolm entered the graduate program in the Biochemistry Department at Louisiana State University in order to complete his graduate studies. While at LSU, he has worked in the laboratory of Dr. Simon H. Chang, investigating the structural basis for differences between the phosphofructokinases from two bacteria, *B. stearothermophilus* and *E. coli*. He was a teaching assistant (3 yrs.) for the senior-level undergraduate biochemistry laboratory course, and was active as a member of the Biochemistry Graduate Student Council (3 yrs.), which organized the first and second annual Biochemistry Research Minisymposia.

During his tenure at LSU, Malcolm has been a part of six publications: (1) Byrnes, M., Zhu, X., Younathan, E. S., & Chang, S. H. (1994) "Kinetic Characteristics

of the Phosphofructokinase from *Bacillus stearothermophilus*: MgATP Non-allosterically Inhibits the Enzyme" *Biochemistry* 33, 3424-3431. (2) Byrnes, M., Hu, W., Younathan, E. S., & Chang, S. H. (1994) "A Chimeric Bacterial Phosphofructokinase Exhibits Cooperativity in the Absence of Heterotropic Regulation" *J. Biol. Chem.* (in press). (3) Byrnes, M., Auzat, I., Garel, J.-R., & Chang, S. H. "The Role of Residue 161 in the Allosteric Transitions of Two Bacterial Phosphofructokinases" (in preparation). (4) Zhu, X., Byrnes, M., & Chang, S. H. "The Role of Glycine 212 in the Allosteric Behavior of Phosphofructokinase from *Bacillus stearothermophilus*" (submitted to *Biochemistry*). (5) Li, J., Zhu, X., Byrnes, M., Nelson, J. W., & Chang, S. H. (1993) "Site-directed Mutagenesis of Rabbit Muscle Phosphofructokinase cDNA: Mutations at Glutamine 200 Affect the Allosteric Properties of the Enzyme" *J. Biol. Chem.* 268, 24599-24606. (6) Li, J., Chen, Z., Lu, L., Byrnes, M., & Chang, S. H. (1990) "Sequence Diversity in the 5'-untranslated Region of Rabbit Muscle Phosphofructokinase mRNA" *Biochem. Biophys. Res. Comm.* 170, 1056-1060.

Malcolm will be leaving LSU in October, 1994 to accept a position as post-doctoral associate in the Department of Pharmacology (College of Veterinary Medicine) at Cornell University in Ithaca, New York, in the laboratory of Dr. Robert Oswald. He and Dr. Oswald have written and submitted an application for an NIH individual research training fellowship.

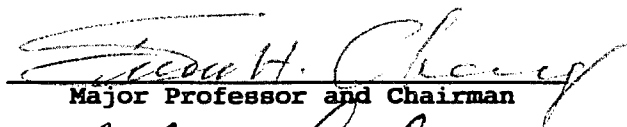
DOCTORAL EXAMINATION AND DISSERTATION REPORT

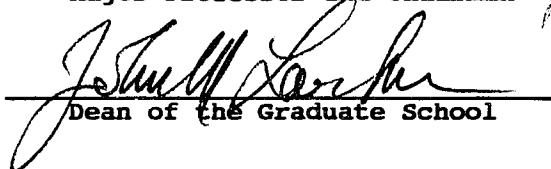
**Candidate:** Walton Malcolm Byrnes

**Major Field:** Biochemistry

**Title of Dissertation:** The Structural Basis for Kinetic and  
Allosteric Differences between Two Bacterial  
Phosphofructokinases

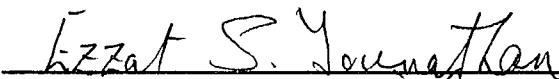
**Approved:**

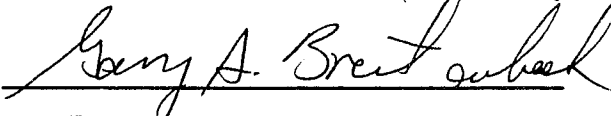
  
Major Professor and Chairman


  
Dean of the Graduate School

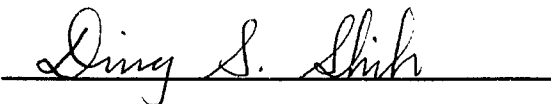
**EXAMINING COMMITTEE:**

  
\_\_\_\_\_

  
\_\_\_\_\_

  
\_\_\_\_\_

  
\_\_\_\_\_

  
\_\_\_\_\_

\_\_\_\_\_

\_\_\_\_\_

**Date of Examination:**

October 11, 1994

\_\_\_\_\_